VNIVERSIDAD NACIONAL
AVFNOMA DE
MÉXICO

UNIVERSIDAD NACIONAL AUTÓNOMA DE MÉXICO

UNIDAD ACADÉMICA DE LOS CICLOS PROFESIONALES Y
POSGRADO DEL COLEGIO DE CIENCIAS Y HUMANIDADES
INSTITUTO DE GEOFÍSICA
POSGRADO EN CIENCIAS DE LA TIERRA

INVESTIGACIONES GEOFÍSICAS E HIDROGEOLÓGICAS EN EL NOROESTE DE LA PENINSULA DE YUCATÁN, MÉXICO

T E S I S

PARA OPTAR AL GRADO DE DOCTOR EN CIENCIAS
(AGUAS SUBTERRÁNEAS)

P R E S E N T A

BIRGIT STEINICH

Ciudad Universitaria Marzo, 1996

UNAM – Dirección General de Bibliotecas Tesis Digitales Restricciones de uso

Investigaciones geofísicas e hidrogeológicas en el noroeste de la Península de Yucatán, México

Birgit Steinich

Abstract

The present investigation focuses on the aquifer of the Peninsula of Yucatan, southeast Mexico. The study area consists of the region between 88°30′ and 90°45′ west and 19°30′ and 21°75′ north. The Peninsula of Yucatan is a limestone platform housing a mature karst system. The ground water flow is determined by secondary porosity present in the form of interconnected fractures, channels and cavities. Permeabilities are high and hydraulic gradients are low. The aquifer consists of a fresh water lens underlain by salt water. The aquifer is unconfined except for a narrow band parallel to the coast. A circular alignment of sinkholes, the Ring of Cenotes, crosses the study area.

The interpretation of electrical surveys shows that various segments of the Ring of Cenotes have increased permeabilities with respect to their surroundings. Nevertheless, a low permeability zone was identified in the southern part of the ring. Variations of the water level near this zone show that the eastern and the western segment, with respect to this zone, are disconnected hydraulically. Comparison of these results with geochemical data suggests that the low permeability zone represents a ground water divide in the aquifer system. The thickness of the fresh water lens varies between 18 m near the coast up to 110 m in the southeastern part of the study area. The upper part of the limestone rocks containing the aquifer is electrically anisotropic as a consequence of one or several systems of aligned fractures causing an anisotropy of the permeability.

The area east of the low permeability zone is characterized by a high variability in its water levels and equipotential lines as a function of surface recharge variations. Those oscilations cause changes of the ground water flow direction, even a reversal of the regional orientation, which is from southeast to northwest, to a southeast to northwest direction. The northwest portion of the affected zone reaches the southern part of the City of Merida. The contamination risk for extended rural areas southeast of the City is increased by contaminants which may reach the aquifer from the City of Merida.

The distribution and size of the karst sinkholes in the study area are not homogeneous. Different alignments and clusters of sinkholes can be observed, the best studied example of these is the Ring of Cenotes. Two topographic platforms can be distinguished in the study area. These are separated by the Sierrita de Ticul, a small landstep that crosses the study area in a northwest to southeast

direction. Altitudes on the lower platform, which surround the upper platform, vary between 0 m near the coast to 20 m near the Sierrita de Ticul. The upper platform has altitudes in the order of 50 m to 100 m and is located in the southern-central part of the study area. Two remarkable local tectonic structures exist within the study area: a transform fault, which is related to the opening of the Gulf of Mexico, and the Chicxulub Crater. Both structures were sedimentary basins in the past. Different compaction rates of these sediments with respect to the surroundings may have caused fracture systems along the former walls of the basins. These fractures represent favorable initial conditions for the karstification process. Hydraulic gradients, climatic conditions, type of vegetation and others may be the selection factors for the fractures that were later opened by the karst corrosion. As long as cavities formed during this process are submerged, the water gives the necessary bouyant support to prevent the total collapse of the cavity roofs. In areas were the water table is not able to support the cave roofs, these are likely to collapse and big dolines can be observed at the surface. Based on the close relationship of local tectonics with the distribution of the permeability of the aquifer, a division of the latter into 'hydrotectonic domains' has been proposed, the Ring of Cenotes being one example.

Vo.Bo.

Luis E. Marín

Dr. Luis E. Marín
Director de Tesis

I N D I C E

Resumen

En este trabajo se estudió el acuífero de la Península de Yucatán en el sureste de México. La zona de estudio está comprendida entre las longitudes $88^o30'$ y $90^o45'$ oeste y las latitudes $19^o30'$ y $21^o75'$ norte. La Península de Yucatán consiste en una plataforma de rocas calcáreas altamente carstificadas. El flujo del agua subterránea es determinado por la porosidad secundaria presente en forma de fracturas, túneles y cavernas interconectadas. La permeabilidad es alta y los gradientes hidráulicos bajos. El acuífero consiste en un lente de agua dulce el cual flota sobre agua salada. El acuífero es libre excepto por una estrecha franja a lo largo de la costa. Existe un marcado alineamiento circular de dolinas, el 'Anillo de Cenotes'.

La interpretación de registros eléctricos muestra que varios segmentos de este anillo tienen permeabilidades altas respecto a los alrededores. Sin embargo, existe una zona de reducida permeabilidad en la parte sur del anillo. Variaciones del nivel del agua observadas cerca de esta zona muestran que esta última desconecta hidráulicamente las partes del anillo al occidente de las que se encuentran al oriente de ella. La comparación de estos resultados con datos geoquímicos sugiere que dicha zona representa un parteaguas en el acuífero de Yucatán. El lente de agua dulce tiene espesores que varían entre 18 m cerca de la costa hasta 110 m en la parte sureste de la zona estudiada. El subsuelo es electricamente anisotrópico lo cual es la consecuencia de uno o varios sistemas de fracturas alineadas que generan una anisotropía en la permeabilidad.

El área al oriente del parteaguas se caracteriza por su alta variabilidad de los niveles de agua y del régimen de las líneas equipotenciales como respuesta a cambios de la recarga superficial. Dichas oscilaciones causan variaciones en la dirección del flujo subterráneo, posiblemente hasta una inversión de una dirección sureste-noroeste (lo cual corresponde a la orientación del flujo regional) a noroeste-sureste. La zona afectada alcanza en su porción noroeste la parte sur de la Ciudad de Mérida. Existe el peligro de contaminación proveniente de la ciudad de una extensa zona rural al

sureste de ella.

La distribución y el tamaño de las dolinas cársticas en la zona de estudio no son homogéneos. Existen diferentes alineamientos y agrupamientos de dolinas siendo el Anillo de Cenotes el mejor estudiado. En la zona de estudio se pueden distinguir dos plataformas, el límite entre ambas es la Sierra de Ticul que atraviesa la zona de noroeste a sureste. Las alturas del terreno varían entre 0 m y 20 m en la plataforma baja que rodea la plataforma alta. Esta última tiene alturas entre 50 m y 100 m y ocupa el área central-sur de la zona de estudio. Dos estructuras de la tectónica local destacan en el área: una falla transforme relacionada con la apertura del Golfo de México y el Cráter de Chicxulub. Las dos estructuras formaron cuencas de sedimentación en su tiempo. Se propone que debido a diferentes grados de la compactación de estos sedimentos respecto al área fuera de las cuencas se creó un sistema de fracturas a lo largo de las antiguas paredes de las cuencas. Estas fracturas representaron condiciones favorables para el inicio del proceso de la carstificación. Un proceso de selección el cual depende de factores como el gradiente hidráulico, las condiciones climatológicas, el tipo de vegetación entre otros, decide si las fracturas se abren finalmente por disolución. Mientras que las cavernas así formadas se encuentran sumergidas, el agua da el apoyo suficiente para evitar el colapso de la totalidad de sus techos. Donde la profundidad al nivel del agua es demasiado grande para ya no cumplir esa condición, se colapsan los techos lo cual se manifiesta con dolinas de mayor tamaño. Con base a la estrecha relación entre la tectónica local y la distribución de la permeabilidad en el acuífero, se propone dividirlo en 'dominios hidrotectónicos', siendo el Anillo de Cenotes uno de ellos.

Abstract

The present investigation focuses on the aquifer of the Peninsula of Yucatan, southeast Mexico. The study area consists of the region between $88^o30'$ and $90^o45'$ west and $19^o30'$ and $21^o75'$ north. The Peninsula of Yucatan is a limestone platform housing a mature karst system. The ground water flow is determined by secondary porosity present in the form of interconnected fractures, channels and cavities. Permeabilities are high and hydraulic gradients are low. The aquifer consists of a fresh water lens underlain by salt water. The aquifer is unconfined except for a narrow band parallel to the coast. A circular alignment of sinkholes, the Ring of Cenotes, crosses the study area.

The interpretation of electrical surveys shows that various segments of the Ring of Cenotes have increased permeabilities with respect to their surroundings. Nevertheless, a low permeability zone was identified in the southern part of the ring. Variations of the water level near this zone show that the eastern and the western segment, with respect to this zone, are disconnected hydraulically. Comparison of these results with geochemical data suggests that the low permeability zone represents a ground water divide in the aquifer system. The thickness of the fresh water lens varies between 18 m near the coast up to 110 m in the southeastern part of the study area. The upper part of the limestone rocks containing the aquifer is electrically anisotropic as a consequence of one or several systems of aligned fractures causing an anisotropy of the permeability.

The area east of the low permeability zone is characterized by a high variability in its water levels and equipotential lines as a function of surface recharge variations. Those oscilations cause changes of the ground water flow direction, even a reversal of the regional orientation, which is from southeast to northwest, to a southeast to northwest direction. The northwest portion of the affected zone reaches the southern part of the City of Merida. The contamination risk for extended rural areas southeast of the City is increased by contaminants which may reach the aquifer from the City

of Merida.

The distribution and size of the karst sinkholes in the study area are not homogeneous. Different alignments and clusters of sinkholes can be observed, the best studied example of these is the Ring of Cenotes. Two topographic platforms can be distinguished in the study area. These are separated by the Sierrita de Ticul, a small landstep that crosses the study area in a northwest to southeast direction. Altitudes on the lower platform, which surround the upper platform, vary between 0 m near the coast to 20 m near the Sierrita de Ticul. The upper platform has altitudes in the order of 50 m to 100 m and is located in the southern-central part of the study area. Two remarkable local tectonic structures exist within the study area: a transform fault, which is related to the opening of the Gulf of Mexico, and the Chicxulub Crater. Both structures were sedimentary basins in the past. Different compaction rates of these sediments with respect to the surroundings may have caused fracture systems along the former walls of the basins. These fractures represent favorable initial conditions for the karstification process. Hydraulic gradients, climatic conditions, type of vegetation and others may be the selection factors for the fractures that were later opened by the karst corrosion. As long as cavities formed during this process are submerged, the water gives the necessary bouyant support to prevent the total collapse of the cavity roofs. In areas were the water table is not able to support the cave roofs, these are likely to collapse and big dolines can be observed at the surface. Based on the close relationship of local tectonics with the distribution of the permeability of the aquifer, a division of the latter into 'hydrotectonic domains' has been proposed, the Ring of Cenotes being one example.

I. Introducción

El área de estudio está comprendida entre las longitudes $88^o30'$ y $90^o45'$ oeste y las latitudes $19^o30'$ y $21^o75'$ norte, lo cual corresponde a la parte noroeste de la Península de Yucatán en el sureste de México.

El clima de la zona de estudio es tropical húmedo. Las temperaturas medias mensuales varían entre 23.9^oC en enero y 29.7^oC en mayo (valores promedios de 32 años para la estación meteorológica de Telchaquillo, Yucatán) (Anónimo, 1994). La temporada de lluvias abarca los meses de junio a octubre con valores máximos de precipitación en los meses julio a septiembre (Anónimo, 1994). La precipitación pluvial media anual varía desde 500 mm cerca de la costa noroeste hasta 1300 mm en la parte sur-central del área de estudio (Anónimo, 1988).

La Península es una plataforma de rocas calcáreas. En el área de estudio afloran formaciones del Terciario y del Cuaternario. En una franja cercana a la línea de la costa aflora el Cuaternario, seguido tierra adentro por capas del Plioceno, Oligoceno en la parte occidente y Eoceno en la parte orientel y Eoceno Medio. A lo largo de la Sierrita de Ticul afloran capas del Paleoceno (Anónimo, 1988).

La Península de Yucatán es un terreno con topografía plana. El único desnivel importante representa la Sierrita de Ticul, que atraviesa el área de estudio en una dirección noroeste-sureste. Al norte de la Sierrita de Ticul, las alturas del terreno varían entre 0 m en la costa a aproximadamente 20 m sobre el nivel medio del mar (NMM) al pie de la misma. La Sierrita de Ticul representa el límite norte de una plataforma ligeramente elevada con alturas entre 50 m y 100 m (Anónimo, 1984). Como consecuencia de la carstificación, el terreno tiene un aspecto ondulado en diferentes zonas del área de estudio con diferencias de altura del orden de metros a decenas de metros.

En la parte noroeste de la Península de Yucatán, no existen arroyos ni ríos. Todo el agua está presente en forma de agua subterránea. La roca tiene una alta permeabilidad, la capa de suelo varía entre unos pocos centímetros hasta inexistente en muchas partes del área de estudio. El nivel freático es somero en la parte norte del área de

estudio, teniendo valores de entre 0 m en la costa a 30 m al pie de la Sierrita de Ticul. Al sur de la Sierrita de Ticul, estos valores están en el rango de 30 m a 140 m (Anónimo, 1988).

El acuífero es libre excepto por una estrecha franja a lo largo de la costa (Perry et al., 1989). El acuífero es cárstico, el flujo del agua subterránea está determinado por la porosidad secundaria, presente en forma de fracturas, túneles y cavernas interconectados. La recarga del acuífero se efectúa durante la temporada de lluvias que comprende los meses de mayo a octubre. El flujo subterráneo regional es de sureste a noroeste, sin embargo, el flujo local puede diferir considerablemente de esta dirección. Se propuso que el Anillo de Cenotes intercepta el flujo del agua subterránea, funge como río subterráneo, descargando su agua en los dos puntos de intercepción con la línea costera cerca de Dzilam de Bravo en la costa norte y de Celestún en la costa occidental (Marín, 1990). La descarga del acuífero al mar se realiza a través de fracturas, túneles y cavernas abiertos hacia el mar a lo largo de toda la línea costera, sin embargo, modelos del acuíferos sugieren que una buena parte de la descarga se concentra en los puntos de intersección del Anillo de Cenotes con la costa (Marín, 1990; Perry et al., 1995).

Esta investigación está divida en cuatro partes, cada cual representada por una publicación. En lo siguiente se dan los objetivos y resultados más importantes de ellas.

Investigaciones hidrogeológicas en el noroeste de Yucatán, México, utilizando registros de resistividad

Estudios geoeléctricos confirman que la permeabilidad del subsuelo aumenta acercándose al Anillo de Cenotes, sin embargo, existen variaciones de la permeabilidad a lo largo de este (Steinich and Marín, en prensa(a)). Los mismos autores identificaron una zona de reducida permeabilidad en el tramo del anillo al sur de la Ciudad de Mérida, cerca de la población de Abalá. Debido a la presencia de fracturas alineadas se cuenta con un medio anisotrópico respecto a su permeabilidad (Steinich y Marín,

en prensa(a)). El acuífero de Yucatán consiste en un lente de agua dulce el cual flota sobre agua salada (Marín, 1990). Se tiene evidencia del interfase hasta más de 90 *km* de la costa, donde alcanza una profundidad de 110 *m* aproximadamente (Steinich y Marín, en prensa(a)).

Determinación de las características de flujo en el acuífero del noroeste de la Península de Yucatán, México

La respuesta del acuífero a las precipitación se realiza en el orden de días. Escasez en la recarga superficial puede causar una disminución del nivel freático por más de un metro lo cual representa más del 50% del valor inicial. La parte con mayores variaciones del nivel observadas se encuentra al este de la zona de reducida permeabilidad. El rápido drenaje de esta 'zona de alta variabilidad' se debe a un alineamiento de los conductos y al hecho que estas estén paralelos a la dirección del flujo (Steinich and Marín, en prensa(b)). La diferencia de la velocidad de drenaje en el acuífero causa cambios importantes en el regimen del flujo subterráneo hasta generar una inversión de carácter temporal de la dirección de flujo de sureste-noroeste (flujo regional) a noroeste-sureste. La zona afectada se extiende hasta los alrededores de la Ciudad de Mérida lo cual implica un peligro de contaminación de amplias áreas rurales en la parte central de la zona de estudio proveniente de la ciudad.

Localización del parteaguas en el acuífero cárstico de Yucatán, México, combinando datos geoquímicos e hidrogeológicos

La hipótesis de que el Anillo de Cenotes funciona como río subterráneo (Marín, 1990) con dos puntos de descarga en los puntos de intersección con la línea costera (Perry et al., 1995) requiere la existencia de un parteaguas en el acuífero de Yucatán. Datos hidráulicos y geoquímicos coinciden en un parteaguas ubicado en la parte sur del Anillo de Cenotes (Steinich et al., aceptado). La zona de reducida permeabilidad

descrita por Steinich y Marín (en prensa(a)) juega un papel importante en la ubicación del parteaguas. Se propone que representa el límite occidental de este último desconectando hidráulicamente los segmentos del Anillo de Cenotes al oriente y al occidente de ella (Steinich et al., aceptado).

El papel de la tectónica local en el desarrollo del carst y la hidrogeología en Yucatán, México

El proceso de carstificación que formó el carst yucateco se desarrolló de una manera heterogénea, lo cual se refleja, entre otras cosas, en la heterogeneidad de la distribución espacial y el tamaño de las dolinas. Una de las manifestaciones más interesantes es el Anillo de Cenotes que representa un alineamiento circular de dolinas. Otros alineamientos y agrupamientos se pueden identificar en la zona de estudio (Steinich y Marín, en arbitraje). Resultados obtenidos por los mismos autores implican que las estructuras de la tectónica local generaron un diseño de fracturas que dió las condiciones necesarias para el inicio del proceso de la carstificación. Otros fenómenos (clima, vegetación, profundidad al nivel del agua, etc.) resultan determinantes para la selección de las fracturas abiertas por la carstificación y para la manifestación de las cavernas en la superficie a causa del colapso de sus techos (Steinich y Marín, en arbitraje). A base de estos resultados se propone definir diferentes 'dominios hidrotectónicos', siendo el Anillo de Cenotes el mejor estudiado.

Referencias

Anónimo, 1984. Cartas Topográficas de Yucatán 1:50 000. *Instituto Nacional de Estadística, Geografía e Informática, Mérida, Yucatán.*

Anónimo, 1988. Sinopsis Geohidrológica del Estado de Yucatán. *Secretaría de Agricultura y Recursos Hidráulicos, México, D.F., 1988.*

Anónimo, 1994. Datos climatológicos. *Comisión Nacional del Agua, Mérida,*

Yucatán.

Marín, L.E. 1990. Field Investigations and Numerical Simulation of Groundwater Flow in the Karstic Aquifer of Northwestern Yucatan, México. *Ph. D. Thesis. 183 pp., Northern Illinois University, DeKalb, IL, USA*

Perry, E.C., L.E. Marín, J. McClain y G. Velázquez; 1995. The Ring of Cenotes (sinkholes), northwest Yucatan, Mexico: its hydrogeologic characteristics and possible association with the Chicxulub Impact Crater. *Geology, 23:17-20*

Perry, E.C., J. Swift, J. Gamboa, A. Reeve, R. Sanborn, L.E. Marín, y M. Villasuso. 1989. Geological and Environmental Aspects of Surface Cementation, North Coast, Yucatan, Mexico. *Geology, 17:818-821*

Steinich, B. y L.E. Marín, en prensa(a). Hydrogeological investigations in northwestern Yucatan, Mexico, using resistivity surveys. *Ground Water*

Steinich, B. y L.E. Marín, en prensa(b). Determination of flow characteristics in the Aquifer of the Northwestern Peninsula of Yucatan, Mexico. *Journal of Hydrology*

Steinich, B., G. Velázquez Olimán y L.E. Marín, E. Perry, aceptado. Determination of the ground water divide in the karst aquifer of Yucatan, Mexico, combining geochemical and hydrogeological data. *Geofísica Internacional*

Steinich, B. y L.E. Marín, en arbitraje. The role of local tectonics on the karst development and the hydrogeology in Yucatan, Mexico. *Water Resources Research*

II. Investigaciones hidrogeológicas en el noroeste de Yucatán, México, utilizando registros de resistividad.

Hydrogeological investigations in northwestern Yucatan, Mexico, using resistivity surveys

Birgit Steinich[a], Luis E. Marin[a]

Instituto de Geofísica, Universidad Nacional Autónoma de México, Cd. Universitaria, Mexico City, Mexico, C.P. 04510

GROUND WATER, 1996, en prensa

Abstract

Eight Schlumberger soundings and four Wenner anisotropy measurements were conducted in the northwestern section of the Yucatan Peninsula for hydrogeological investigations of a karst aquifer. This system is influenced by a circular high permeability zone (Ring of Cenotes) probably related to the Chicxulub Impact Crater. Schlumberger soundings and Wenner anisotropy measurements show that the karst aquifer can be modeled as an electrically anisotropic medium. Anisotropy is related to preferential permeability directions channeling ground water flow within the aquifer. Directions of maximum permeability were determined using Wenner anisotropy measurements. Electrical soundings were conducted at different sites near the Ring of Cenotes. Resistivity values decrease toward the Ring of Cenotes supporting the hypothesis that selected segments of the Ring have high permeability. Several soundings were conducted in order to study lateral permeability variations along the Ring. A high permeability section can be identified by low resistivity models and is related to a zone of high cenote density. A low permeability section of the Ring was found showing high resistivity models. This zone overlaps with an area of low cenote den-

sity. Electrical soundings were used to determine the depth of the fresh water lens; the interface was detected along two profiles perpendicular and parallel to the Ring of Cenotes resulting in a depth that ranged from 18 m near the coast up to 110 m in the southeastern part of the study area. The predicted depths of the interface using electrical methods showed a good correlation with Ghyben-Herzberg and measured interface depths at some sites. Discrepancies between calculated and interpreted interface depths at two sites may by explained by horizontal-to-vertical permeability anisotropy.

Introduction

The study area is the northwestern section of the Yucatan Peninsula located in southeastern Mexico (Fig. 1). The hydrogeology of the Yucatan Peninsula consists of a thin lens of fresh water underlain by a salt water intrusion that penetrates more than 40 km inland. This lens has an approximate thickness of 45 m at Merida and is less than 120 m thick within the study area. The rocks in the upper hundred meters consist primarily of limestone. Small chert fragments have also been found (Marín, 1994). Dissolution of the carbonate rocks have resulted in a lack of aquitards. The aquifer consists of a mature karstic medium with a well developed system of interconnected caverns and conduits. It is unconfined except for a narrow band parallel to the coast (Perry et al., 1989). The aquifer has a low hydraulic gradient, on the order of $7 - 10$ mm/km, suggesting very high permeabilities (Marín, 1990). Limited data suggest that the Ghyben-Herzberg relation holds for northwestern Yucatan except near the coast (Marín, 1990; Marín et al., in review).

It has recently been proposed that Yucatan is the site of an extraterrestrial impact event that struck the Earth 65 million years ago (Hildebrand et al., 1991; Sharpton et al., 1992). This structure, known as the Chicxulub Impact Crater, has been proposed to have a diameter of approximately 300 km. A steep gravity gradient according to the geophysical model, occurs at an approximate diameter of 180 km, location

that coincides with that of the Ring of Cenotes (Sharpton et al., 1993). It has been reported by Pope et al. (1991), Marín (1990) and Marín et al. (1990) that the Ring of Cenotes has a cenote spacing varying from three cenotes per kilometer to less than one cenote per kilometer forming a $5 - 20$ *km* wide band. Marín (1990) and Marín et al. (in review) have proposed that the Ring channels ground water and acts as a flow conduit.

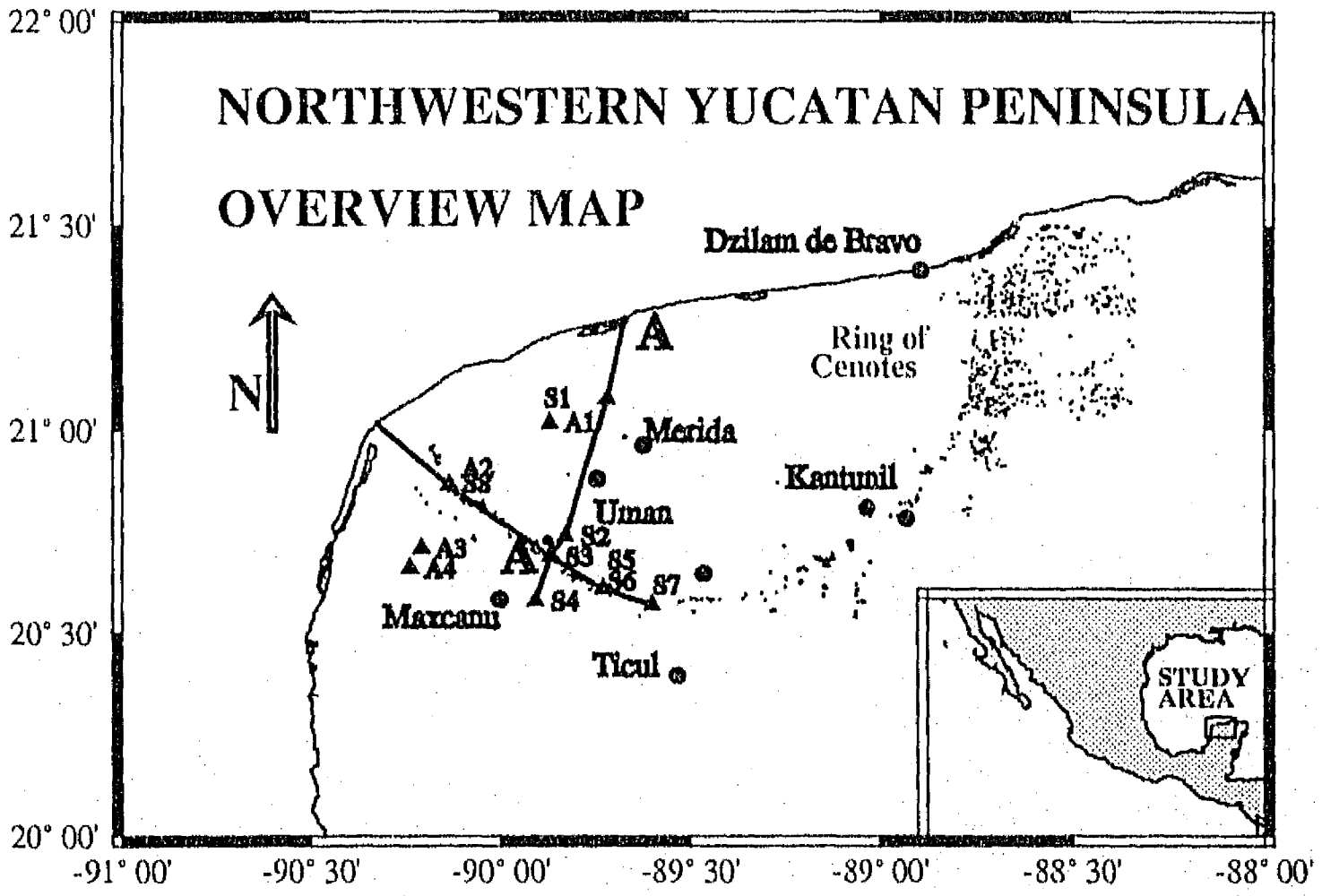

Fig. 1 Overview map of the study area showing electrical survey location and profile positions.

Hydrogeological data supporting the hypothesis that the Ring has high permeability include: 1) the localized abundance of cenotes, which elsewhere represent partially collapsed cavern systems; 2) anomalously high discharge of ground water where the Ring intercepts the coast; 3) water level measurements that drop as they cross the

Ring (Fig. 2), and 4) broken sand bars at the two intersections of the Ring with the coast (Marín, 1990; Marín et al., in review; Perry et al., 1995).

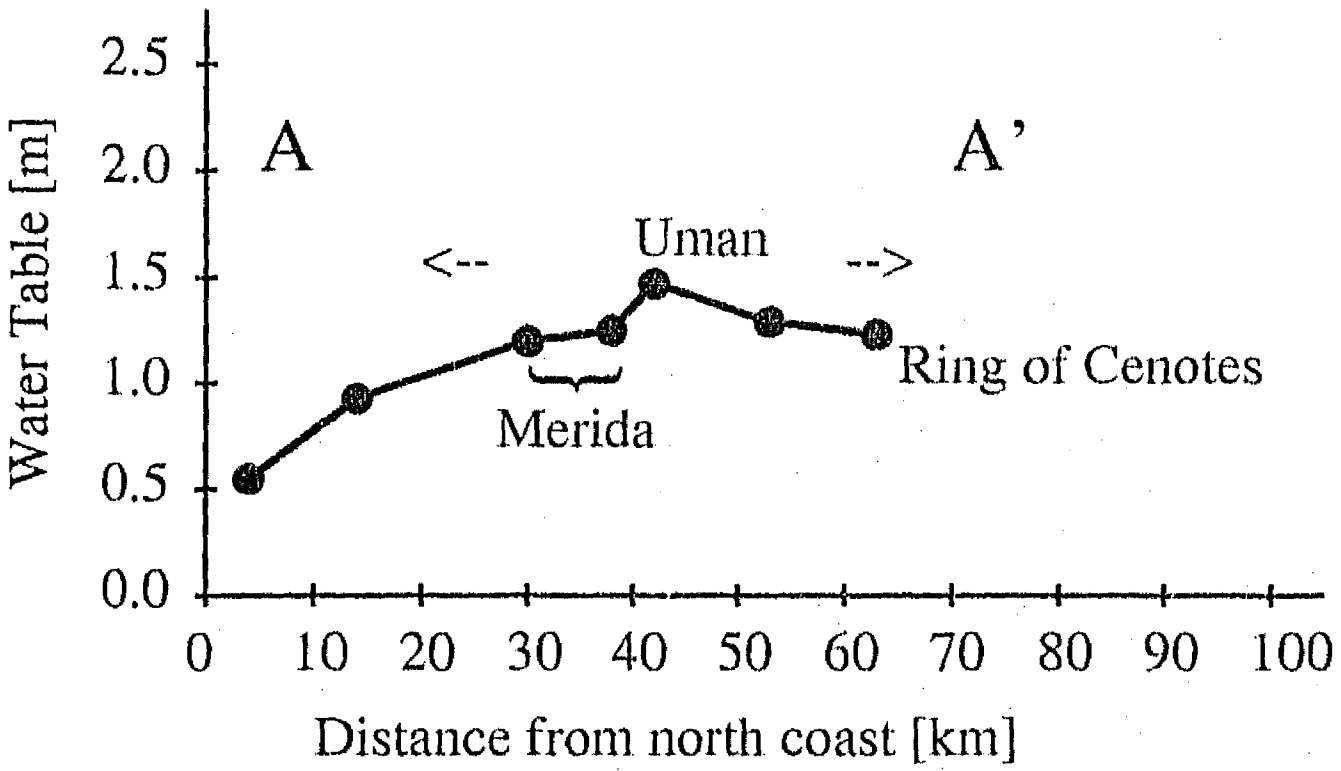

Fig. 2 Cross-section of the north-south profile on the line A-A' (Fig.1). Arrows show ground water flow direction.

Objectives

The objectives of this study were: 1) to determine whether the Ring of Cenotes is a high permeability zone; 2) to use electrical surveys to determine major directions of permeability anisotropy in the Yucatan karst aquifer; 3) to determine the depth of the ground water lens along two profiles parallel and perpendicular to the Ring of Cenotes.

Methodology

Twelve electrical measurements were conducted in June 1993 using two different types of arrays: eight Schlumberger soundings at several locations are shown in Figure 1 marked as S1 to S8. Spacings $AB/2$ ranged between 160 m to 290 m; four Wenner anisotropy measurements are shown as A1 to A4, having spacings of $a = 10$ m (A1), $a = 14$ m (A2) and $a = 20$ m (A3, A4). All measurements were made with an ABEM Terrameter 300B. The field data were interpreted using a FORTRAN code written by the senior author, based on digital linear filter theory as described in Koefoed (1979).

Results and discussion

1. Permeability characteristics of the Ring of Cenotes

The rocks in the upper hundred meters consist of karstic limestone. In such a medium electrical conductivity takes place through water-filled voids. In general, horizontal changes of the resistivity magnitude is a function of interconnected void volume and thus of permeability (Milanović, 1981). The presence of clay lenses can be considered as an exception to this rule. Clay lenses can be present in karstic limestones as infilling material of dissolution cavities (Jennings, 1985). Clay was observed in cores of various wells drilled in the Peninsula of Yucatan (Marín, 1994).

Vertical changes in resistivity can be caused by both phenomena mentioned above as well as a function of salinity of the ground water (Milanović, 1981).

Marin (1990) and Marin et al. (in review) suggested that the Ring of Cenotes is a zone of high permeability. Their results are based on hydrogeological data. Studying the superficial evidence, it can be observed (anonymous, 1984), that cenote-density is highest along a circular line, the Ring of Cenotes, and it decreases rapidly with distance from this zone (Fig. 1).

A local scale study shows, however, that the cenote-density varies also along the Ring

of Cenotes. Electrical soundings can help to determine whether the variations of cenote density is related to variations in subsurface permeability.
In order to investigate the hypothesis concerning the high permeability zone, several Schlumberger soundings were made to observe variations of the resistivity in a zone containing the Ring of Cenotes.

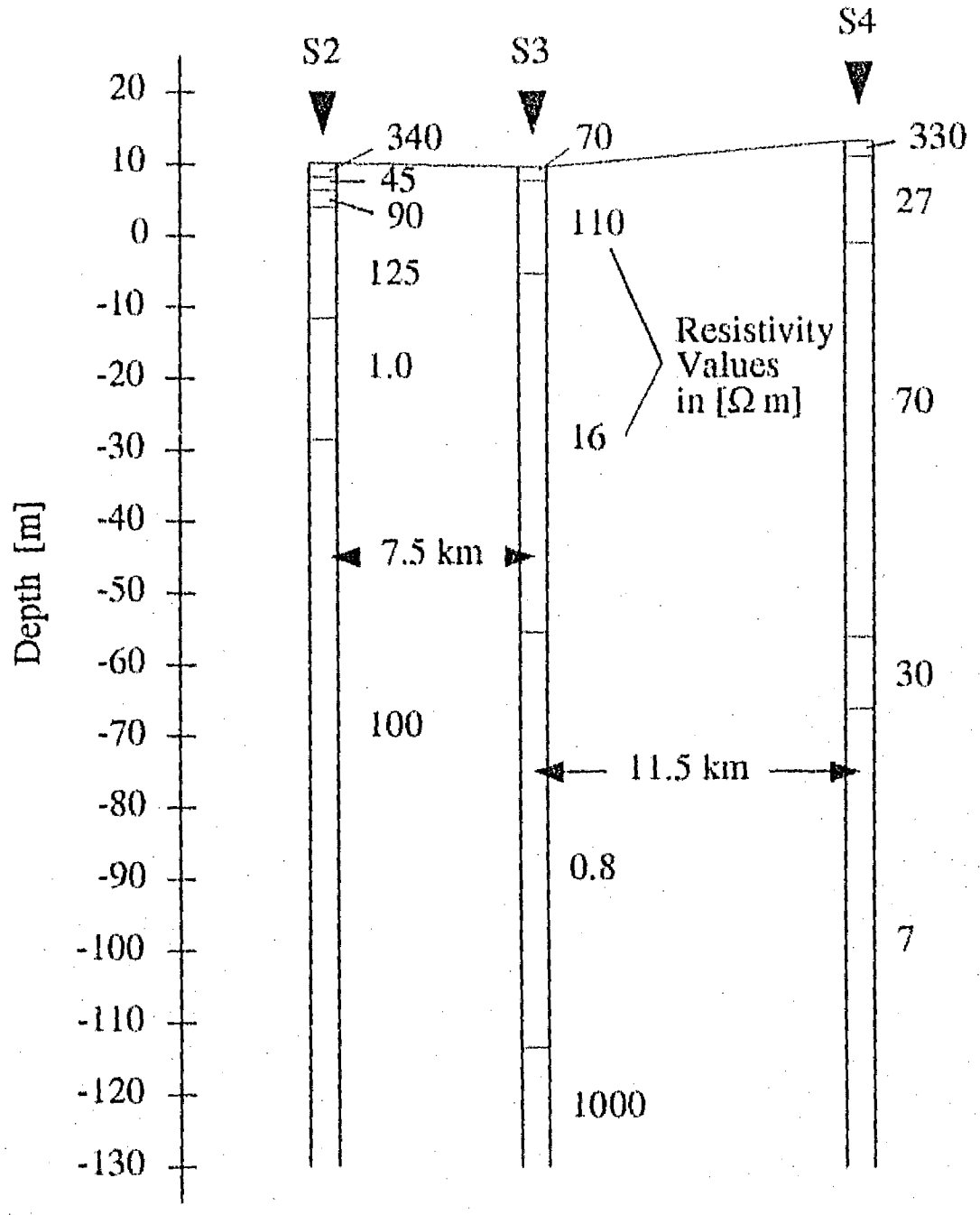

Fig. 3 Lateral resistivity changes perpendicular to the Ring of Cenotes.

Figure 3 compares the interpreted models of three Schlumberger soundings realized at three different sites on a line perpendicular to the Ring. S3 is a site on the Ring where cenote density is high. S4 is a profile approximately 12 km south of the Ring, i.e. outside of the Ring, and S2 was conducted inside the Ring, about 8 km to the north (Fig. 1).

For S3, the best-fit model indicates that there is an increasing resistivity trend in the upper 15 meters with a maximum value of 110 Ωm. Underneath, a resistivity change to the relatively low value of 16 Ωm was observed. These resistivity values are in the range of rocks satured with fresh water, however, the lower the value, the higher the permeability. This indicates a thick, high permeability layer ranging from -5 m to -55 m. Another sudden resistivity decrease can be observed at a depth of -55 m which is interpreted to be the fresh/salt water interface.

The sounding S4, located south of the Ring, also shows fresh water typical resistivity values down to a depth of -68 m, being in the range from 27 Ωm to 70 Ωm. In the depth interval from -5 m to -55 m, where the model of S3 has its high permeability layer, the model S4 has a higher resistivity than S3.

This implies that the permeability decreases from the Ring to the south to it.

The sounding S2, located north of the Ring shows a low-resistivity layer with 1.0 Ωm from -12 m to -30 m. Additional information (water level measurements and application of the Ghyben-Herzberg formula) predicts an interface depth of approximately -65 m (compare with Fig. 8) thus we believe that this low-resistivity layer is a clay lens. Apart from this postulated clay lens, resistivity values of the S2 profile are higher than those of the S3 model, which again indicates decreasing permeability moving away from the Ring of Cenotes.

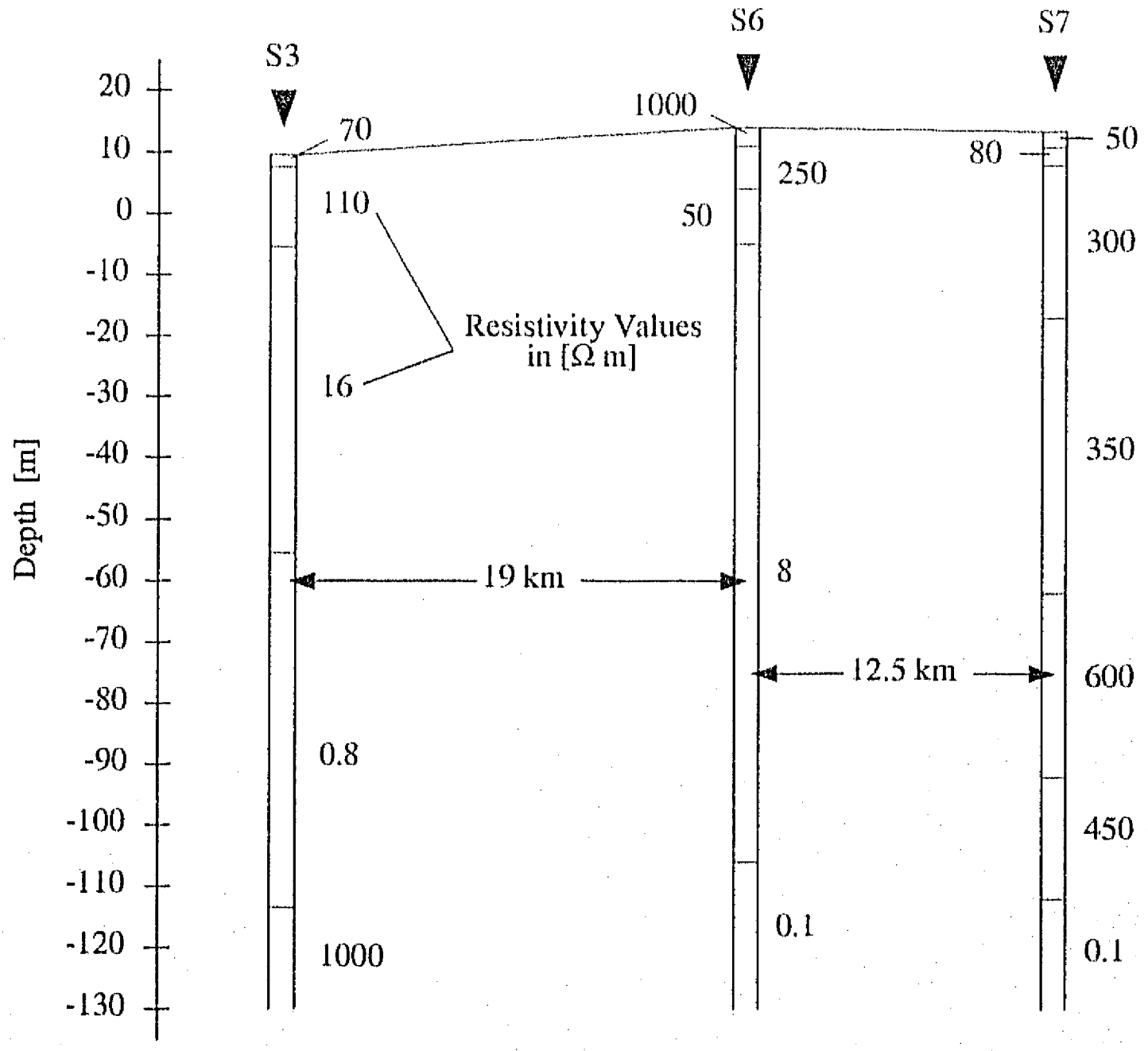

Fig. 4 Lateral resistivity changes in the Ring of Cenotes.

Figure 4 compares the models of three soundings, all conducted in the Ring of Cenotes. S3, described above, and S6 lie in a zone of high cenote density, S7 in a region where there are only very few cenotes reported (Fig. 1).

Interpreted models show important resistivity changes along the Ring. S6 has resistivity values in the range of 8 Ωm to 50 Ωm in almost the whole column above the salt/fresh water interface, with the exception of two high resistivity layers near the

surface.

In a wide depth range, resistivity values are therefore comparable to those of S3. S7, however, shows high resistivities in the major part of the column with values ranging from 300 Ωm to 450 Ωm.

In terms of permeability that means that the permeability at S7 is significantly lower than that at S3 and S6. The high permeability layer present at S3 and S4, disappears at S7. This absence of high permeability occurs in a zone of low cenote-density which supports the hypothesis of the narrow relationship between the cenote-density and the permeability.

Summarizing the results it can be seen, that in the studied area, the Ring of Cenotes is a high permeability zone with respect to its surroundings only on a selected segment. The above discussion leads to the conclusion, that the medium is highly permeable in the subsurface only where the surface cenote density is also high. It can therefore be concluded that the high permeability zone, postulated by Marín (1990) is not continuous along the whole Ring of Cenotes.

2. Permeability anisotropy

2.1 Theoretical model

Ground water flow in a karst medium takes place mainly through dissolution voids such as fractures, channels and caverns rather than through the matrix (Gordon, 1986). The Ring of Cenotes is an alignment of fractures and voids due to increased dissolution and collapse of the limestone (Pope et al., 1991). Such a medium can be described by the theoretical model shown in Figure 5.

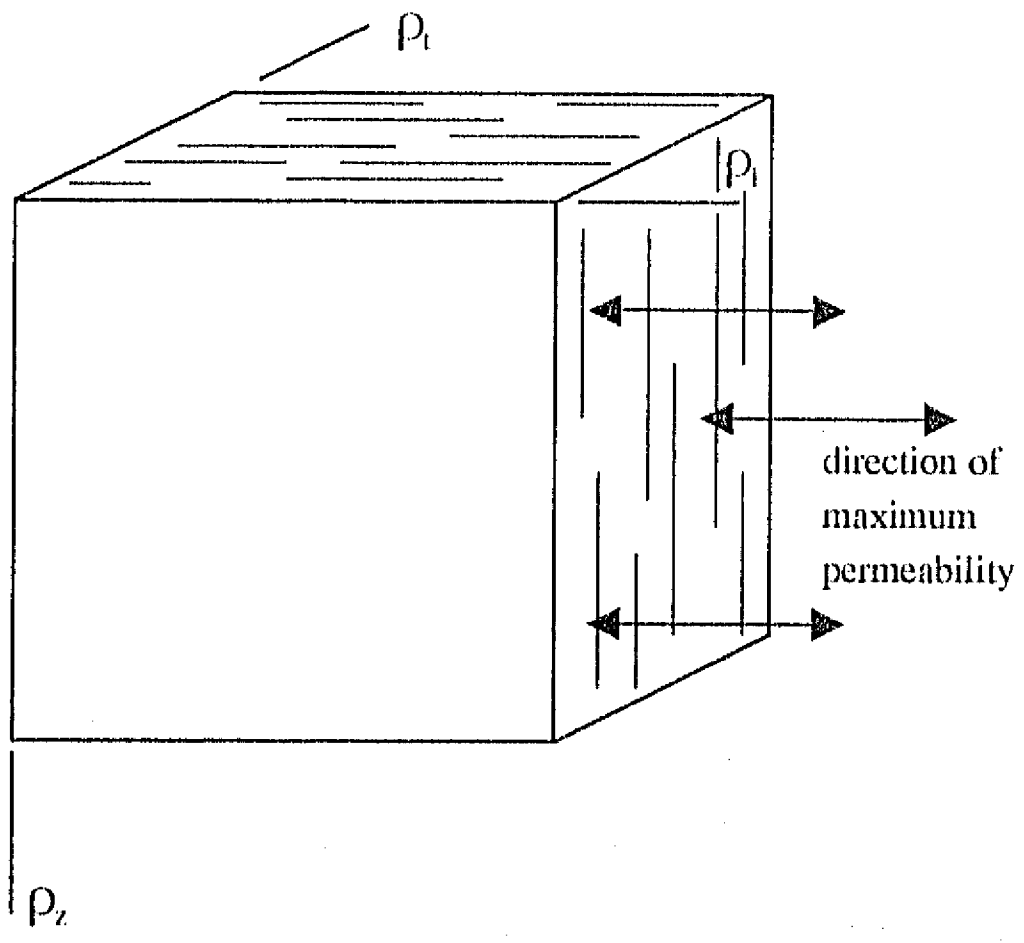

Fig. 5 Theoretical model of the electrically anisotropic medium.

A fractured medium is electrically anisotropic (Ritzi and Andolsek, 1992), i. e. resistivities in any of the three orthogonal directions can be different from the other two. Resistivity measurements made above such a medium would record the apparent resistivities (i.e. Militzer and Weber, 1985):

$$\varrho_{at} = \sqrt{\varrho_t \varrho_z} \qquad \varrho_{at} = \sqrt{\varrho_t \varrho_z} \qquad \varrho_{az} = \sqrt{\varrho_t \varrho_t} \tag{1}$$

where:

ϱ_{at} : apparent resistivity in transverse direction

ϱ_{al} : apparent resistivity in longitudinal direction

ϱ_{az} : apparent resistivity in vertical direction

for the transverse t and longitudinal l directions with respect to the main fracture plane and in the vertical z direction, respectively. The apparent resistivity in one direction is then determined by the real resistivities in the other two directions (Carpenter et al., 1990). This is called the 'paradox of anisotropy' (Keller et al., 1966). In order to apply this model to Yucatan, we made the following assumptions based on the orientation shown in Figure 5:

1. t is the direction of lowest permeability.
2. l is the direction of highest permeability.
3. Vertical resistivity changes can be due to variations in permeability or in water quality.

Furthermore it can be assumed from Pope et al. (1991) that the inclination of the fractures is predominantly vertical. This was confirmed by cores of various wells drilled in the studied area (Marín, 1994). So the direction of the ϱ_z-axes can be assumed to be within the fracture planes. Considering the three points, the theoretical model would have the following characteristics, where the terms where defined in Figure 5 and equation (1).

$$\varrho_t < \varrho_l, \varrho_z \tag{2}$$

hence:

$$\begin{aligned} \varrho_{at} = \sqrt{\varrho_l \varrho_z} &> \varrho_{al} = \sqrt{\varrho_t \varrho_z} \\ \varrho_{az} = \sqrt{\varrho_t \varrho_l} &> \varrho_{al} = \sqrt{\varrho_t \varrho_z} \end{aligned} \tag{3}$$

The two apparent resistivities that are measured in a Wenner anisotropy survey are ϱ_{at} and ϱ_{al}. It follows from equation (3) that the direction of maximum permeability is marked by the direction of the maximum apparent resistivity measured.
A parameter to quantify anisotropy is defined by:

$$\lambda = \sqrt{\frac{\varrho_t}{\varrho_l}} \tag{4}$$

2.2 Wenner anisotropy measurements

In order to investigate the anisotropic characteristics of the aquifer, four Wenner anisotropic measurements were made in the western section of the study area. Following the theoretical model for the medium, the form of the data curve as a function of the direction is related to the hydraulic characteristics. Based on the discussion in section (2.1), real resistivity is highest in the t-direction and lowest in the l-direction. However, the anisotropy paradox states that the highest apparent resistivity is measured in the l-direction and the lowest apparent resistivity in the t-direction. Low real resistivity is related to high density of interconnected fractures and therefore to the direction of highest permeability.
The data curve of a Wenner anisotropy measurement in an isotropic medium is supposed to be a circle, that of an anisotropic medium is supposed to be an elliptic type one. Figure 6 shows the original data of the four experiment sites labeled A1 to A4.

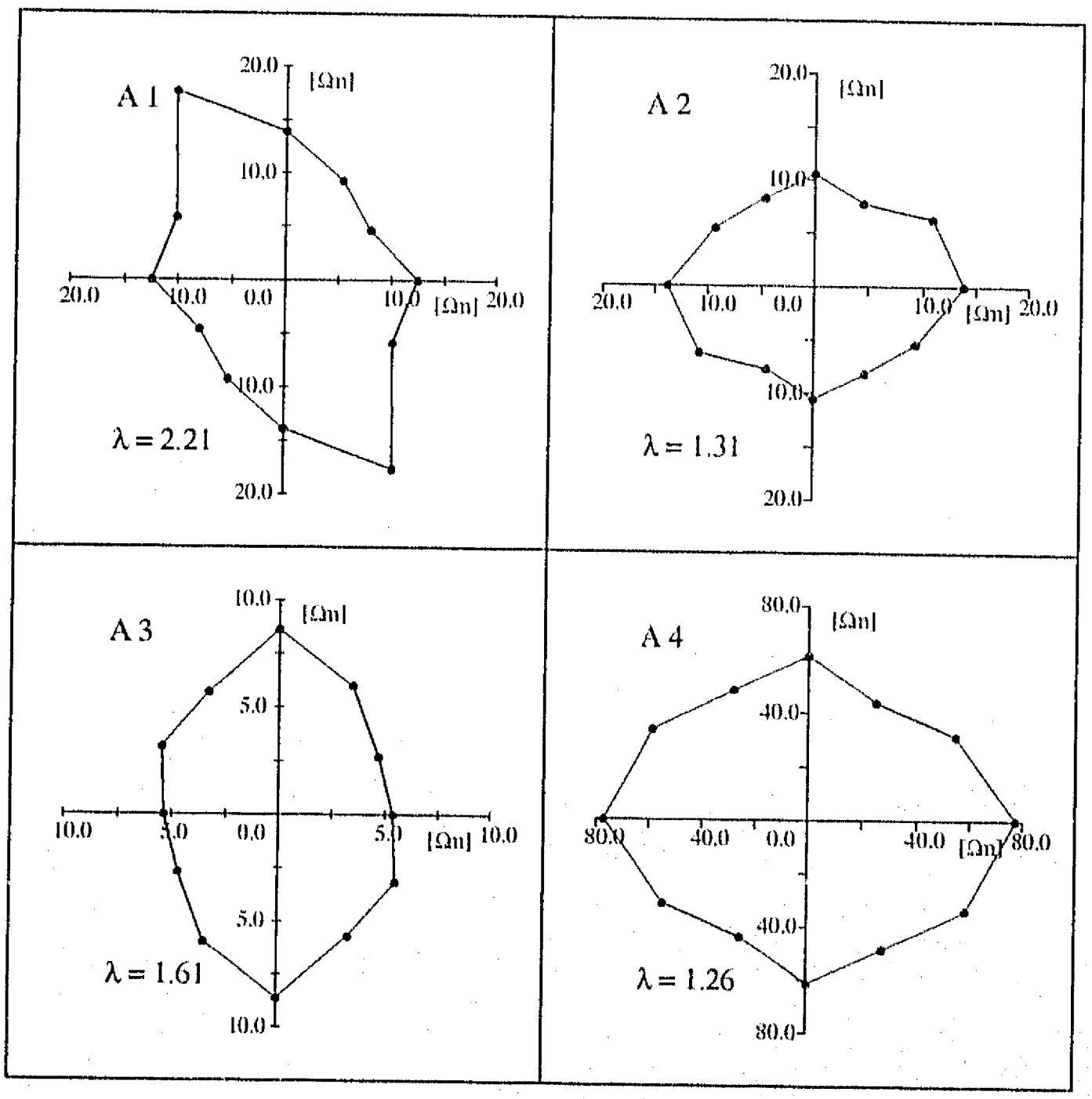

Fig. 6 Original data of four anisotropy measurements.

All anisotropy measurements realized in the western section of the study area have elliptical type data curves and therefore point to anisotropic medium. Their respective anisotropy coefficients are 2.21 (A1), 1.31 (A2), 1.61 (A3), and 1.26 (A4). Figure 7 shows interpreted maximum permeability directions.

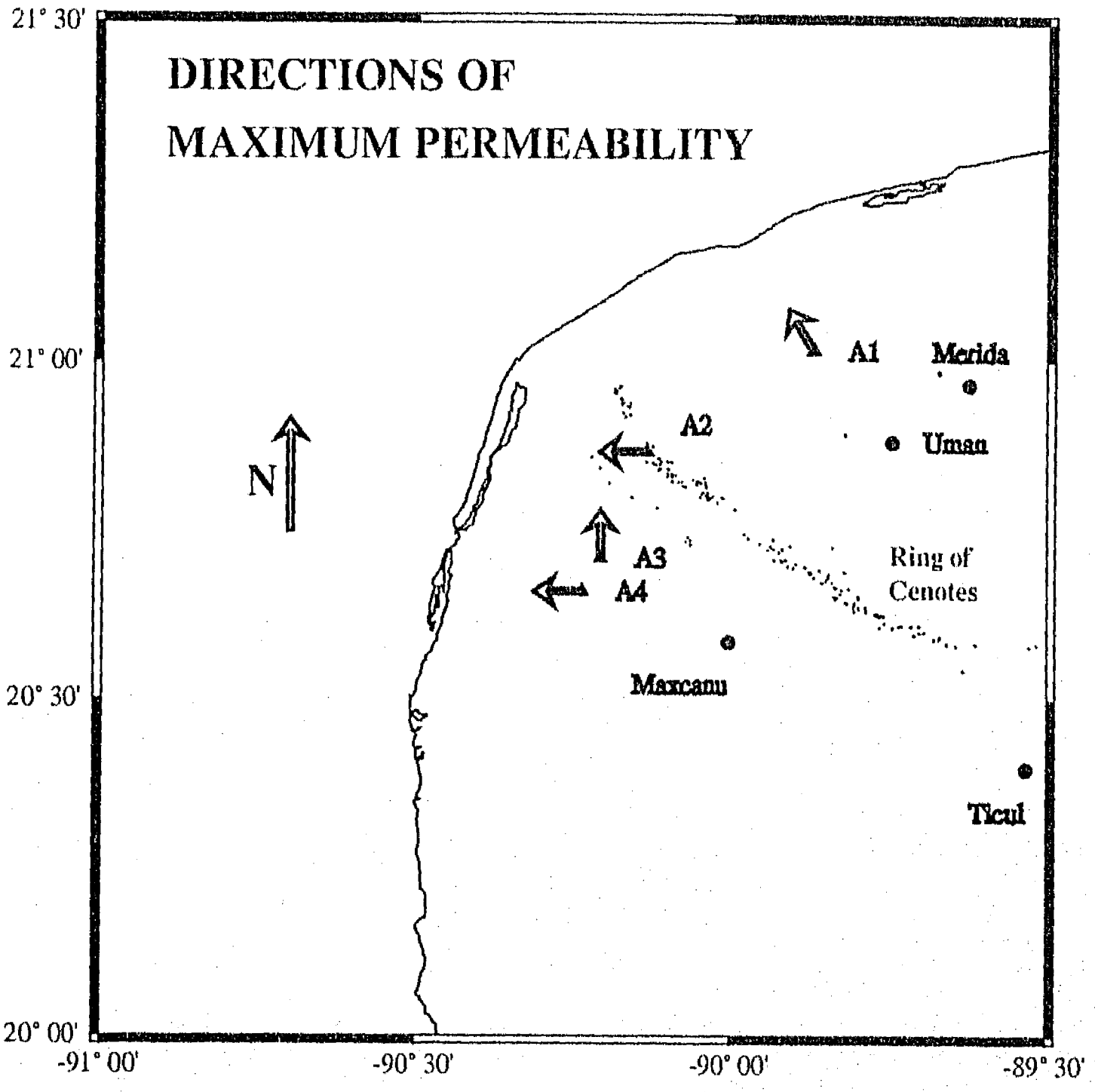

Fig. 7 Interpreted directions of maximum permeability using the anisotropic measurements.

Permeability anisotropy is most pronounced at the (A1)-site. The direction of maximum permeability coincides in this case with the shortest direction to the coast as is the case for the (A4) site. (A1) and (A4) are located relatively far from the Ring of Cenotes. Based on Figure 2 and on results from Marín (1990) we know that at the (A1)-site the aquifer discharge is towards the coast. In this case the interpreted

direction of maximum permeability coincides with the discharge direction. The same conclusion may be true also for the (A4)-site, however, there are no aquifer data available for this region.

Direction of maximum permeability at (A2) is oblique to the Ring of Cenotes. Figure 7 shows that the (A2) is a transition location between zones of high and low cenote densities. We know from the discussion in section 1 that the high permeability Ring of Cenotes is interrupted at some places. Change in cenote density implies that the (A2)-site is another example for this. We think that the observed direction of maximum permeability at this site may be that of a system of fractures orientated obliquely to the Ring direction. Dissolution could have been acting along this fracture system and resulting in the abrupt cutoff of the high permeability zone that extends southeast of (A2). In the same area the Ring of Cenotes is composed of two arcs, 8 *km* apart (Perry et al., 1995), (Fig. 7). The direction of maximum permeability of (A3) is oriented towards the second arc. We think that (A2) and (A3) may be the manifestation of a local fracture system responsible for the interruption of the mayor arc of the Ring of Cenotes and related with the formation of the second arc segment reported by Perry et al. (1995).

2.3 Depth of anisotropy

Electrical anisotropy can also be observed in an experiment composed of two Schlumberger soundings that have the same center point, but are orientated perpendicular to each other.

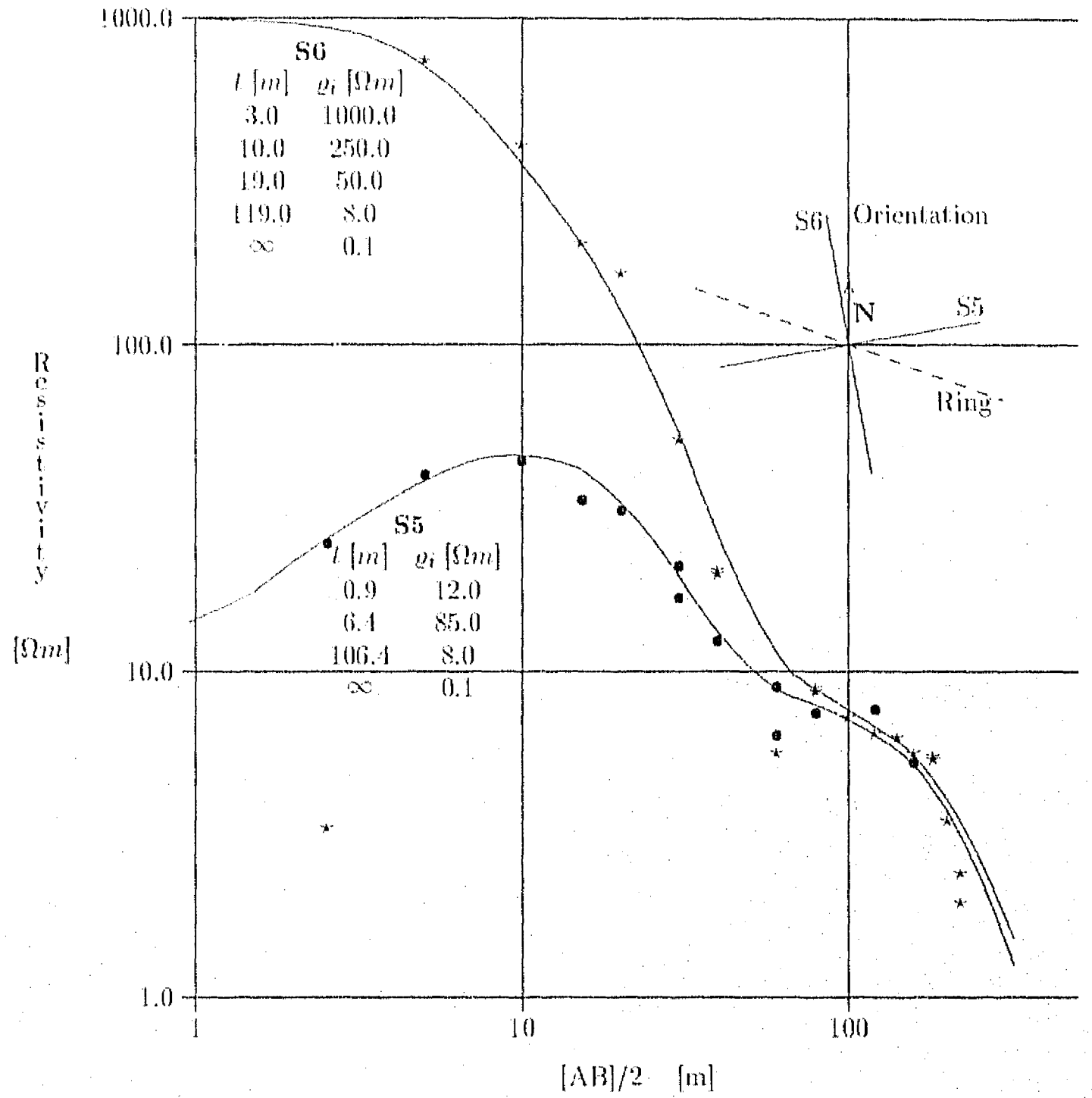

Fig. 8 Original data points and interpreted models of two soundings perpendicular to each other, S5 and S6.

Figure 8 shows the field data and the model curves of two perpendicular soundings, labeled S5 and S6. Both curves show significant differences of apparent resistivities for $AB/2$ -spacings up to 40 m. This discrepancy can be explained assuming a permeability anisotropic medium as discussed in section 2.1.

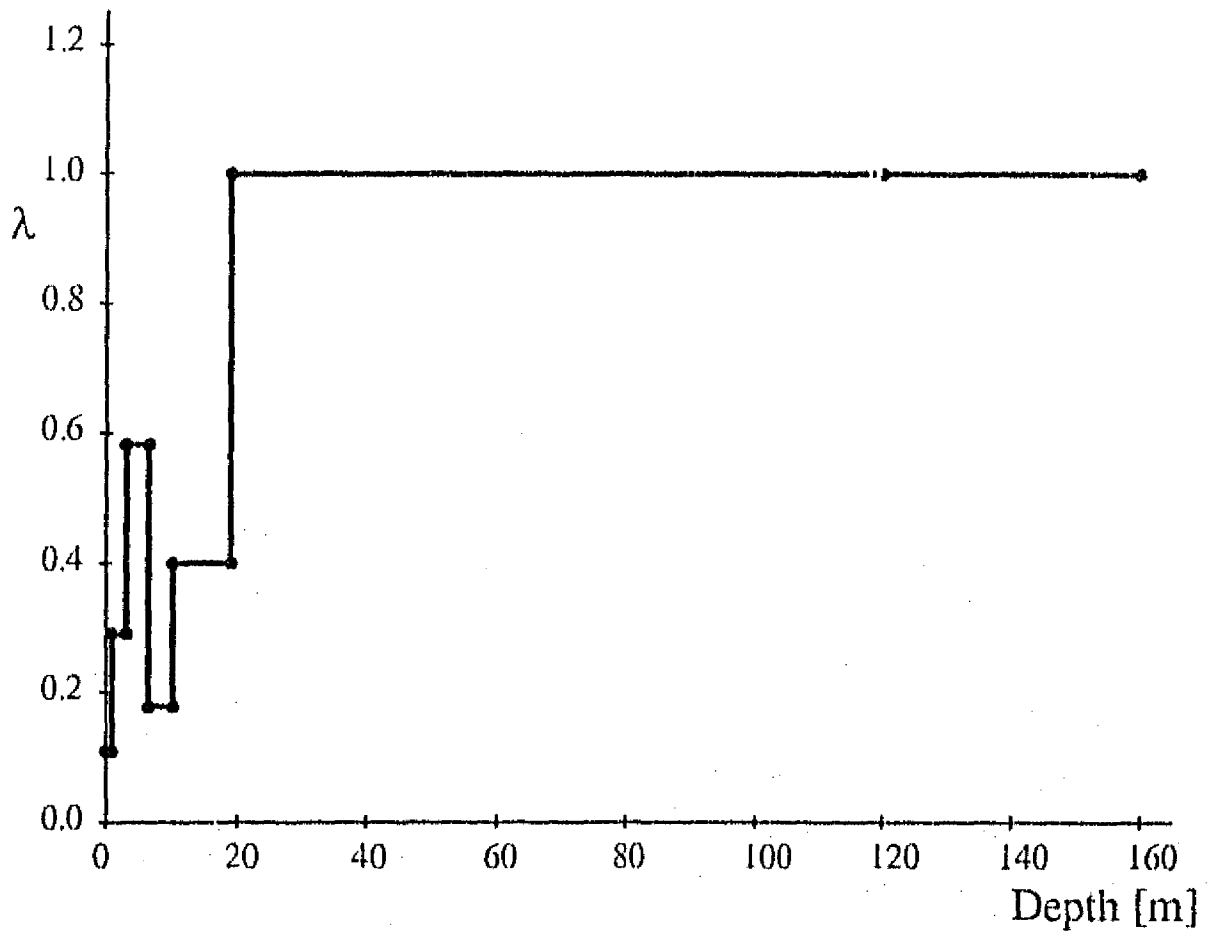

Fig. 9 Anisotropic coefficient λ for the models of Fig. 8.

Figure 9 shows the values of the anisotropy coefficient λ, calculated with the resistivity values of the two models of S5 and S6. Permeability anisotropy can be assumed at this site for the upper 19 m of the subsurface medium.

3. Depth of the fresh/salt water interface

Electrical soundings were used to estimate the depth of the fresh/salt water interface. Two profiles were studied, one in a north-south direction that is perpendicular to the north coast of the Peninsula and perpendicular to the southwestern part of the Ring of Cenotes (Fig. 10). The second profile lies in a west-east direction and is parallel to the southwestern part of the Ring of Cenotes (Fig. 11). The profiles cross at point

S3 at the Ring of Cenotes (Fig. 1).

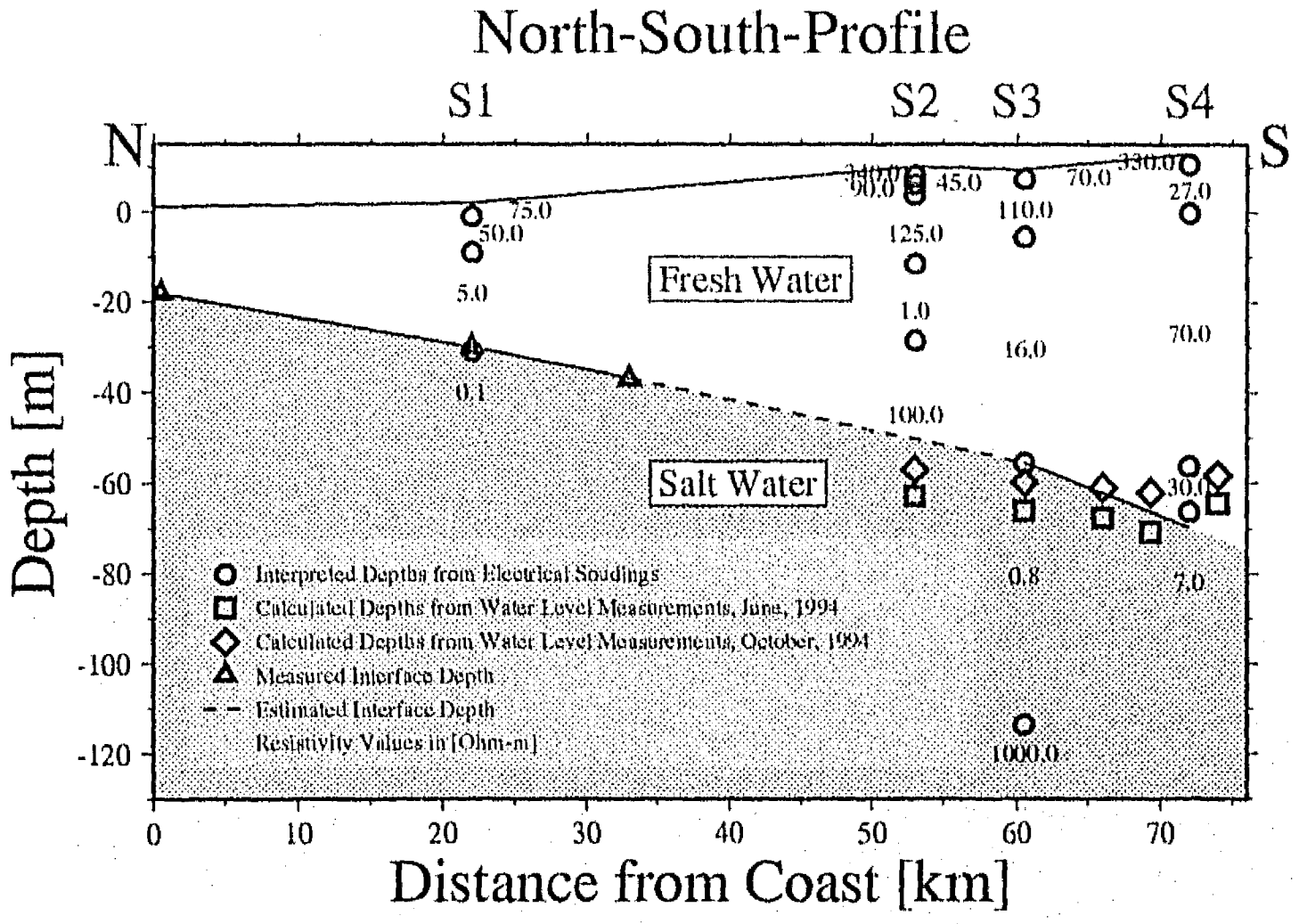

Fig. 10 Interpreted fresh/salt water interface on the North-South-Profile.

Interpreted interface depths from electrical soundings are plotted together with available measured and calculated interface depths. The measured interface depths are taken from Marín et al. (1990) and Marin et al. (in review). Interface depths were calculated with the Ghyben-Herzberg Formula from two sets of water level measurements realized in June and October 1994. Variations of water levels resulted in a variation of calculated interface depth of approximately 10 m.

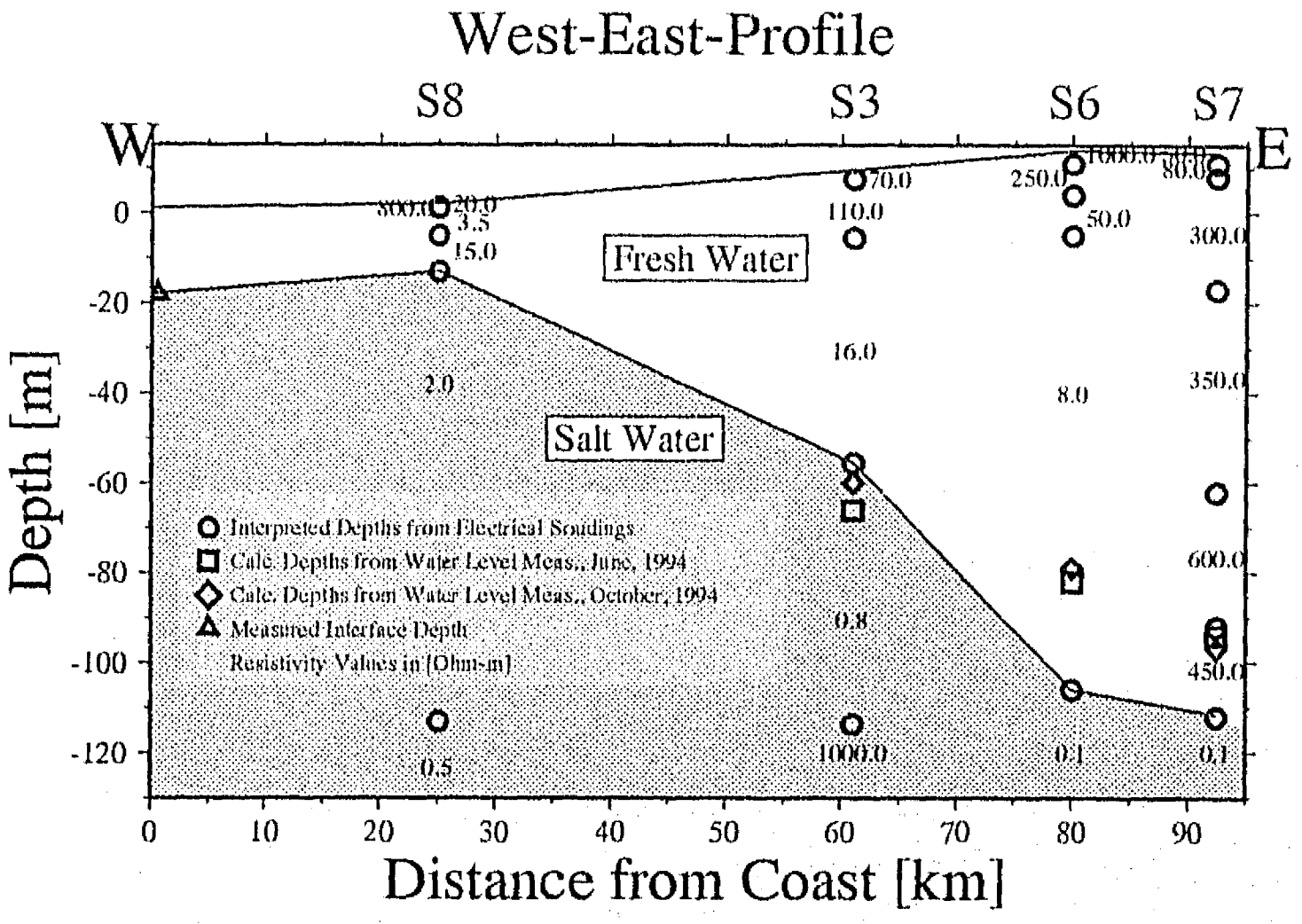

Fig. 11 Interpreted fresh/salt water interface on the West-East-Profile.

Moore et al. (1992) showed that the discrepancy between measured interface depth and the one calculated by the Ghyben-Herzberg Formula can be important in coastal regions. This was attributed to the fast salt water flow contradicting the 'static-sea-water-condition' for the Ghyben-Herzberg model.

Nevertheless, we calculated the interface depths with the Ghyben-Herzberg formula, assuming its validity in our case due to the distance of the studied region from the coast. We also assume that the interface is sharp. This is supported by results from Moore et al. (1992), Marín (1990) and Marín et al. (in review). Results are summarized in Figures 10 and 11, showing depth values in the north-south profile and in the west-east profile, respectively.

Interface depth could be interpreted from the electrical data in all but one point in the

north-south profile at 55 *km* from the coast. At this site (S2) a low resistivity layer is found between a 12 meters and 29 meters below the surface. Due to the interference of the low resistivity layer, it was not possible to predict where the fresh/salt water interface is. Taking into account the interface depth variations due to the water level changes and considering an interval of ± 5 *m* for the determination of the interface depth from the electrical measurements, results of calculated and interpreted depths can be considered consistent for nearly all sites. However, this is not the case for the sites S6 and S7 (Fig. 11). Differences between calculated and interpreted depths are as high as 25 *m*.

In an electrically anisotropic medium depths are overestimated if anisotropy is due to horizontal layering (Koefoed, 1979). In this case, layering could stand for variations of permeability in the vertical direction. For both soundings (S6 and S7), an average coefficient of anisotropy on the order of 1.2 can explain the high difference between the calculated and interpreted interface depths.

The results suggest that the salt water intrusion penetrates more than 70 *km* inland and perhaps as much as 90 *km*. On both profiles the interface shows a clear trend of increasing depth with distance from the coast resulting in a ground water lens thickness of about 15 meters near the coast up to 110 meters 90 *km* inland. A question presently being addressed is whether the salt water predicted to be found in this area is marine in origin or whether it is a result of dissolution of evaporites as Perry et al. (1995) have suggested.

Conclusions

The interpretation of eight Schlumberger electrical surveys realized in northwestern Yucatan have shown that the Ring of Cenotes is a high permeability zone on selected segments, characterized at the surface by a high density of cenotes. It was also shown that there are significant resistivity changes along the Ring which supports the conclusion that the highly permeable Ring is not continuous. The places of

discontinuity can be related to the discontinuity of cenote density.

Wenner anisotropy surveys have shown that the upper part of the Yucatan Aquifer can be described as an electrically anisotropic medium. The anisotropic characteristics may be due to preferential permeability directions. The Wenner surveys were used to determine directions of maximum permeability at four sites. Schlumberger soundings perpendicular to each other had differing apparent resistivity values. The interpretation of this data required an anisotropic model for the first 19 m.

Finally, the depth of the fresh/salt water interface was be determined along two profiles perpendicular and parallel to the Ring of Cenotes. The interface was detected with electrical soundings up to 90 km from the coast and compared with calculated and measured interface depths. Depth of fresh water lens varied in the study area from 18 meters near the coast to 110 meters in the southeastern part of this area.

Acknowledgments

B. Steinich thanks the Deutschen Akademischen Austausch Dienst (DAAD) and the Secretaría de Relaciones Exteriores of Mexico for financial support. Field work was funded by Consejo Nacional de Ciencia y Tecnología (grant no. 9302-T2057) and Dirección General de Asuntos del Personal Académico of the Mexican National University (grant no. IN106891). We thank P. Carpenter from Northern Illinois University for lending the geoelectric equipment and S. Tulaczyk and E. C. Perry for participation in field work and for important discussions.

References

anonymous, 1984. Cartas Topográficas de Yucatán 1:50 000. *Instituto Nacional de Estadística, Geografía e Informática, Mérida, Yucatán.*

Carpenter, P.J., Kaufmann, R.S. and Price, B. 1990. Use of Resistivity Soundings to Determine Landfill Structure. *Ground Water. v. 28. no. 4. pp.*

560-575

Gordon, M.J. 1986. Dependence of Effective Porosity on Fracture Continuity in Fractured Media. *Ground Water, v. 24, no. 4, pp. 446-452*

Hildebrand, A.R., Penfield, G.T., Kring, D.A., Pilkington, M., Camargo, A., Jacobsen, S.B., and Boynton, W.V. 1991. Chicxulub Crater: A possible Cretaceous/Tertiary boundary impact crater on the Yucatán Peninsula, Mexico. *Geology, no. 19, pp. 867-871*

Keller, G.V. and Frischknecht, F.C. 1966. Electrical Methods in Geophysical Prospecting. *Pergamon Press. New York. 519 pp.*

Koefoed, O. 1979. Geosounding Principles, 1: Resistivity Sounding Measurements. *Elsevier. Amsterdam. 276 pp.*

Jennings, J. N., 1995. Karst Geomorphology. *Basil Blackwell Ltd., New York, 293 pp.*

Marín, L.E. 1990. Field Investigations and Numerical Simulation of Groundwater Flow in the Karstic Aquifer of Northwestern Yucatan, Mexico. *Ph. D. thesis. Northern Illinois University, DeKalb, Il. 183 pp.*

Marín, L.E., Perry, E.C., Pope, K.O., Duller, C.E., Booth, C.J., and Villasuso, M. 1990. Hurricane Gilbert, its Effects on the Aquifer in Northwestern Yucatan, Mexico. *International Association of Hydrogeologists, Selected Papers on Hydrogeology from the 28th International Geologic Congress, Washington, D.C. July 9-19, 1989*

Marín, L.E. 1994. Informe Final sobre las perforaciones en Yucatán. *Reporte Técnico, IGF-UNAM, 1994*

Marín, L.E., Perry, E.C., and Essaid, H.I. in review. Numerical simulation of groundwater flow in the karstic aquifer of northwestern Yucatan, Mexico. *Internal Review, USGS*

Milanović, P.T. 1981. Karst Hydrogeology. *Water Resources Publications. Littleton. Colorado. 434 pp.*

Militzer, H. und Weber, F., Ed. 1985. Angewandte Geophysik, Bd. 2.

Springer Verlag Wien/Akademie-Verlag Berlin. 371 pp.

Moore, Y.H., Stoessell, R.K., and Easley, D.H. 1992. Fresh-Water/Sea-Water Relationship Within a Ground-Water Flow System, Northern Coast of the Yucatan Peninsula. *Ground Water. v. 30. no. 3. pp. 343-350*

Perry, E.C., Swift, J., Gamboa, J., Reeve, A., Sanbonr, R., Marín, L.E., and Villasuso, M. 1989. Geological and Environmental Aspects of Surface Cementation, North Coast, Yucatan, Mexico. *Geology. v. 17. pp 818-821*

Perry, E.C., Marín, L.E., McClain, and J., Velázquez, G.; 1995. The Ring of Cenotes (sinkholes), northwest Yucatan, Mexico: its hydrogeologic characteristics and possible association with the Chicxulub Impact Crater. *Geology. v. 23. pp. 17-20*

Pope, K.O., Ocampo, C., and Duller, C.E. 1991. Mexican site for K/T impact crater?. *Nature. v. 351. p. 105*

Ritzi, R.W., Jr., and Andolsek, R.H. 1992. Relation Between Anisotropic Transmissivity and Azimuthal Resistivity Surveys in Shallow, Fractured, Carbonate Flow Systems. *Ground Water. v. 30. no. 5. pp. 774-780*

Sharpton, V.L., Dalrymple, G.B., Marín, L.E., Ryder, G., Schuraytz, B.C., and Urrutia-Fucugauchi, J. 1992. New Links Between the Chicxulub Impact Structure and the Cretaceous-Tertiary Boundary. *Nature. v. 359. pp. 819-821*

Sharpton, V.L., Burke, K., Camargo, A., Hall, S.A., Marín, L.E., Suárez, G., Quezada, J.M., Spudis, P.D., and Urrutia-Fucugauchi, J. 1993. The gravity expression of the Chicxulub multiring impact basin: size, morpholgy, and basement characteristics. *Science. v. 261. pp. 1564-1567*

Taylor, R.W., and Fleming, A.H. 1988. Characterizing Jointed Systems by Azimuthal Resistivity Surveys. *Ground Water. v. 26. no. 4. pp. 464-474*

III. Determinación de las características de flujo en el acuífero del noroeste de la Península de Yucatán, México.

Determination of flow characteristics in the Aquifer of the Northwestern Peninsula of Yucatan, Mexico

Birgit Steinich[a], Luis E. Marín[a]

[a]Instituto de Geofísica, Universidad Nacional Autónoma de México,
Cd. Universitaria, Mexico City, Mexico, C.P. 04510

Journal of Hydrology, en prensa

Abstract

Flow characteristics were studied in the Northwestern Peninsula of Yucatan, Mexico. The Yucatan aquifer is a mature karst system, influenced by the Ring of Cenotes (sinkholes). This zone of aligned sinkholes is a high permeability zone with respect to its surroundings. The aquifer is unconfined within the study area. Water level measurements at 48 locations were made in June and October of 1994. Water levels were measured up to four times in October. Water levels in a limited group of wells showed variations up to 60 % during October '94 whereas others had variations on the order of 5 % in the same period. By studying the resulting equipotential regimes, a highly variable zone (HVZ) was identified. Drain characteristics are significantly different from the rest of the study area which leads to the hypothesis that the HVZ represents an independent subsystem of interconnected fractures. In order to determine directions of high permeability within the study area, azimuthal resistivity surveys were conducted at 22 locations. Resistivity curves particularly in the HVZ show two or more peaks, each indicating a direction of high permeability. Directions of high permeability are interpreted to be preferential directions of aligned fractures.

Comparison with the two different equipotential regimes in October '94 shows that in the majority of the cases the direction of the hydraulic gradient coincides with the direction of one fracture system. The hydraulic gradient can be considered to be the major control in the dissolution process at least in the HVZ, resulting in the selective opening of the fractures. Peaks in the resistivity curves are of the same order of magnitude. This shows that both regimes of equipotential lines and the corresponding changes of the hydraulic gradients are sufficiently frequent to be able to create different fracture systems with a comparable fracture density. The variations of the equipotential regime in time may have severe consequences in terms of the risk of aquifer contamination in the highly variable zone. Contaminants, generated mainly in the City of Merida, are generally believed to flow towards the north coast of the Peninsula. However, reversals in the hydraulic gradient may allow contaminants to flow towards the southeast of the City, at least for limited periods in the year.

1. Introduction

The aquifer in the Peninsula of Yucatan consists of a mature karstic system. The upper hundreds of meters consist of almost pure Tertiary and Quaternary carbonate sequences with no major tectonic deformation (Morán Z., 1985). A review of the stratigraphic column for northwestern Yucatan is presented in Sharpton et al. (in press). There is some evidence for clay lenses (Steinich & Marín, in press; Marín, 1994), but they tend to be local in extent and therefore don't act as significant aquitards (Perry et al., 1995). When dissolved, the carbonate rocks leave almost no residue (Marín & Perry, 1994). The aquifer is unconfined, except for a narrow band parallel to the coast (Perry et al., 1989). The porosity ranges between 7% and 41% (González Herrera, 1984). All types of dissolution voids are described with sizes ranging from the order of centimeters found in several cores of wells drilled in the study area (Marín, 1994) up to caverns with diameters in the order of tens of meters. Many of the latter can be easily visited in numerous places and diving was made in

some of them (Marín & Perry, unpublished). The presence of the dissolution voids of considerable size imply that ground water flow is predominantly determined by this secondary porosity.

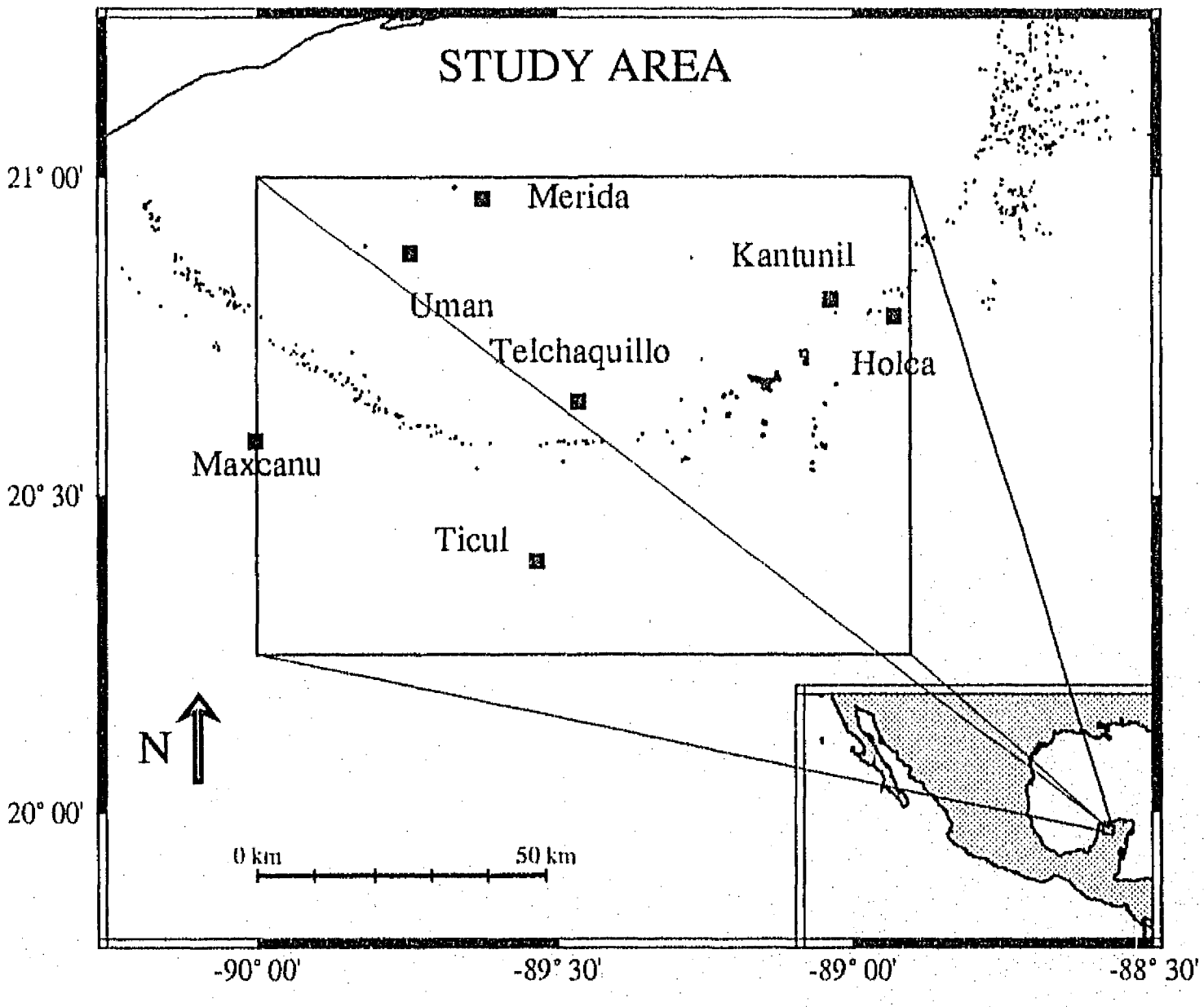

Fig. 1 Overview map showing the study area.

The aquifer is in general terms characterized by high permeabilities and a very low hydraulic gradient (Marín, 1990). The aquifer is a coastal aquifer. Tidal influences, however, could not be observed in the study area, due to its considerable distance from the coast line. These observations are supported by Reeve & Perry (1990).

The hydrogeological characteristics of the aquifer are influenced by the Ring of Cenotes. This circular alignment of sinkholes is probably related to the Chicxulub impact crater underlying the Yucatan aquifer at depths ranging from 300 to 1000 meters approximately (Perry et al., 1995). Marín (1990) has postulated that the Ring of Cenotes forms a subsurface river system, with the water draining towards it and discharging into the sea at its intersection points with the coast line. Marín (1990) suggested that the Ring represents a no flow barrier except in the southeastern segment of the Ring where ground water flow is probably crossing the Ring. Steinich & Marín (in press) found a low permeability zone in the western edge of the same segment. The region itself is characterized by a wider spacing of the sinkhole locations, which is in strong contrast to the remaining western segment of the Ring (Anonymous, 1984 and Fig.1). These circumstances indicate that the southeastern part of the Yucatan aquifer is of special interest in order to understand the influence of the Ring of Cenotes on the ground water flow regime. The fresh water is present as a thin lens having thicknesses of 15 m near the coast, 45 m at Merida, and approximately 120 m 90 km from the coast (Marín, 1990; Steinich & Marín, in press). Except for the narrow cementation band along the coast, there is no layer that protects the ground water from direct infiltration of contaminants. There is some evidence for the existence of clay lenses (Marín, 1994). Nevertheless, this clay represents only cave infilling material and can not be considered to be present as a continuous layer or to act as an aquitard (Steinich & Marín, in press). The aquifer is therefore highly vulnerable to contamination (Marín & Perry, 1994). The City of Merida is the most important concentration of population and industry in the Peninsula of Yucatan. Most of the drinking water is needed there but most of the contamination is generated there as well (Méndez R. 1993). The fresh water lens is the only source of drinking water in Peninsula so there is an urgent need for information concerning the hydrogeology of this region.

2. Objectives

The objectives of this study were: 1) to map the water table in the region south of the City of Merida; 2) to describe water table variations and their consequences for ground water movement; 3) to find the relationship between the hydraulic gradient and fracture orientation; and 4) to estimate the risk of contamination in the study area as a consequence of water table variations.

3. Methodology

Water level measurements were made in 48 wells distributed in the study area as shown by numbered small rectangles in the map of Figure 5. Observation wells are in the majority of the cases hand-driven water supply wells in villages and some water-filled caverns (cenotes in the local language). A first-order topographic survey conducted by INEGI exists for the area. Wells were tied to this network using a level and stadia. Wells were selected so that the nearest benchmark was not more than 300 m away, for most wells, however, this distance was much smaller. Elevation of the wells were determined with a maximum error of 0.2 cm. Water level was measured with respect to the leveled reference point with a maximum error of 1 cm. Water levels in 24 of the observation wells were measured in June and in October of 1994. The other 24 wells were measured only in October of 1994. In order to observe short time scale variations of the water levels, some of the wells were visited up to four times during October '94. Water level data were gridded using a $1' \times 1'$ grid and the water table surface was calculated by an interpolation algorithm as used by Wessel & Smith (1992).

Twenty-two electrical surveys were conducted within the study area. The array chosen was that of azimuthal resistivity surveys in order to determine the orientation of fractures. Azimuthal resistivity surveys are Wenner type arrays, conducted with the same center point for different angles with respect to the north direction. Within an

isotropic medium, measured resistivity is the same for all directions. The presence of fractures, however, imply anisotropy in the electrical characteristics of the rocks. Resistivity values vary as a function of the angle with respect to the north direction related to the orientation of the fractures. This makes azimuthal resistivity surveys a useful method for the determination of directions of enhanced permeability as a consequence of the presence of fracture systems (Taylor & Fleming, 1988; Steinich & Marín, in press).

For the azimuthal surveys in this study, spacings $AB/3$ equal to 20 m (eight cases), 24 m (three cases), 25 m (one case), 26 m (two cases) and 30 m (eight cases) were chosen. Electrical surveys were conducted using a Syskal RI Resistivity meter.

4. Study Area

The study area is located in the Peninsula of Yucatan, southeastern Mexico. It is composed of the region between $90^o00'$ and $88^o54'$ west, $20^o15'$ and $21^o00'$ north.

The Ring of Cenotes crosses this area from west to northeast (Fig.1). Cenote density within the Ring is variable (Steinich & Marín, in press; Perry et al., 1995; Marín et al., 1990). The ring is best developed in its western segment which is followed eastward by a zone of low cenote density. A remarkable segment is the one southwest of Kantunil, characterized by a wider spacing in cenote locations (Fig. 1).

The study area is characterized by a very heterogeneous distribution of population and industrial plants. Its major concentration is in the northwest part of the study area represented by the cities of Merida and Uman, the former being the largest City in the Peninsula and that with the best developed infrastructure. Another regional center is Ticul, located in the south. The southeastern part of the area has only small villages.

The density of observation wells varies within the study area. Namely in a zone southwest of Kantunil there are very few wells available for water level measurements due to the lack of bench marks. Azimuthal resistivity surveys were made in the whole

study area with a concentration in the zone southwest of Kantunil. This was to study in more detail this area of enhanced interest.

Results and Discussion

5. Water table maps

Based on the water table measurements in the 48 observation wells, water table maps were made for three different times , June of 1994, beginning of October (Fig. 2) and end of October of 1994 (Fig. 3). The configuration of the equipotential lines in June '94 is nearly identical to that at the end of October '94 so we omitted the June '94 map here. Figure 4a shows precipitation curves for two meteorological stations, Telchaquillo and Holca (Fig. 1). Precipitation values are monthly average values over a period of 32 years (Telchaquillo) and 12 years (Holca) (Anonymous, 1994). The rainy season in the study area is from June to September, with the highest precipitation in September. The water table of June corresponds therefore to the period at the beginning of the rainy season, the water table maps of October represent two water table configurations in the transition period from the rainy to the dry season. This transition period is characterized by a lower monthly precipitation (Fig. 4a) as well as by a decrease of the number of rainy days in a month (Fig. 4b). At the climatological station of Holca, only seven days with precipitation where observed in October of 1994, and 60 % of the total monthly precipitation was registered on only one day (October 14th.).

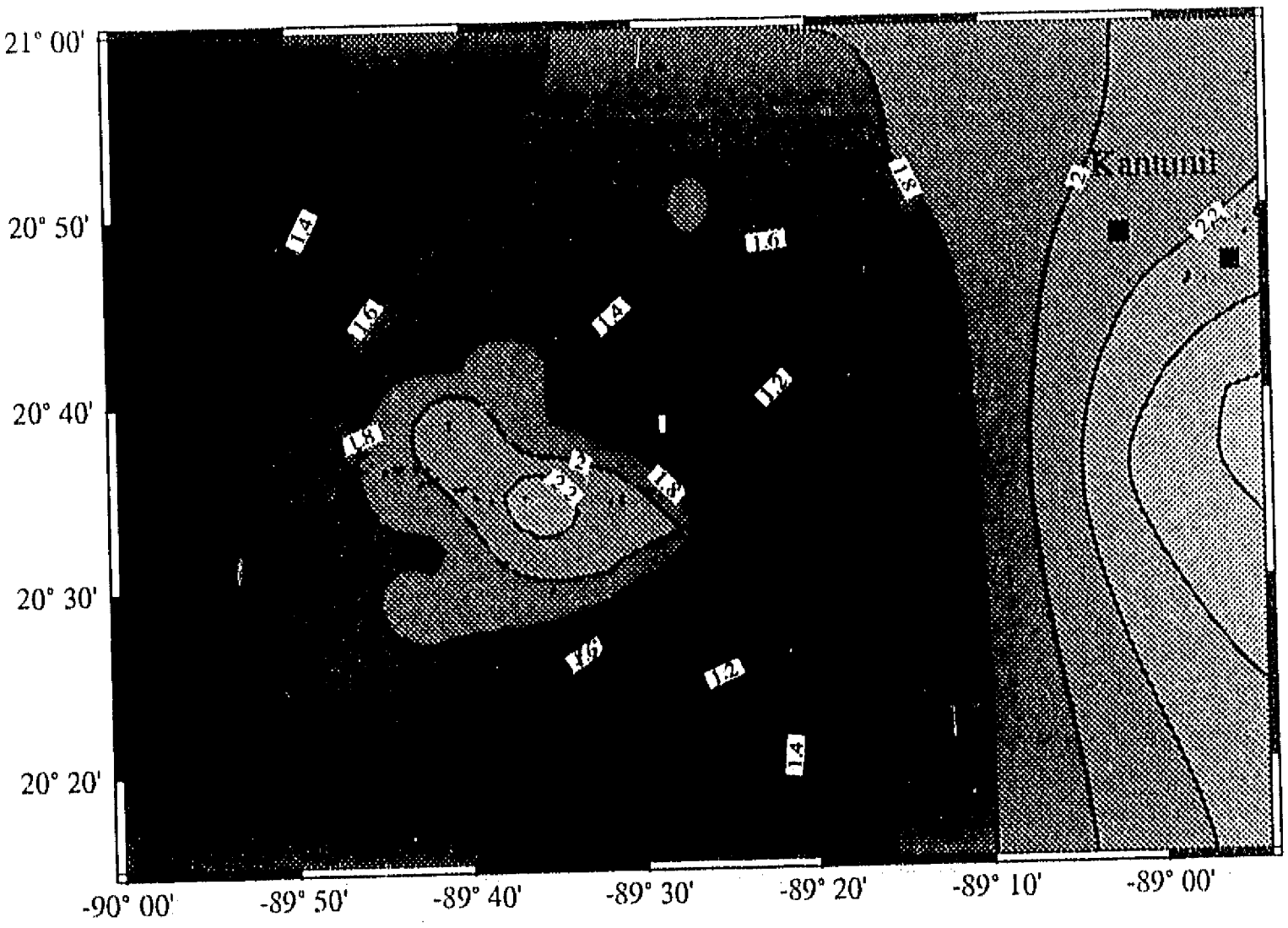

Fig. 2 Equipotential lines at the beginning of October '94, i.e. during the low water level period in meters above mean sea level.

In spite of the significant variations of the water levels that will be discussed later, the three water table configurations show some similarities. In the center left part of the study area there is a remarkable head maximum. This high coincides in space with a zone of low cenote density (Fig. 1). Study of precipitation and evaporation data show no indication for an increased recharge to the aquifer in this zone. However, former investigations using electrical resistivity surveys showed that this is a zone of relatively low permeability (Steinich & Marín, in press). This may account for the head maximum in this zone. In the western part of the study area, equipotential lines

are perpendicular to the Ring of Cenotes which implies that there is no ground water flow crossing the Ring, as predicted by Marín (1990). Discharge direction in this zone is towards the west coast of the Peninsula (Fig. 1).

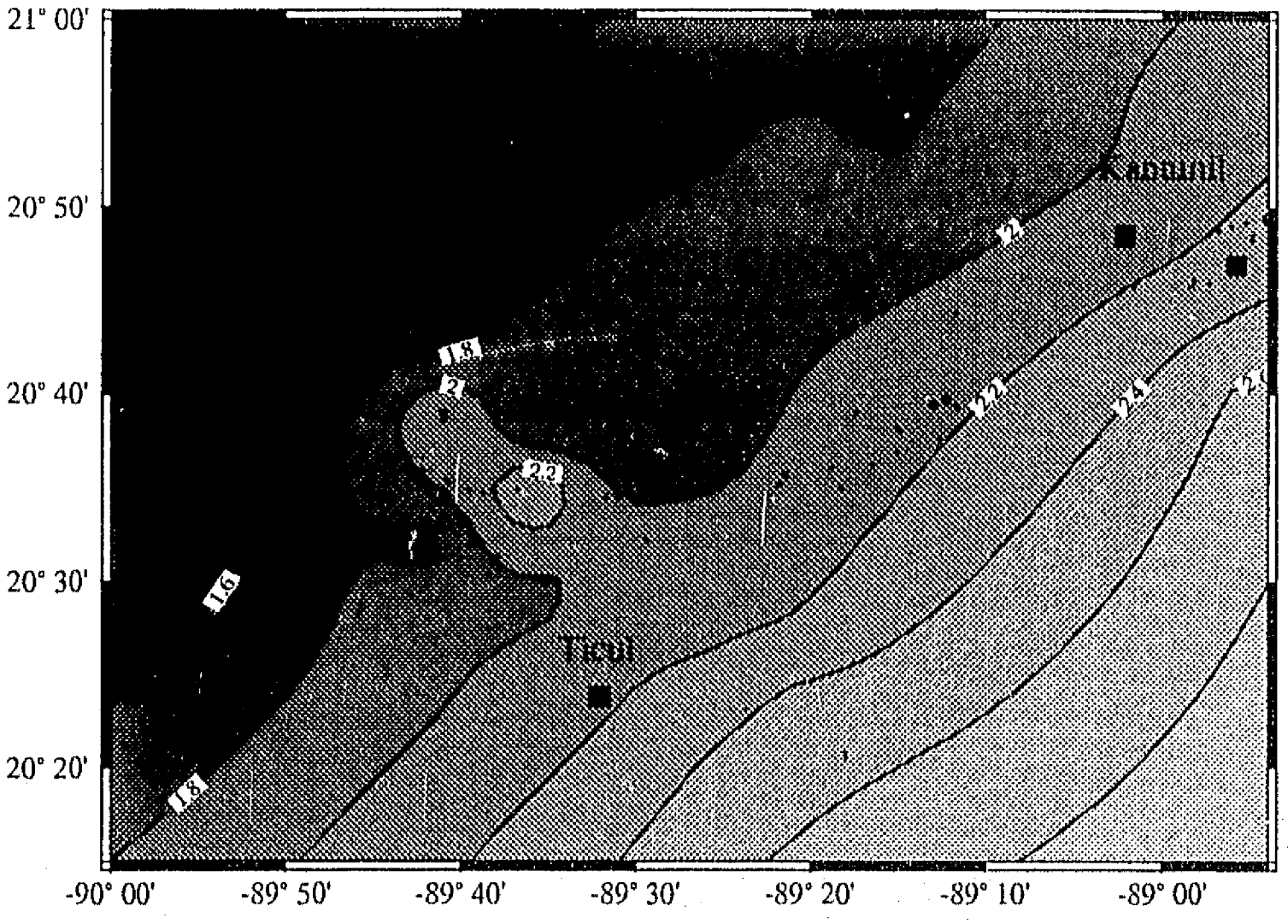

Fig. 3 Equipotential lines at the end of October '94, i.e. after recuperation to the high water levels in meters above mean sea level.

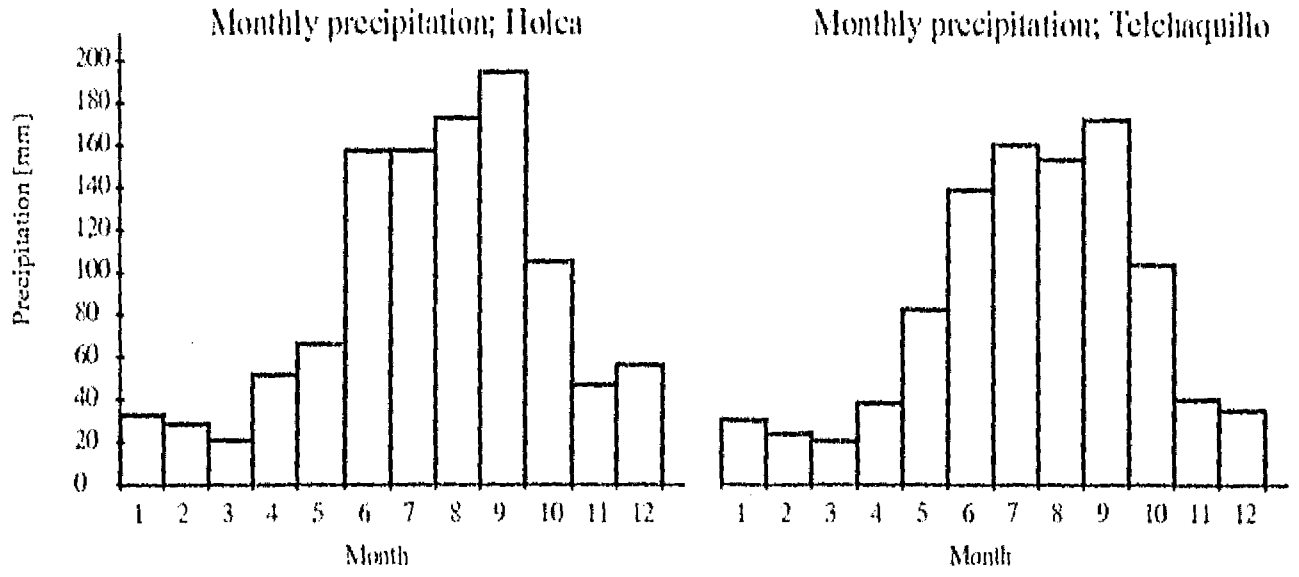

Fig. 4a Average monthly precipitation at climatological stations at Telchaquillo and Holca. Averages are taken over 32 years and 12 years, respectively.

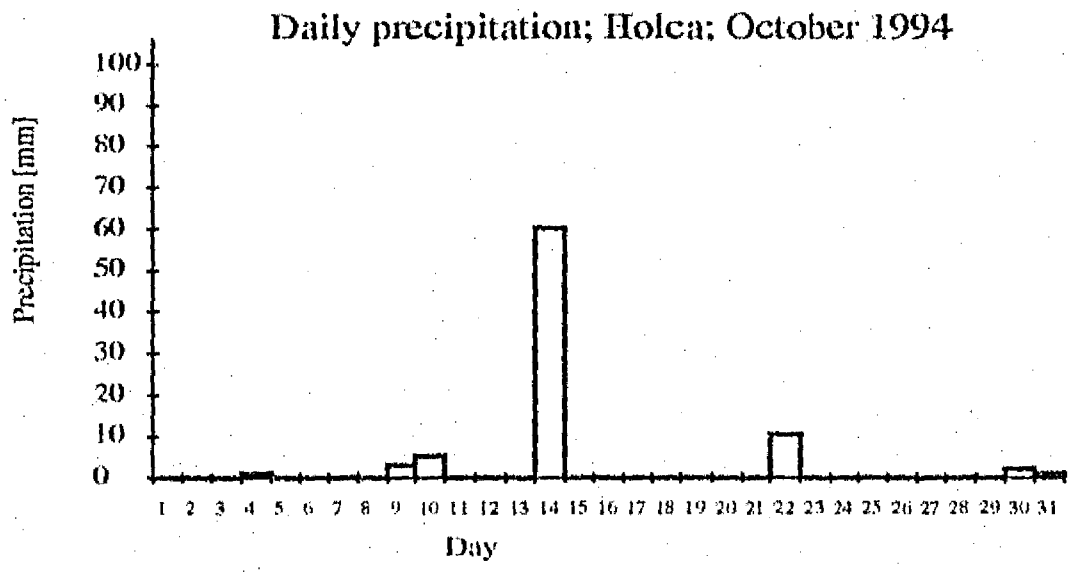

Fig. 4b Daily precipitation at the climatological station Holca for October of 1994.

6. Water table variations

During the observation period significant water level variations occured in some wells. Table 1 shows some examples of the water levels measured in different wells at different times. With respect to measurements in June '94, water levels were low in the period of October 9th to 11th and returned to values similar to those of June '94 after October 19th.

Water level at different times in meters above sea level

	Jun.94	10-09-94	10-10-94	10-11-94	10-19-94	10-20-94
well 14	2.19	1.97			2.01	
well 11	2.35	2.42			2.30	
well 17	1.95	0.84	0.85		1.88	1.87
well 23	2.23			1.06	2.42	
well 16	2.00		0.91			1.96
well 24	2.52			1.40		2.41
well 21	2.34			1.26		2.29
well 20	2.18			1.07		2.11
well 22	2.28			1.18		2.23

Tab. 1 Examples of the water levels measured in different wells at different times in June and October '94. For well numbers refer to Figure 5.

According to the magnitude of variation, wells can be divided into two groups. 1) Wells that show small water level variations in the order of 5% with respect to the June '94 values, and 2) wells that show very high variations up to 60%. Wells of the second group are located in southeastern part of the study area which will be referred

to as the 'highly variable zone (HVZ)' (Fig. 5).

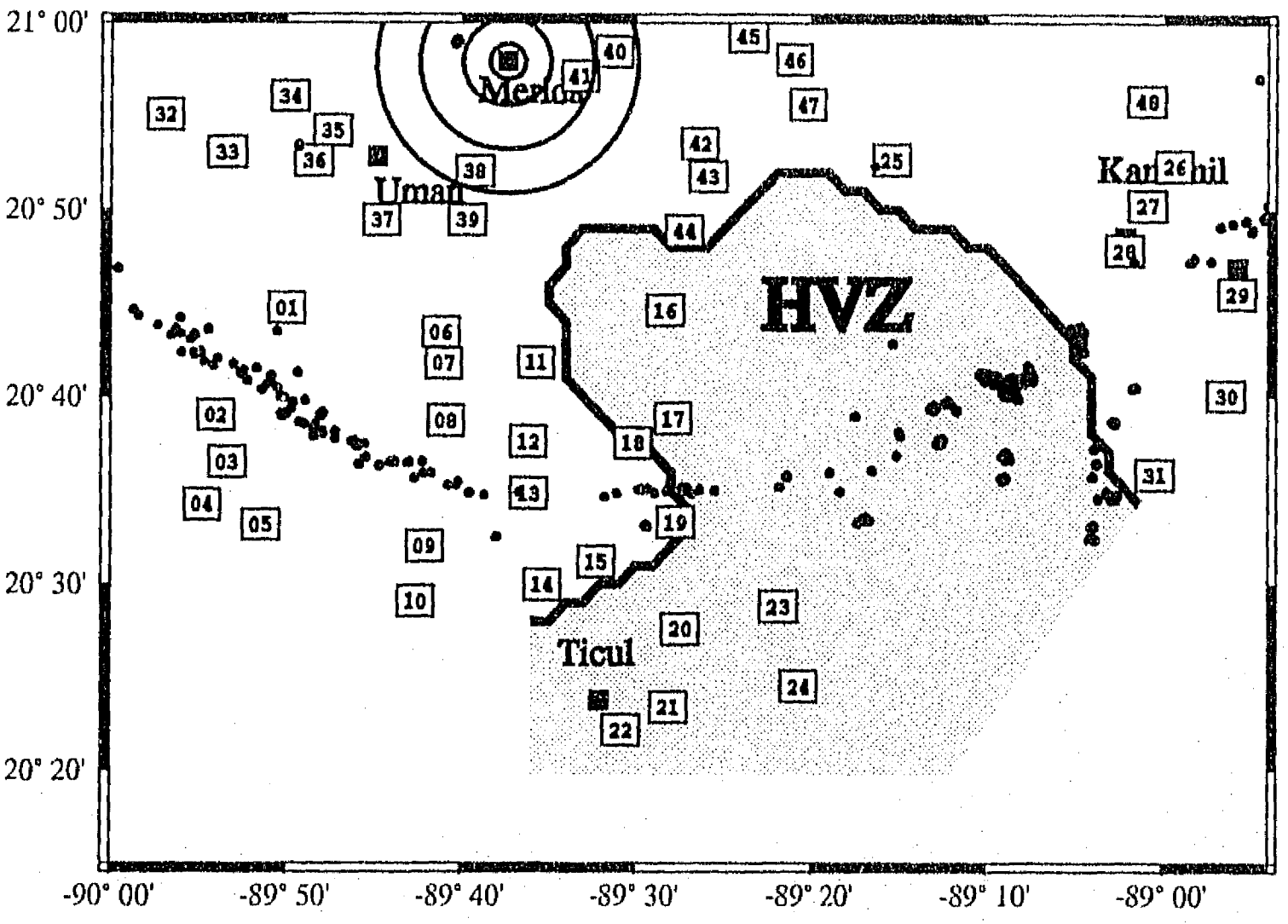

Fig. 5 Highly Variable Zone (HVZ). Numbers indicate observation wells.

The recuperation from the low level at the beginning of October to the high level occured in one week or less. Figure 4b shows that a heavy rain occured on October 14th, whereas the first 13 days of this month were almost dry. The amount of surficial recharge to the aquifer was low during these 13 days which is thought to be the reason for the low water levels measured at the beginning of October (Table 1 and Fig. 2). The draining process caused by this lack of recharge affected different areas in different manners. This implies that different independent fracture systems exist which have very small or no connection between each other. Water table oscillations in such independent systems can be very different to each other (Milanović, 1981;

Bonacci, 1995). Water in the HVZ drained very quickly while the effect in the rest of the study area was relatively small. Fast drainage as observed in the HVZ is typical for an emptying process of large caverns and channels (Milanović, 1981). The surroundings of the HVZ, especially the reported low permeability zone west of it (Steinich & Marín, in press) may be representative of a diffuse flow zone as described by Beck (1986).

The fast drainage of the HVZ causes the build up of a high hydraulic gradient towards the low permeability zone west of it. A steep gradient in karst, however, is not necessarily related to a real flow (Thrailkill, 1986). This may be especially true when nearby wells penetrate different subsystems of the aquifer. We propose that the two different groups of wells fulfill this condition. This would lead to the conclusion that in spite of the observed steep hydraulic gradient there is none or very slow flow between the HVZ and the nearby low permeability zone.

The heavy rain observed on October 14th (Fig. 4b) stopped the drainage process and caused an increase of the water levels of the wells in the HVZ within a few days.

As a conclusion we postulate that the HVZ is an independent subsystem of interconnected fractures, channels and caverns which is characterized by a high permeability with respect to its surroundings. This zone has preferred routes for ground water circulation facilitating very quick draining and recuperation of the aquifer.

7. Ground water flow direction

The observed water level variations in the HVZ cause the important changes in the configuration of the equipotential lines in the study area presented in Figures 2 and 3. As a consequence, ground water flow direction would therefore change substantially between the beginning and the end of October '94. There are examples reported in the literature that show that water table variations can actually cause such a change in direction of the ground water circulation (Milanović, 1981).

Figure 3 shows that the general ground water flow at the end of October '94 is from

southeast to northwest, i.e. towards the north and west coast of the Peninsula. The same situation was found in June '94. The equipotential lines in the eastern part of the study area show the tendency to turn east. This implies that flow is towards the north coast of the Peninsula. However, more data are needed in this zone to confirm this trend. Flow in the HVZ is orientated nearly perpendicular to the Ring of Cenotes, crossing it from southeast to northwest along the entire segment east of the mentioned head maximum.

A significant increase in the water level was observed in the wells of the HVZ at the end of October '94. A consequence of these oscillations is a quite different configuration of equipotential lines in nearly the whole study area (Fig. 2). The flow direction in the HVZ is from east to west, i.e. parallel to the Ring of Cenotes rather than from southeast to northwest as at the end of October 1994. In the center part of the study area a depression zone was formed as a consequence of the lack of surficial recharge and the quicker drainage of the HVZ with respect to its surrounding. The depression zone may be explained by the presence of karst conduits with high transmission capacities located below the afected zone (Milanović, 1981). This is in accordance with the statement made above that ground water flow is mainly determined by karst secondary porosity. This depression reverses the ground water flow direction in an extended area around it. A change of its hydrogeological situation from discharging water in June and at the end of October '94 to recharging water at the beginning of October '94 can be observed in the HVZ.

8. Azimuthal resistivity surveys and fracture orientation

The water level measurements described so far were used to determine the direction of hydraulic gradients. The mean ground water flow direction is supposed to follow the hydraulic gradient. On the other hand, real ground water movement in karst is mainly through dissolution voids such as fractures, channels and caverns (Gordon, 1986), and these conduits are not necessarily parallel to the hydraulic gradient. As

shown by Groves & Howard (1994), hydraulic gradient is only one of the parameters that control solutional enlargement. Initial fracture width can cause the enlargement of fissures in a direction other than the hydraulic gradients.

The Yucatan karstic aquifer is in general a mature system. Fracture openings on the order of centimeters are frequently found in cores of various wells drilled in the study area (Marín, 1994). Flow in fractures of this size can be assumed to be turbulent. Dissolution processes in the Yucatan Karst aquifer have been active at least for the last 125,000 years (Marín, 1990). Following a simulation study made by Howard & Groves (1995), this time period is sufficient for the formation of a maze flow system. The dominant flow regime is probably conduit flow although there may be zones where diffuse flow prevails.

Azimuthal resistivity surveys can be used to determine directions of high permeability i.e. preferential directions of dissolution of the limestone (Steinich & Marín, in press; Ritzi & Andolsek, 1992; Taylor & Fleming, 1988). Azimuthal resistivity surveys conducted for this study had spacings between 20 m and 30 m. Statements about interpreted directions of high permeability are valid for lengths within this order of magnitude. Azimuthal surveys were conducted at 22 locations in the the study area, 14 of them within the HVZ. Figure 6 shows four examples of the surveys. A circular curve would be expected in a terrain without a preferential direction of dissolution. Only one of the 22 data curves shows a circular shape and is presented in Figure 6a. The other 21 azimuthal surveys differ from a circular curve. In two data curves, one direction for high permeability can be identified, in the other 19 cases, two or more directions of enhanced permeability can be found. Each peak can be interpreted as representing the direction for one set of enlarged fractures, marked in the example in Figure 6b by two arrows.

The three sites with less than two fracture directions are outside of the HVZ. All 14 sites in the HVZ have two or more interpreted fracture directions. Frequent change of hydraulic gradient as observed in the HVZ may therefore be related to active enlargement of fissures and the formation of a complex conduit system as observed

in the HVZ.

6 a.

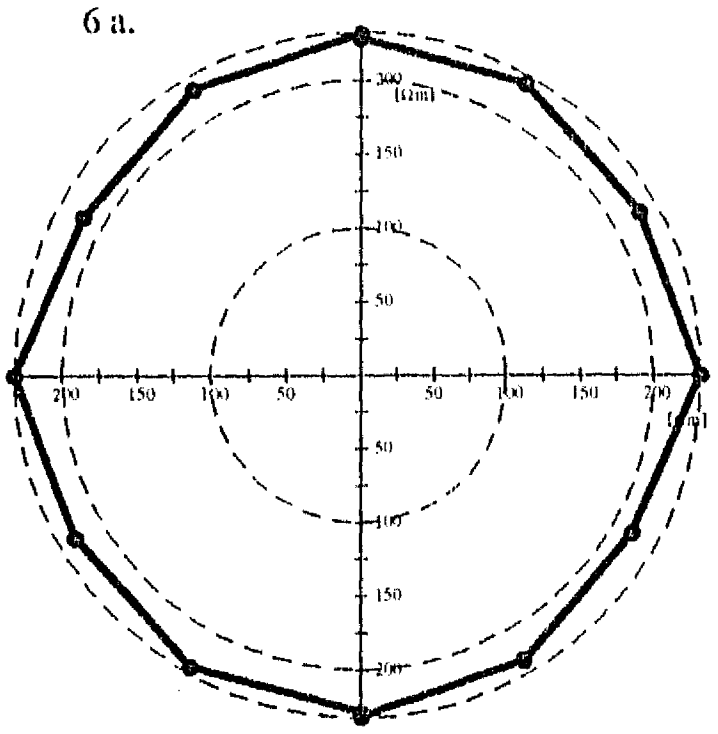

6 b.

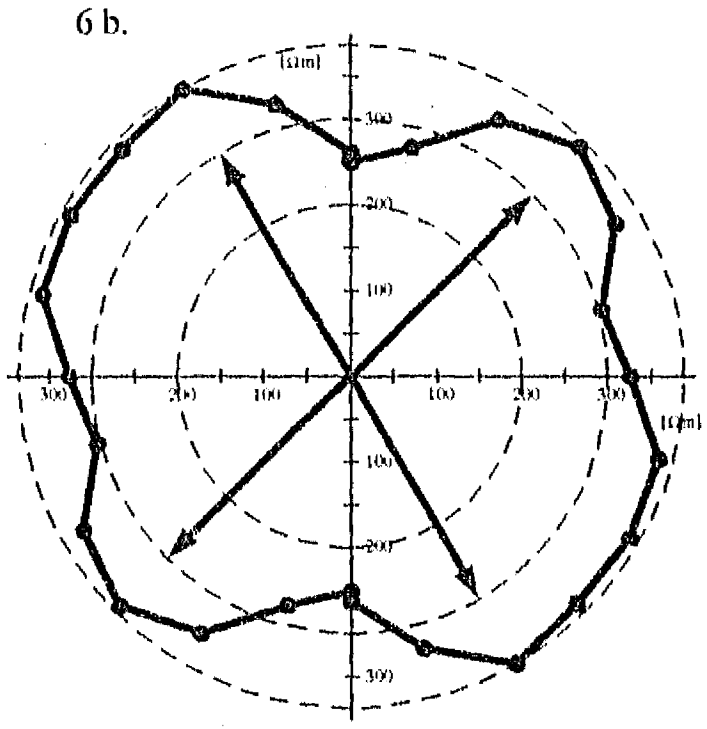

6 c.

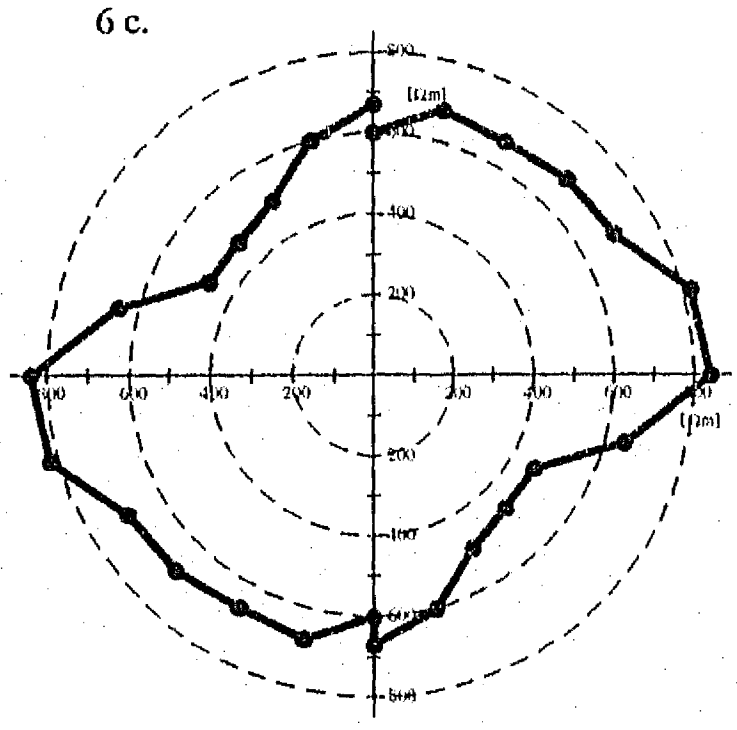

6 d.

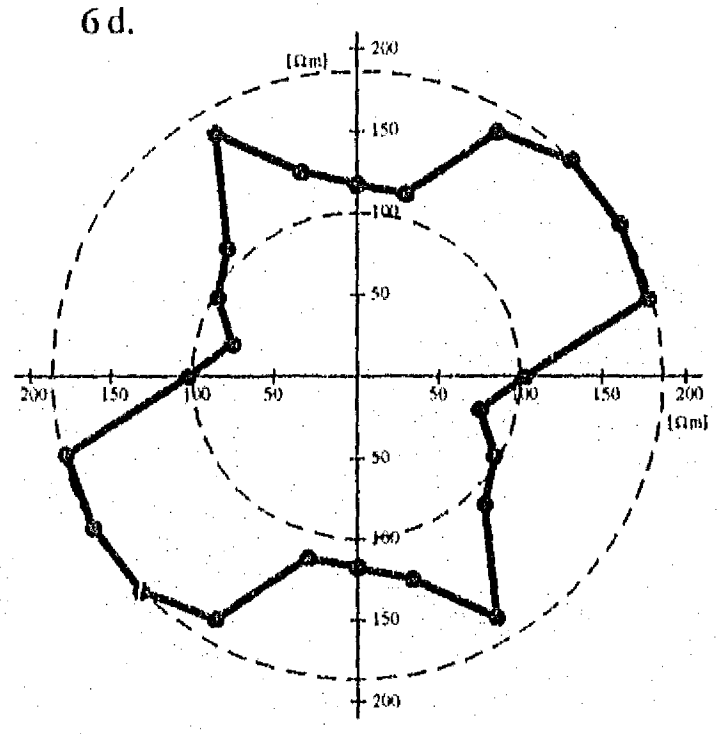

Fig. 6a-d 4 Examples of the 22 azimuthal resistivity surveys conducted in the study area. 6a is from the southwest part of the study area, 6b and 6c lay in the HVZ, 6d is from the northeastern part of the study area. 6a shows a nearly circular curve, typical for an isotropic medium. 6b shows the two interpreted directions of enlarged fractures, each marked by an arrow.

9. Relationship between hydraulic gradients and fracture orientations

Figure 7 shows the interpreted high permeability directions in the study area, where each of these directions is represented by an arrow. As in section 8, a fracture set is assigned to each direction of high permeability.

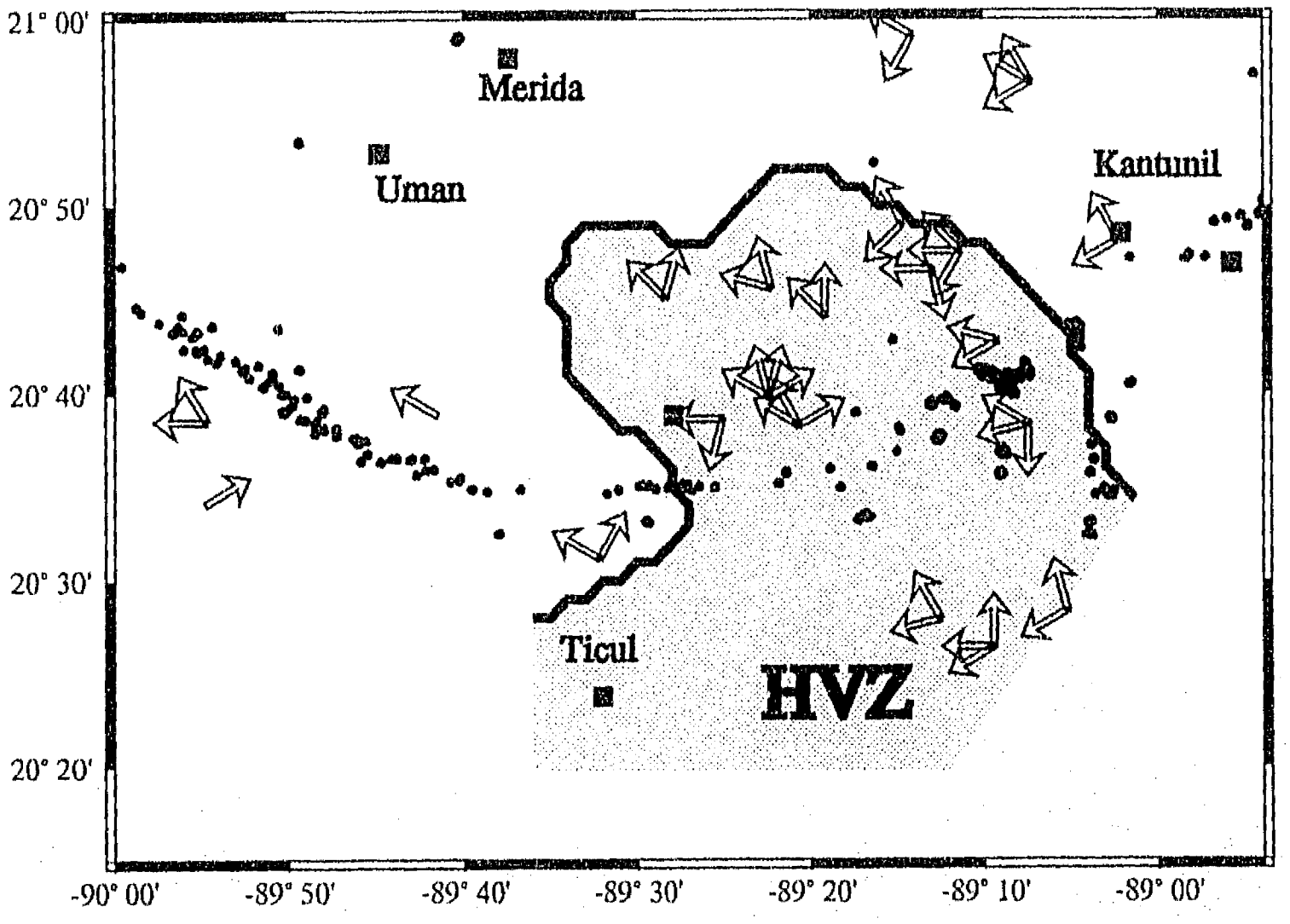

Fig. 7 Interpreted directions of high permeability using 22 Azimuthal Resistivity Surveys in the Study Area. Each arrow represents one direction of high permeability. Arrows start at its respective resistivity survey's location.

Comparison of the two different equipotential regimes (Fig. 2 and 3) with the equipotential lines and interpreted high permeability directions (Fig. 7) show that the regional hydraulic gradient coincides with a high permeability direction in 15 cases,

whereas in the other seven cases, no correlation can be found. This observation implies that in the majority of the sites, there is a direct relationship between hydraulic gradient and fracture orientation. Ground water flow in these cases can be assumed to be parallel to the hydraulic gradient, which on the other hand implies favorable conditions for further solution enlargement of the existing conduits.

In the cases where there is no correlation between the hydraulic gradient and the fracture orientation, local ground water flow differs from the regional direction of hydraulic gradient. Half of the sites outside the HVZ are representative of this situation but only one out of five sites inside the HVZ. Individual conduit segments may tend to be well aligned inside the HVZ while tending to meander outside. Tortuosity of the flowpaths may therefore tend to be lower inside than outside the HVZ. This implies that radial distances covered by the water are high in the HVZ within a specific time interval and this could favor a more rapid spreading of contaminants in the HVZ with respect to its surroundings.

Taylor & Fleming (1988) showed that the magnitude of the peaks of the resistivity curves can be related to the density of the fracture subsystems. Densities of the same order of magnitude result in peaks of comparable size. The peaks of the resistivity curves are generally of comparable magnitude (Fig. 6b-d), which suggests that the different fracture systems are all well developed.

It can be concluded from the alignment of the directions of the fracture systems and hydraulic gradient that the hydraulic gradient is a determinant factor in the enlargement of fractures by dissolution, especially in the HVZ. The existence of different, equally developed fracture systems implies that changes of the hydraulic gradient are frequent in the HVZ so that neither of the observed equipotential regimes can be assumed to be an exceptional situation.

10. Consequences of the reversals in hydraulic gradients with respect to the contamination risk

The conclusions concerning the frequency of either of the two equipotential regimes have severe consequences for the contamination risk of different zones of the study area. The City of Merida has the main accumulation of population and industry in northwestern Yucatan. The actual extension of the City is marked in Figure 5. This makes the City of Merida the main source of contamination in the Peninsula of Yucatan. Ground water flow in the Merida area is assumed to be from southeast to northwest (Méndez, 1993; Marín, 1990). This configuration is supported by the equipotential regimes found in June '94 and end of October '94. Contaminants that dissolve in or float on water flow towards the north coast of the Peninsula. The equipotential regime as found at the beginning of October '94 reverses the hydraulic gradients towards the southeast. The region affected by this variation is the HVZ. As shown in Figure 5, the area of the City of Merida is located on the rim of the HVZ. The presence of the industrial zone, which is located further to the south of the City, increases the risk of bringing contaminants to the extended area southeast of the City. Furthermore, is has been reported that a large well field is located to the southeast of Merida. Extensive pumping of this field has caused a cone of depression to form. Thus, the gradient has probably been reversed on the southeastern outskirts of the city (Escolero, pers. commun., 1994). Low tortuosity of the pathways contribute significantly to the magnitude of this risk.

This risk should not be underestimated if one considers that there are no state-owned treatment plants in the Peninsula and neither is there a natural elimination of contaminants from the waste water before it reaches the ground water. Reaction of water movement to variations of the hydraulic gradient is fast and movement of any contaminated water that enters into the aquifer must be assumed to spread out rapidly (Milanović, 1981; Felton & Currens, 1994). Low tortuosity of the pathways may aggravate this situation.

11. Conclusions

Three sets of water level measurements were made in the study area in June '94 and at the beginning and end of October '94. Water levels in a selected group of observation wells showed variations up to 60 % with respect to the June levels, whereas the variations in the other wells were in the order of 5 %. Based on the water level measurements, two different equipotential regimes were found. Major variations occur only in a limited zone in the southeast portion of the study area, which was referred to as the highly variable zone (HVZ). The HVZ shows varying drainage characteristics with respect to its surroundings, namely drain velocities seem to be very high. We postulate that the HVZ represents a widely independent subsystem of interconnected fractures.

Twenty-two azimuthal resistivity surveys were conducted in the study area to study preferential directions of high permeability. Namely in the HVZ zone, resistivity curves show two or more peaks, generally being of the same order of magnitude. A direction of high permeability has been suggested to be a consequence of the existence of aligned interconnected fractures. Each peak of a resistivity curve may represent therefore one system of such aligned fractures. Directions of these aligned fractures could be related to directions of the hydraulic gradient in the majority of the cases in the way that for each hydraulic gradient there is one corresponding parallel system of aligned fractures. This close relationship between hydraulic gradient and fracture systems show that the hydraulic gradient played a major role in the development of the fracture systems especially in the HVZ. The fact that peaks in the resistivity curves are of the same order of magnitude shows that different fracture systems are equally well developed. Both equipotential regimes must therefore be equally frequent, otherwise one of the fracture systems would exceed the other in importance. These results show that azimuthal resistivity surveys have a lot of potential for the investigation of aquifers in fractured media, especially when combined with hydraulic data.

The variability of the equipotential regime may have severe consequences for the

vulnerability of the aquifer to contamination. The major source of contaminants is the City of Merida, located at the northwestern rim of the highly variable zone. Ground water flow in this area is different in the two equipotential regimes. In the case of June '94 as well as end of October of '94, ground water flow is from southeast to northwest. This is considered as the normal ground water flow direction. At the beginning of October '94, however, the southern part of the City is located on a plateau of the equipotential surface at the rim of HVZ. Water could then also flow towards the southeast of the City. This can also be the case for contaminants reaching the aquifer in the southern part of the City, namely for those contaminants that dissolve in or float on the water.

Acknowledgments

B. Steinich thanks the Deutschen Akademischen Austausch Dienst (DAAD), the Secretaría de Relaciones Exteriores of Mexico and Dirección General de Asuntos del Personal Académico (grant no. IN101594) for financial support. Field work was funded by Consejo Nacional de Ciencia y Tecnología (grant no. T9457-0293). Frank Ohlsen and Saul Hernández helped with the field work. We thank the personal of INEGI/Merida for their important help during preparation of the field work and the National Water Commission in Mexico City and in Mérida, Yucatán, for making available the meteorological data.

References

Anonymous, 1994. Data for Monthly and Daily Precipitation. *Comisión Nacional del Agua, Mérida, Yucatán*

Anonymous, 1984. Cartas Topográficas de Yucatán 1:50 000. *Instiuto Nacional de Estadística, Geografía e Informática, Mérida, Yucatán.*

Beck, B.F., 1986. Ground Water Monitoring Considerations in Karst of Young

Limestones. *Proc. of the Environmental Problems in Karst Terranes and Their Solutions Conference, Bowling Green, Kentucky, October 1986, pp.229-248*

Bonacci, O., 1995. Ground water behaviour in karst: example of the Ombla Spring (Croatia). *J. Hydrol., 165(2):113-134*

Felton, G.K., & J.C. Currens, 1994. Peak flow rate and recession-curve characteristics of a karst spring in the Inner Bluegrass, central Kentucky. *J. Hydrol., 162(2):99-118*

González Herrera, R.A., 1984. Correlación de muestras de roca en pozos de la Ciudad de Mérida. *Senior Thesis, Universidad Autónoma de Yucatán, Mérida, México*

Gordon, M.J. 1986. Dependence of Effective Porosity on Fracture Continuity in Fractured Media. *Ground Water, 24(4):446-452*

Groves, C.G. & A.D. Howard, 1994. Early development of karst systems: 1. Preferential flow path enlargement under laminar flow. *Water Resour. Res., 30(10): 2837-2846*

Howard, A.D. and C.G. Groves, 1995. Early development of karst systems: 2. Turbulent flow. *Water Resour. Res., 31(1):19-26*

Marín, L.E. 1990. Field Investigations and Numerical Simulation of Groundwater Flow in the Karstic Aquifer of Northwestern Yucatan, México. *Ph. D. Thesis. 183 pp., Northern Illinois University, DeKalb, IL, USA*

Marín, L.E., 1994. Informe Final sobre las perforaciones en Yucatán. *Reporte Técnico, IGF-UNAM, 1994*

Marín, L.E. and Perry, E.C., 1994. The hydrogeology and contamination potential of northwestern Yucatán, Mexico. *Geofísica Internacional, 33(4):619-623*

Marín, L.E., Perry, E.C., Pope, K.O., Duller, C.E., Booth, C.J., and Villasuso, M. 1990. Hurricane Gilbert, its Effects on the Aquifer in Northwestern Yucatan, Mexico. *International Association of Hydrogeologists, Selected Papers on Hydrogeology from the 28th International Geologic Congress, Washington, D.C. July 9-19, 1989*

Méndez R., R. 1993. Modelo de comportamiento del acuífero de la Ciudad de Mérida, Yucatán. *Abstract, Memorias de la Primera Reunión Nacional Sobre Aguas Subterráneas. Mexico City, Mexico. May, 1994, IGF-UNAM, p. 28*

Milanović, P.T., 1981. Karst Hydrogeology. *Water Resources Publications. Littleton, CO, 434 pp.*

Morán Z., D.J., 1985. Geología de la República Mexicana. *Facultad de Ingeniería (UNAM) and Instituto Nacional de Estadística, Geografía e Informatica, México, 2a. Edición, 88 pp.*

Perry, E.C., Marín, L.E., McClain, and J., Velázquez, G.; 1995. The Ring of Cenotes (sinkholes), northwest Yucatan, Mexico: its hydrogeologic characteristics and possible association with the Chicxulub Impact Crater. *Geology, 23:17-20*

Perry, E.C., J. Swift, J. Gamboa, A. Reeve, R. Sanbon, L.E. Marín, M. Villasuso. 1989. Geological and Environmental Aspects of Surface Cementation, North Coast, Yucatan, Mexico. *Geology, 17:818-821*

Reeve, A., and E.C. Perry, 1990. Hydrogeology and tidal analysis along the western north coast of the Yucatan Peninsula, Mexico. *In: J.H. Krishna, V. Quiñones-Aponte, F. Gomez-Gomez and G.L. Morris (Editors), Tropical Hydrology and Caribbean Water Resources, Am. Water Resour. Assoc., Bethesda, Md., 327-337*

Ritzi, R.W.Jr., and Andolsek, R.H., 1992. Relation Between Anisotropic Transmissivity and Azimuthal Resistivity Surveys in Shallow, Fractured, Carbonate Flow Systems. *Ground Water, 30(5):774-780*

Sharpton, V.L., L.E. Marín, C. Carney, S. Lee, G. Ryder, B.C. Schuraytz, P. Sikora, P.D. Spudis, in press. A Model of the Chicxulub Impact Basin Based on Evaluation of Geophysical Data, Well Logs and Drill Core Samples. *Geological Society of America Special Paper 307*

Steinich, B. and L.E. Marín, in press. Hydrogeological investigations in northwestern Yucatan, Mexico, using resistivity surveys. *Ground Water*

Taylor, R.W., and Fleming, A.H., 1988. Characterizing Jointed Systems by Azimuthal Resistivity Surveys. *Ground Water, 26(4):464-474*

Thrailkill, J., 1986. Models and Methods for Shallow Conduit-Flow Carbonate Aquifers. *in: Proceedings of the Environmental Problems in Karst Terranes and Their Solutions Conference, National Water Well Association, Dublin, Ohio: 17-31*

Wessel, P. and W.H.F. Smith. 1992. The GMT-SYSTEM v. 2.1. Technical Reference & Cookbook. *SOEST/SIO*

IV. Localización del parteaguas en el acuífero cárstico de Yucatán, México, combinando datos geoquímicos e hidrogeológicos.

Determination of the ground water divide in the karst aquifer of Yucatan, Mexico, combining geochemical and hydrogeological data

Birgit Steinich[a], Guadalupe Velázquez Olimán[a], Luis E. Marín[a], Eugene Perry[b]

[a]Instituto de Geofísica, Universidad Nacional Autónoma de México, Cd. Universitaria, Mexico City, Mexico, C.P. 04510

[b]Department of Geology, Northern Illinois University, DeKalb, Illinois 60115

Geofísica Internacional, aceptado

Resumen

El acuífero de la Peninsula de Yucatán es un acuífero cárstico, el cual se caracteriza por su alta permeabilidad. Huellas del proceso de la carstificación, como los túneles y las cavernas (cenotes) subterráneos, se pueden apreciar en toda la Península. Sin embargo, hay una acumulación de los mismos a lo largo de una línea circular, el Anillo de Cenotes. El anillo está relacionado con el Cráter de Chicxulub, una estructura de impacto enterrada que data del límite del Cretácico/Terciario. El Anillo de Cenotes representa en varios de sus segmentos, una zona de alta permeabilidad y se ha propuesto que actúa como un río subterráneo, el cual concentra el agua subterránea y la conduce hacia sus puntos de intersection con la línea costera cerca de Celestún y Dzilam de Bravo. Basado en datos hidrogeológicos, se describe una zona que separa hidráulicamente dos segmentos del anillo. Se usó la relación SO_4/Cl como trazador

natural para determinar direcciones de flujo en el área de estudio. La combinación de los resultados permite la identificación del parteaguas del sistema del río subterráneo y su ubicación en la parte sur del área de estudio cruzando el Anillo de Cenotes cerca de la población de Abalá.

Palabras clave: Acuífero Cárstico de Yucatán, Anillo de Cenotes, Parteaguas

Abstract

The aquifer of the Peninsula of Yucatan is a karstic aquifer characterized by its high permeability. Karst features such as underground channels and collapsed caverns (cenotes) are widely present throughout the whole Peninsula. However, there is an accumulation of cenotes along a circular line, the Ring of Cenotes. The ring is related to the Crater of Chicxulub, a buried impact structure that dates from the K/T-boundary. The Ring of Cenotes represents on several segments a high permeability zone and is assumed to act as an underground river that collects ground water and brings it to its two intersection points with the coast line near Celestun and Dzilam de Bravo. Based on hydrogeological data, a dividing zone is described that hydraulically separates two segments of the Ring. Using the SO_4/Cl ratio as a natural tracer, ground water flow directions in the study area are described. Combining the results, the location of the ground water divide of the underground river system is proposed to be located at the southern part of the study area, crossing the Ring of Cenotes near the village of Abala.

Key words: Karstic Aquifer of Yucatan, Ring of Cenotes, Ground Water Divide

1. Introduction

The aquifer of the Peninsula of Yucatan is a coastal karstic aquifer. It is unconfined,

except for a narrow band parallel to the coast (Perry et al., 1989). The Yucatan platform consists of a mature karst system, with corresponding high permeabilities and low hydraulic gradients (Back and Hanshaw, 1970; Marín, 1990; Marín et al., 1987). The regional ground water flow is from southeast to northwest (Steinich & Marín, in press(b)). However, there are several phenomena which cause changes in the flow regime of the aquifer, altering locally the regional southeast to northwest flow direction. 1) The Ring of Cenotes (sinkholes) is a circular zone of high cenote density. The permeability along several segments of this ring is enhanced, intercepting the regional ground water flow and causing a concentrated discharge at its intersection points with the coast near Celestun at the west coast and near Dzilam de Bravo at the north coast of the Peninsula (Marín, 1990; Perry et al., 1995; Pope and Duller, 1989; Pope et al., 1993;). The Ring of Cenotes is related to the Chicxulub Crater (Hildebrand et al., 1995; Perry et al., 1995; Pope et al., 1993), a buried impact structure that dates from the K/T-boundary (Hildebrand et al., 1991; Sharpton et al., 1992; Swisher et al., 1992). (2) The aquifer's permeability is dominated by secondary porosity, present as fractures, underground channels and caverns. Steinich & Marín (in press(a)) and Steinich & Marín (in press(b)) described a zone of decreased permeability in the southern part of the ring of cenotes near Abala (Fig. 1) neighboring a zone with good interconnection of voids and typically low tortuosity of the flow path. The chemistry of the ground water is controlled by water-rock interactions including mixing of the fresh/salt water, dissolution of the carbonate rocks, evaporation/precipitation (essentially loss or gain of pure water) and redox reactions (Velázquez Olimán, 1995; Perry et al., in review), as well as dissolution of an evaporitic body found in the southern section of the study area (Urrutia-Fucugauchi et al., in press).

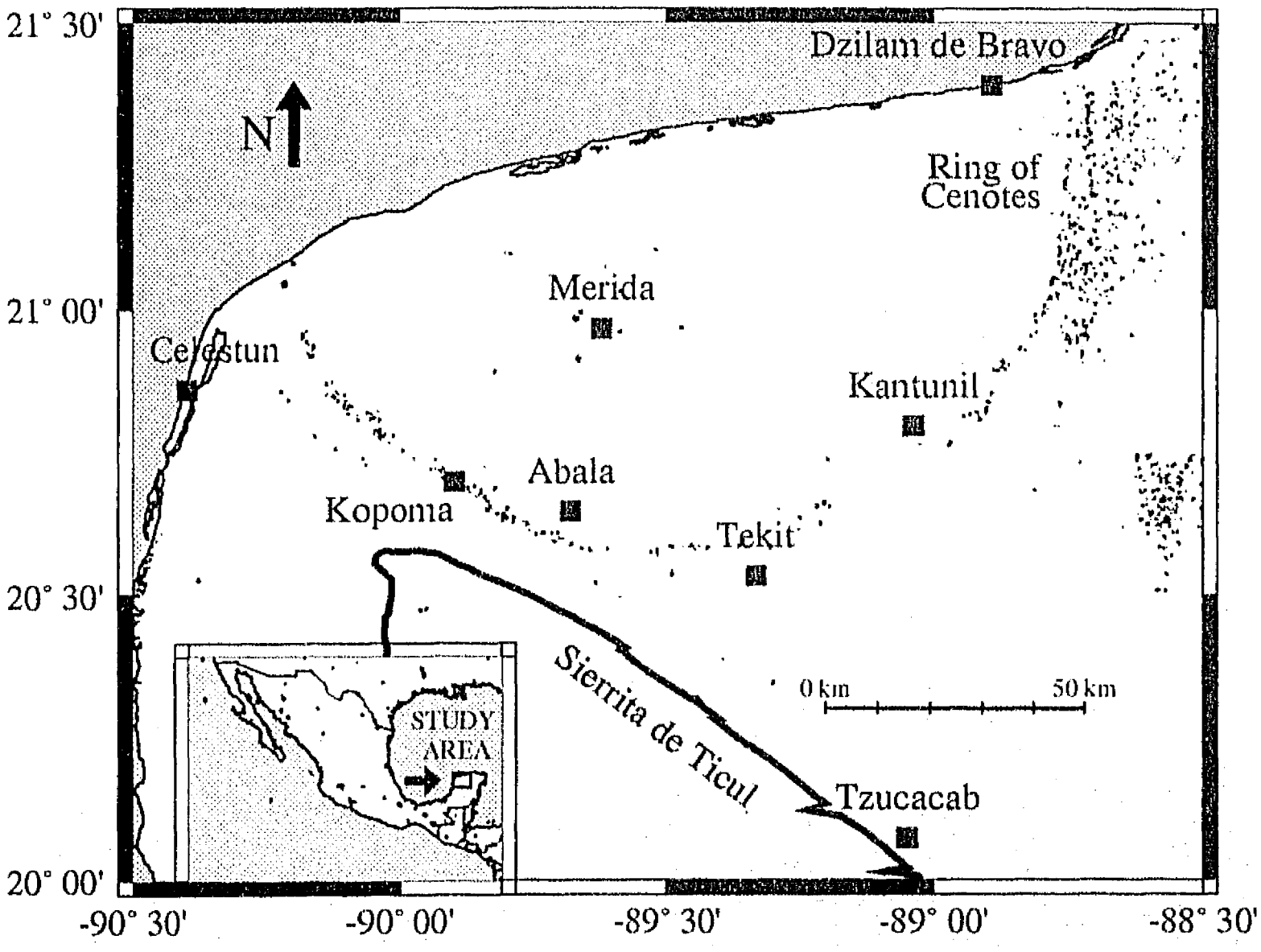

Fig. 1 Study area in the northwestern part of the Peninsula of Yucatan, Mexico. Black points are cenotes that were digitized by the senior author from topographic maps (Anonymous, 1984).

2. Objectives

The objectives of this study are: to investigate local flow directions with 1) hydrogeological and 2) geochemical data, and 3) to integrate the results in order to determine the location of the ground water divide in the aquifer of northwestern Yucatan.

3. Study Area

This study was conducted in the western section of the Peninsula of Yucatan, Mexico. The study area consists of the region between $88^o30'$ and $90^o30'$ west and $20^o00'$ and $21^o30'$ north (Fig. 1). The Ring of Cenotes traverses the study area from west (near Celestun) to northeast (near Dzilam de Bravo) (Fig. 1). The study area is characterized by a flat topography which is cut by the Sierrita de Ticul (Fig. 1), a small land step elevating levels from typically 15 meters above mean sea level (MSL) north of it, to levels in the range of 50 to 100 meters in the south (Anonymous, 1984).

4. Methodology

Water level measurements were made in nine observation wells within the central part of the study area. Most of these wells are hand-driven water supply wells and some are cenotes (water filled sinkholes). A first-order topographic survey conducted by the Instituto Nacional de Estadística, Geografía e Informática (INEGI) exists for the area. Distances from the wells to the nearest benchmark are less than 300 m; well elevations were determined using a level and stadia with a maximum error of 0.2 cm. Water levels were measured with respect to the leveled reference point with a maximum error of 1 cm. Data was taken in October of 1994. Measurements in the observation wells were repeated up to four times within a two weeks period in order to compare the oscillations of the water levels.

Twenty-one water samples were collected from actively pumping municipal wells. Parameters measured in the field were temperature, pH, conductivity, dissolved oxygen, and redox potential using a Datasonde 3. Three samples were taken at each site for the determination of alkalinity, anions, and cations. Alkalinity was determined within 24 hours by Gran titration (Stumm & Morgan, 1981), using a Hach kit and 1.6 N H_2SO_4. Samples for anions and cations were collected in 125 ml plastic bottles previously washed in dilute 10% HNO_3 acid. Water samples were filtered using

a 0.2 μm pore diameter. Samples were stored in a cooler and previous to analysis were stored in a dark refrigerator at 4^o C. Anions were analyzed using an ion chromatograph with a Dionex ion suppressor and a conductivity cell. The cations were analyzed using a Beckman V DC plasma. The laboratory analysis were conducted at the Geology Department at Northern Illinois University. All samples had a mass balance error less than 5% (Velázquez Olimán, 1995). The pH-meter was calibrated using 4.0 and 7.0 buffers. The electrodes for redox were calibrated using quinhydrone. A flow-through device was used for the field parameters. Readings were taken once the samples had stabilized.

Results and discussion

5. Hydrogeological Data

Marín (1990) and Marín et al. (1989) have proposed that the Ring of Cenotes is a high permeability zone that acts as an underground river intersecting ground water flow as it flows from south to north. Ground water is intercepted by the Ring, and it discharges at either of two intersections with the sea.

Since ground water is discharging at both ends, somewhere within the Ring must exist a ground water divide. This hypothesis is supported by three lines of evidence: 1) on two north-south transects, water level with respect to mean sea level first increases with distance away from the sea, and then decreases, having local minima at the intersection with the Ring. 2) A higher density of submarine springs is observed using Thematic Mapper images at Dzilam de Bravo, the intersection of the eastern portion of the Ring with the sea (Marín et al., 1989). 3) Sand bars at the two intersections, Celestun and Dzilam de Bravo, (Fig. 1) remain open (sand transport occurs from East to West along the coast) (Marín, 1990). The same author mentions that ground water flow is probably crossing the Ring in its southern part.

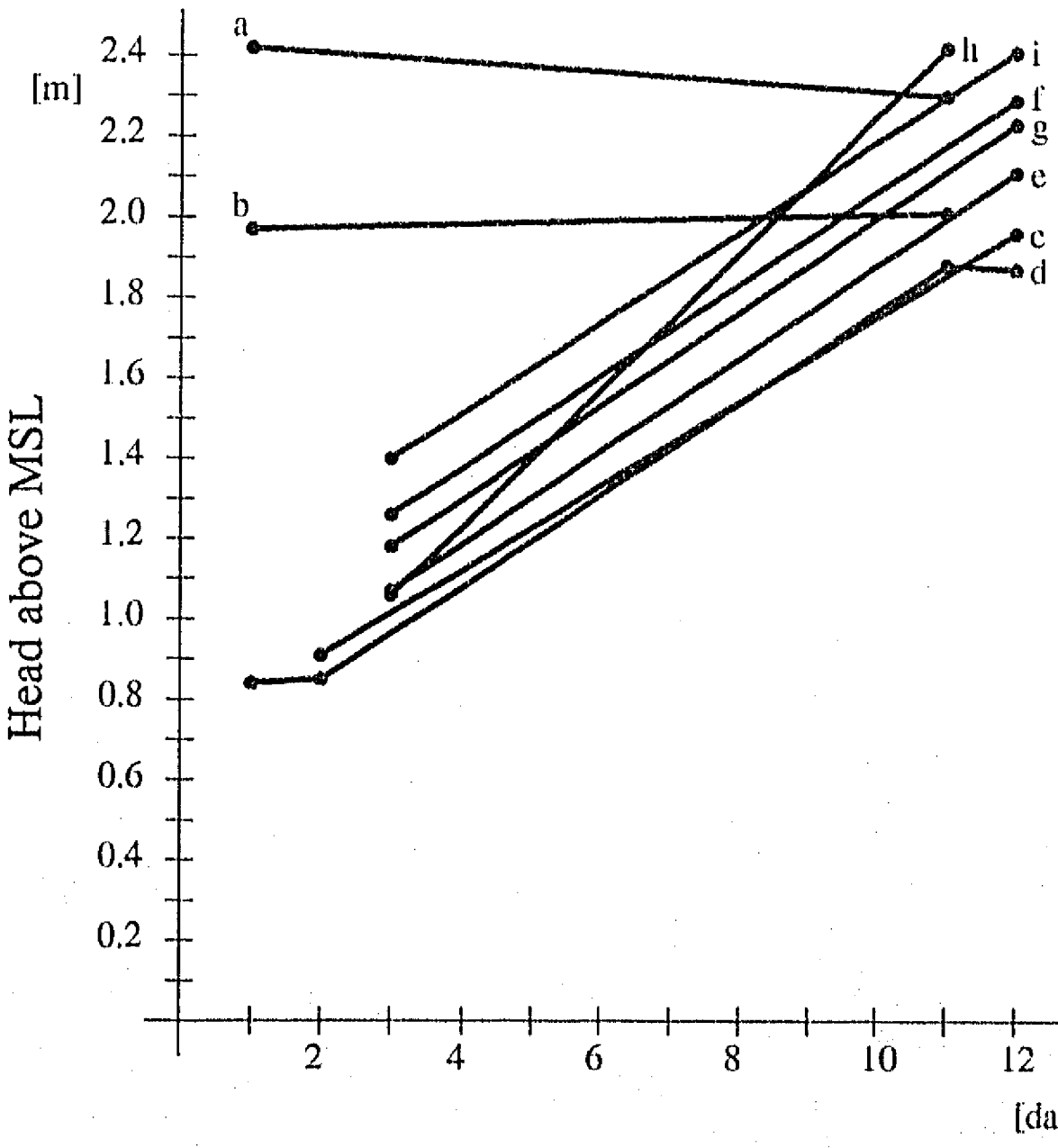

Fig. 2 Water level variations in nine observation wells in the central part of the study area. Measurements are from a two weeks period in October of 1994, day one is Oct. 9. Well locations are shown in Figure 3. Wells (a) and (b) are located west and wells (c) to (i) east of the interpreted dividing zone. Water levels are in meters above mean sea level.

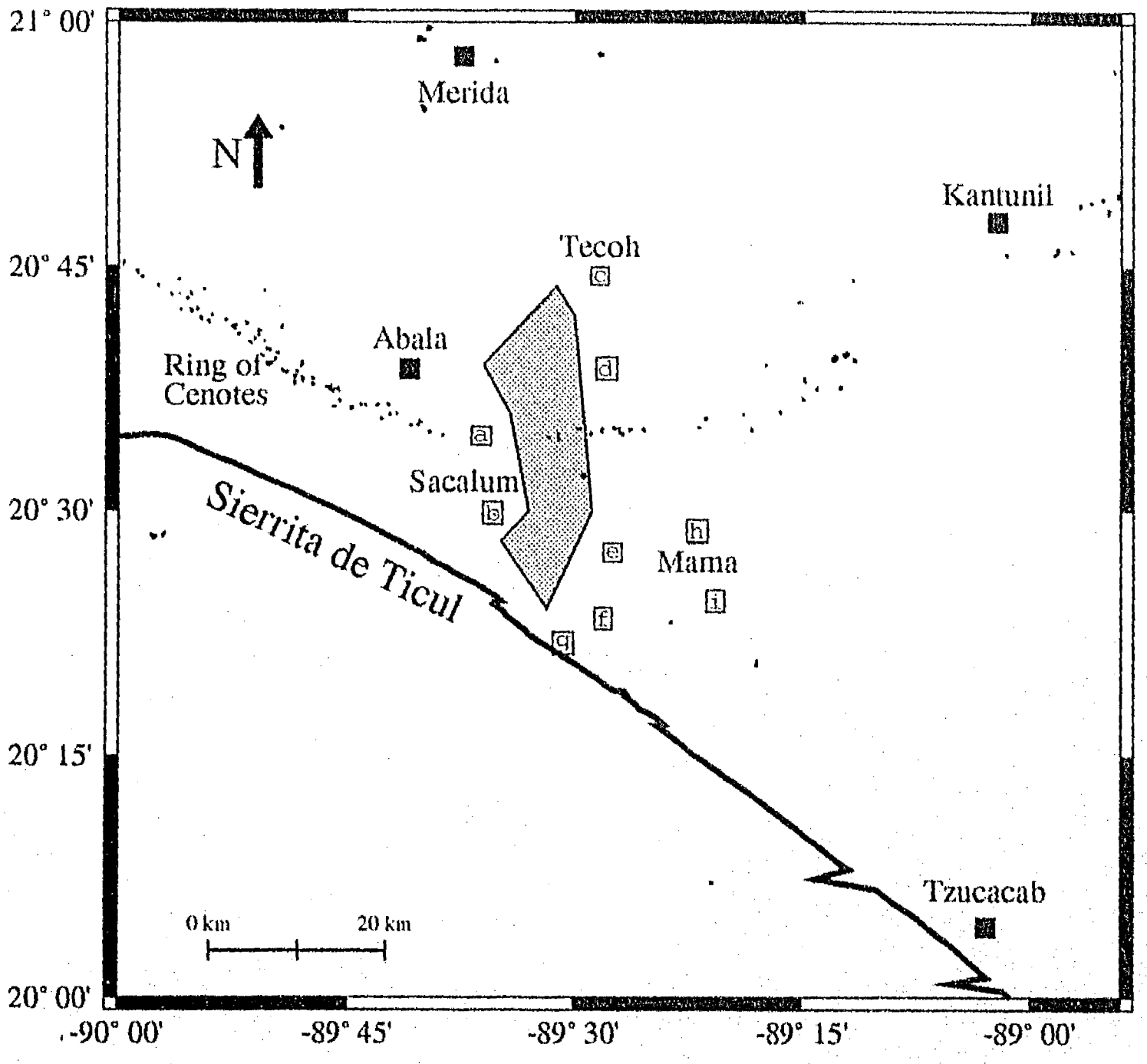

Fig. 3 Gray shaded area is the proposed location for the dividing zone as deduced from the hydrogeological data. [a] to [i] are the observation wells.

Steinich and Marín (in press(a)) described lateral permeability variations along the Ring. Using electrical soundings they identified a zone of relatively low permeability near Abala (Fig. 1). While the Ring west of Abala is characterized by a narrow band with high cenote density, the segment near Tekit (Fig. 1) shows a broad band

and lower cenote density. Marín (1990) suggested that ground water flow could cross the Ring near Kantunil. Steinich and Marín (in press(b)) proposed that this zone is a highly variable zone with respect to water levels and flow regime. The nine wells monitored are located within the transition area between the low permeability and the highly variable zone. Figure 2 shows the water level variations within a time period of 14 days in October of 1994. The graph shows that water level changes drastically in some wells while the level in another group of wells stayed nearly stable. Even though the distance between these two groups of wells is only several kilometers and the karst aquifer is assumed to be highly permeable, during the first three days of the observation period, water loss in the low level wells (c to i in Fig. 2) was not compensated by flow from the high level wells (a and b in Fig. 2). Based on these hydrogeological data, it is assumed that there is a zone that disconnects hydraulically the two subsystems within the aquifer. This dividing zone is characterized by no flow or very slow flow through it. Figure 3 shows its location as a gray shaded area and the observation wells.

6. Geochemical Data

The following discussion is based on geochemical data presented in more detail elsewhere (Velázquez Olimán, 1995; Perry et al., in review). The geochemistry of the ground water in Yucatan is primarily determined by mixing of water in a fresh water lens with an underlying salt water intrusion and by the dissolution of evaporite and carbonate rocks. Dissolution of evaporite leads to an enrichment of natural waters in sulfate, so the ratio of SO_4/Cl can be used as a natural tracer (Velázquez Olimán, 1995; Perry et al., 1995). Values for SO_4, Cl and the ratio SO_4/Cl of twenty-one observation wells are reported in Table 1.

Sample site	Sampling date	SO4 [meq/l]	Cl [meq/l]	SO4/Cl x 1000
Abala [01]	08/25/94	3.75	7.62	492.1
Chochola [02]	08/22/94	2.76	10.91	253.0
Homun [03]	06/22/93	0.35	3.11	112.5
Huhi [04]	06/22/93	0.38	3.36	113.1
Kantunil [05]	04/25/94	0.46	4.63	99.4
Kinchil [06]	12/20/93	1.30	9.42	138.0
Kopoma [07]	09/10/93	7.31	17.25	423.8
Mama [08]	06/22/93	3.20	5.23	611.9
Mani [09]	06/24/93	4.82	5.76	836.8
Opichen [10]	08/25/94	7.74	13.11	590.4
Oxkutzcab [11]	09/10/93	2.45	5.30	462.3
Sacalum [12]	08/25/94	5.85	11.80	495.8
S.Antonio T. [13]	12/22/93	3.08	12.44	247.6
S.Jose T. [14]	12/18/93	8.30	14.56	570.1
Sotuta [15]	06/22/93	0.52	3.52	147.7
Tecoh [16]	08/23/94	0.47	4.46	105.4
Tekax [17]	09/10/93	2.45	6.99	350.5
Tekit [18]	09/09/93	0.90	3.57	252.1
Telchaquillo [19]	06/24/93	0.55	3.42	160.8
Ticul [20]	12/17/93	3.91	6.99	559.4
Tzucacab [21]	09/09/93	11.36	10.37	1095.5
Sea water*		56.42	545.84	103.4

Table 1 Values of SO_4, Cl, and ratio of $(SO_4/Cl)x1000$ for the twenty-one ground water samples. Numbers behind the site names in the first column are the same as in Figure 4.

* The ratio $(SO_4/Cl)x1000$ for sea water is taken from Drever (1988).

Waters from the fresh water lens can be grouped as follows: 1) samples with a sulfate to chloride ratio similar to that of sea water, 103.4 (Drever, 1988); and 2) samples with a ratio of SO_4/Cl greater than 300.0. In the first group SO_4/Cl is controlled primarily by mixing of the fresh water lens with the salt water intrusion. This group

includes water from the area circumscribed by the Ring and ground water southeast of the Ring (Fig 4.).

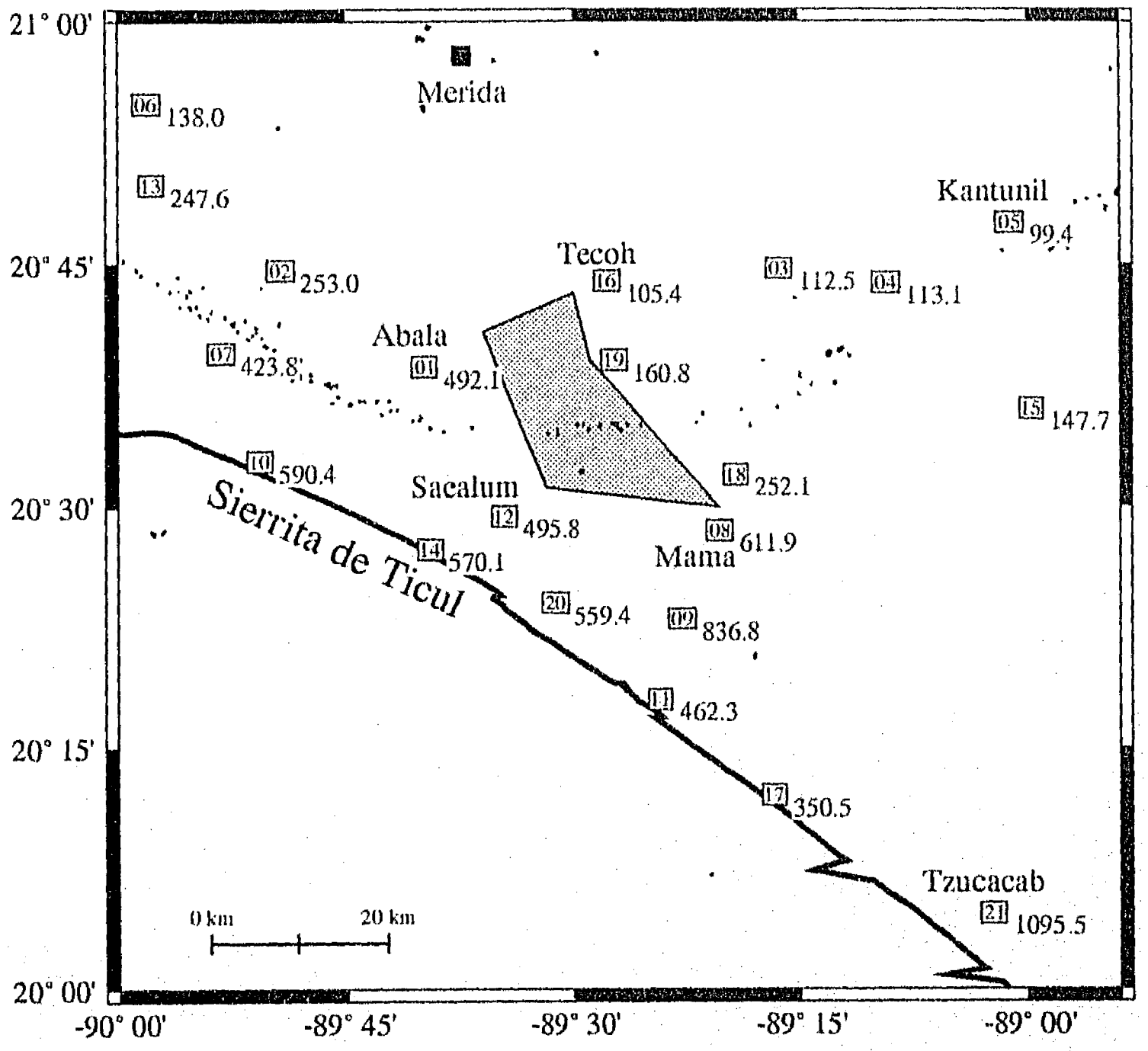

Fig. 4 $(SO_4/Cl)x1000$ for 21 ground water samples. Sample site locations are shown as small numbered rectangles (numbers refer to Table 1).

Perry et al. (in review) present evidence that samples of the second group are mainly influenced by the contact with and dissolution of evaporites located in the southern part of the study area. Highest values extend in a zone about 20 *km* wide that is more

or less parallel to the Sierrita de Ticul (Fig. 4). The highest ratio of SO_4/Cl (1095.5) is found in the southeastern part of the study area at Tzucacab (−89.05 west, 20.08 north, Fig. 4). Although we can deduce that there is, in this zone, an evaporite source of sulfate lying in or above the fresh water lens, from the data available it is not possible to locate more precisely this source or sources because none of these waters is near saturation with respect to gypsum. There is a gradual decrease of SO_4/Cl toward the north of the evaporite zone. It is probable that the preferred flow direction of the sulfate-enriched water from the evaporite zone is towards the west coast. As shown by Perry et al. (1995) the water from the Celestun water works (near the east coast, Fig. 1) has a SO_4/Cl ratio similar to that at Kopoma. This ground water flow direction was also proposed by Steinich and Marín (in press(b)). Within the gray shaded area in Figure 4, bounded by Abala, Tecoh, Sacalum and Mama, the contours of SO_4/Cl cross the Ring of Cenotes at a sharp angle. In contrast, the SO_4/Cl ratio decreases gradually northward in the western part of the study area as has already been mentioned.

7. Location of the ground water divide

Comparison of the results of the hydrogeological data (Fig. 3) and the geochemical data (Fig. 4 and Table 1) show a good correspondence between the location of the proposed dividing zone and the sharp decrease of the SO_4/Cl ratio. We propose that this zone dividing the flow system of the aquifer, which is characterized by the observed drop in the ground water SO_4/Cl ratio, is a ground water divide. Thus, we envision that sulfate-enriched water from the evaporite zone near Tzucacab initially flows to the north, but the flow is then deviated towards the west on a flow path between the Sierrita de Ticul and the western segment of the Ring of Cenotes. This sulfate-enriched water from Tzucacab, therefore does not cross the Ring of Cenotes to reach sites like Tecoh (well 16) and Telchaquillo (well 19) (Fig. 4, Table 1). Based on these results, we propose that the ground water divide is located on a line that, in the

north, lies east of Abala (well 01), but west of Tecoh and Telchaquillo (sampling sites 16 and 19, respectively). It crosses the Ring of Cenotes west of Tekit and northeast of Sacalum (sampling sites 18, and 12, respectively) on its southern section. The possible area of the ground water divide location is shown in Figure 4 as a gray shaded area. Farther to the east, we lack sufficient geochemical data to trace the movement of the sulfate-enriched plume.

8. The low permeability zone near Abala

The only sample north of the Ring of Cenotes having a high SO_4/Cl ratio is Abala (Fig. 4) which is apparently in contrast to the ground water divide-hypothesis proposed in Section Seven. Steinich & Marín (in press(a)) showed that there is a zone of relatively low permeability near the village of Abala. Peak values of water level with respect to mean sea level were found in the same area (Steinich & Marín, in press(b)). The area near Abala seems to be of special interest for the hydrogeology of the aquifer.

There are two possible reasons to account for a "high tracer site" north of the Ring of Cenotes: 1) the high content of SO_4 is due to sulfate-enriched ground water flowing from south to north, or 2) there is a source of SO_4 near the area of Abala.

Steinich & Marín (in press(b)) showed that ground water may cross the Ring from southeast to northwest through the segment between the low permeability zone and Kantunil. This flow is assumed to be focused on a flow path along a system of aligned fractures having this same direction (Steinich & Marín, in press(b)). Based on the discussion of Section Five, this flow must occur east of the dividing zone. If sulfate enriched ground water reaches the area near Abala, the dividing zone must be interrupted in some place and a hydraulic gradient from east to west must be present. Measured peak values of the water level in different periods of the year (Steinich & Marín, in press(b)) seem to reject this hypothesis, although a temporary reversal in hydraulic gradient can not be ruled out in such a highly permeable karstic aquifer.

9. Conclusions

Integration of hydrogeological and geochemical data was used to identify the ground water divide in the aquifer of northwestern Yucatan. This conclusion is based on: 1) results of hydrogeological data which made it possible to identify a zone dividing the aquifer into two subzones. Water of either of the subzones is unlikely to reach the other subzone. 2) Geochemical analysis of 21 ground water samples taken in the study area show that the ground water in the aquifer can be divided into two families, one in contact with an evaporite body located in the southern part of the study area and therefore subject to enrichment with sulfate and another family which is relatively poor in sulfate and can therefore be assumed not to be in contact with the evaporites. The sulfate-enriched water could be used as a natural tracer to allow determination of local flow directions of the ground water and the location of the ground water divide within the aquifer. The proposed ground water divide has a southeast to northwest direction and is located between Abala and Sacalum on the west and Tecoh and Mama on the east side.

10. Acknowledgments

B. Steinich thanks the Deutschen Akademischen Austausch Dienst (DAAD) and the Secretaría de Relaciones Exteriores of Mexico for financial support. Field work was funded through grants to L. Marín from Dirección General de Asuntos del Personal Académico (DGAPA: IN106891, IN101594) and Consejo Nacional de Ciencia y Tecnología (CONACyT: T9457-0293). G. Velázquez was supported through a CONACyT graduate fellowship. E. Perry acknowledges the National Science Foundation (EAR 9304840).

11. References

Anonymous, 1984. Cartas Topográficas de Yucatán 1:50 000. *Instituto Nacional*

de Estadística, Geografía e Informática, Mérida, Yucatán.

Back, W. and B.B. Hanshaw, 1970. Comparison of chemical hydrogeology of the carbonate Peninsulas of Florida and Yucatan. *Journal of Hydrology, 10: 330-368*

Drever, J.I., 1988. The Geochemistry of Natural Waters. *Prentice Hall, Inc., Englewood Cliffs, N.J., USA, 437 pp.*

Hildebrand, H.A., G.T. Penfield, D.A. Kring, M. Pilkington, A. Camargo, S.B. Jacobsen, W.V. Boynton, 1991. Chicxulub Crater: A possible Cretaceous-Tertiary boundary impact crater on the Yucatan Peninsula, Mexico. *Geology, 19:867-871*

Hildebrand, A.R., M. Pilkington, M. Connors, C. Ortíz-Alemán, and R.E. Chávez, 1995. Size and structure of the Chicxulub crater revealed by horizontal gravity gradients and cenotes,. *Nature, vol. 376, pp. 415-417*

Marín, L.E. 1990. Field Investigations and Numerical Simulation of Groundwater Flow in the Karstic Aquifer of Northwestern Yucatan, México. *Ph. D. Thesis. 183 pp., Northern Illinois University, DeKalb, IL, USA*

Marín, L.E., Perry, E.C., Booth, C., and Villasuso, M., 1987. Hydrogeology of the northwestern Peninsula of Yucatan, Mexico. *EOS (Transactions), American Geophysical Union, 69:1292*

Marín, L.E., Perry, E.C., Booth, C., and Villasuso, M., 1987. Hydrogeology of the northwestern Peninsula of Yucatan, Mexico. *EOS (Transactions), American Geophysical Union, 69:1292*

Marín, L.E., Perry, E.C., Pope, K.O., Duller, C.E., Booth, C.J., and Villasuso, M., 1989. Hurricane Gilbert, its Effects on the Aquifer in Northwestern Yucatan, Mexico. *International Association of Hydrogeologists, Selected Papers on Hydrogeology from the 28th International Geologic Congress, Washington, D.C. July 9-19, 1989*

Perry, E.C., Marín, L.E., McClain, and J., Velázquez, G.; 1995. The Ring of Cenotes (sinkholes), northwest Yucatan, Mexico: its hydrogeologic characteristics and possible association with the Chicxulub Impact Crater. *Geology, 23:17-20*

Perry, E.C., J. Swift, J. Gamboa, A. Reeve, R. Sanbon, L.E. Marín, M. Villasuso. 1989. Geological and Environmental Aspects of Surface Cementation, North Coast, Yucatan, Mexico. *Geology, 17:818-821*

Perry, E.C., G. Velázquez Olimán, L.E. Marín, in review. The hydrogeochemistry of the northwest Yucatan (Mexico) karst aquifer and its relation to walt water intrusion and evaporite dissolution. *Submitted to Water Resources Research*

Pope, K.O., C.E. Duller, 1989. Satellite observations of ancient and modern water resources in the Yucatan Peninsula. *In: R. Álvarez (ed.), Simposio Latinoamericano Sobre Sensores Remotos, Memoria, Mexico, Sociedad de Especialistas Latinoamericana en Percepción Remota and Instituto de Geografía, Universidad Nacional Autónoma de México: 91-98*

Pope, K.O., A.C. Ocampo, C.E. Duller, 1993. Surficial Geology of the Chicxulub Impact Crater, Yucatan, Mexico. *Earth, Moon, and Planets, 63:93-104*

Sharpton, V.L., G.B. Dalrymple, L.E. Marín, G. Ryder, B.C. Schuraytz, J. Urrutia-Fucugauchi, 1992. New Links Between the Chicxulub Impact Structure and the Cretaceous-Tertiary Boundary. *Nature, 359:819-821*

Steinich, B. and L.E. Marín, in press(a). Hydrogeological investigations in northwestern Yucatan, Mexico, using resistivity surveys. *Ground Water*

Steinich, B. and L.E. Marín, in press(b). Determination of flow characteristics in the Aquifer of the Northwestern Peninsula of Yucatan, Mexico. *Journal of Hydrology*

Stumm, W., and J.J. Morgan, 1981. Aquatic Chemistry: An Introduction Emphasizing Chemical Equilibria in Natural Waters. *2nd. Ed., Wiley Interscience, New York, USA, 780 pp.*

Swisher, C.C., J.M. Grajales-Nishimura, A. Montanari, S.V. Margolis, P.Claeys, W. Alvarez, P. Renne, E. Cedillo-Pardo, F.J.-M.R. Maurrasse, G.H. Curtis, J. Smit, and M.O. McWilliams, 1992. Coeval $^{40}Ar/^{39}Ar$ ages of 65.0 million years ago from Chicxulub melt rock and Cretaceous-Tertiary boundary tektites. *Science, 257:954-958*

Urrutia-Fucugauchi, J., L.E. Marín, A. Trejo, in press. First results of the UNAM Scientific Drilling Program on the Chicxulub Impact Structure, Yucatan Peninsula, Mexico. *Geofísica Internacional*

Velázquez Olimán, G., 1995. Estudio Geoquímico del Anillo de Cenotes, Yucatán (Geochemical study of the Ring of Cenotes, Yucatan; in spanish). *M.S. Thesis, Instituto de Geofísica, Universidad Nacional Autónoma de México, Mexico City, Mexico, 77 pp.*

V. El papel de la tectónica local en el desarrollo del carst y la hidrogeología en Yucatán, México.

The role of local tectonics on the karst development and the hydrogeology in Yucatan, Mexico

Birgit Steinich[a], Luis E. Marín[a]

[a]Instituto de Geofísica, Universidad Nacional Autónoma de México, Cd. Universitaria, Mexico City, Mexico, C.P. 04510

Water Resources Research, en arbitraje

Abstract

The spatial distribution and size of nearly 7000 sinkholes of the Yucatan karst, Mexico, was studied. The Yucatan Peninsula can be divided topographically into an upper and a lower platform, both showing intensive karstification. Sinkhole distribution in both platforms is not homogeneous; several clusters and alignments can be identified throughout the study area. Sinkholes in the upper, older, platform tend to be larger than those on the lower platform. This is explained as a consequence of the removal of buoyant support and the subsequent collapse of the cavity roofs on the upper platform due to greater depth to the water table. Two local tectonic features are relevant for the spatial distribution of the sinkholes, a transform fault, related to the opening of the Gulf of Mexico, and an impact structure, the Crater of Chicxulub. Both structures formed sedimentation basins in the past and are now buried beneath several hundreds of meters of Tertiary sediments. Sinkhole density is high upon the ancient walls of the sedimentary basins and low upon their bottoms and crests. Stress release fracturing along the walls as a consequence of differential compactation

rates is proposed to provide initial fracturing and create good initial conditions for the karstification process. Based on the observed close relationship between local tectonics and distribution of karst features, different 'hydrotectonic domains' can be identified for the Yucatan karst. The most striking example is the Ring of Cenotes, a circular alignment of sinkholes, identified by former studies as a high permeability zone. As a model for the formation of the Yucatan karst, we propose that local tectonics provide the initial fracturing to the limestone, climatic and mixed water corrosion act as selection factors for the opening of the existing fractures and that the variations of the water level in time represent the decisive factor for the collapse of the cavity roofs. Following this formation model, the existence of a second circular high permeability zone is proposed related to the Crater of Chicxulub similar to the Ring of Cenotes, located within the first ring.

1. Introduction

The study area is located in the Peninsula of Yucatan, southeast Mexico (Fig. 1). The peninsula of Yucatan is a flat Karst platform with a smooth topography ranging from a few meters above mean sea level (MMSL) near the coast to a maximum of approximately 100 MMSL in the southwestern part of the study area [Anonymous, 1984]. The Peninsula of Yucatan is characterized by the presence of hundreds of sinkholes. Due to the flatness of the topography and a shallow water table, numerous sinkholes are filled with fresh water, called "cenotes" in the local language. An unknown percentage of the caverns have collapsed roofs and are mapped as small circular lakes [Anonymous, 1984]. The cenotes represent a superficial evidence of a well developed subsurface karst system with interconnected fractures and channels which control the hydrogeology of the Peninsula of Yucatan [e.g. Marín, 1990; Steinich & Marín, 1996; Steinich & Marín, in review]. The spatial distribution of the sinkholes is not homogeneous throughout the Peninsula. The most striking feature is the Ring of Cenotes, a circular alignment of cenotes [Anonymous, 1984]. Several authors have

proposed that there is a spatial coincidence of this Ring of Cenotes with the Chicxulub Crater [e.g Pope, 1991; Pope et al., 1993; Perry et al., 1995]. The Chicxulub Crater was described by several authors as a meteorite impact event that occured at the K/T-boundary some 65 Million years ago [Penfield & Camargo, 1981; Hildebrand et al., 1991; Sharpton et al., 1992].

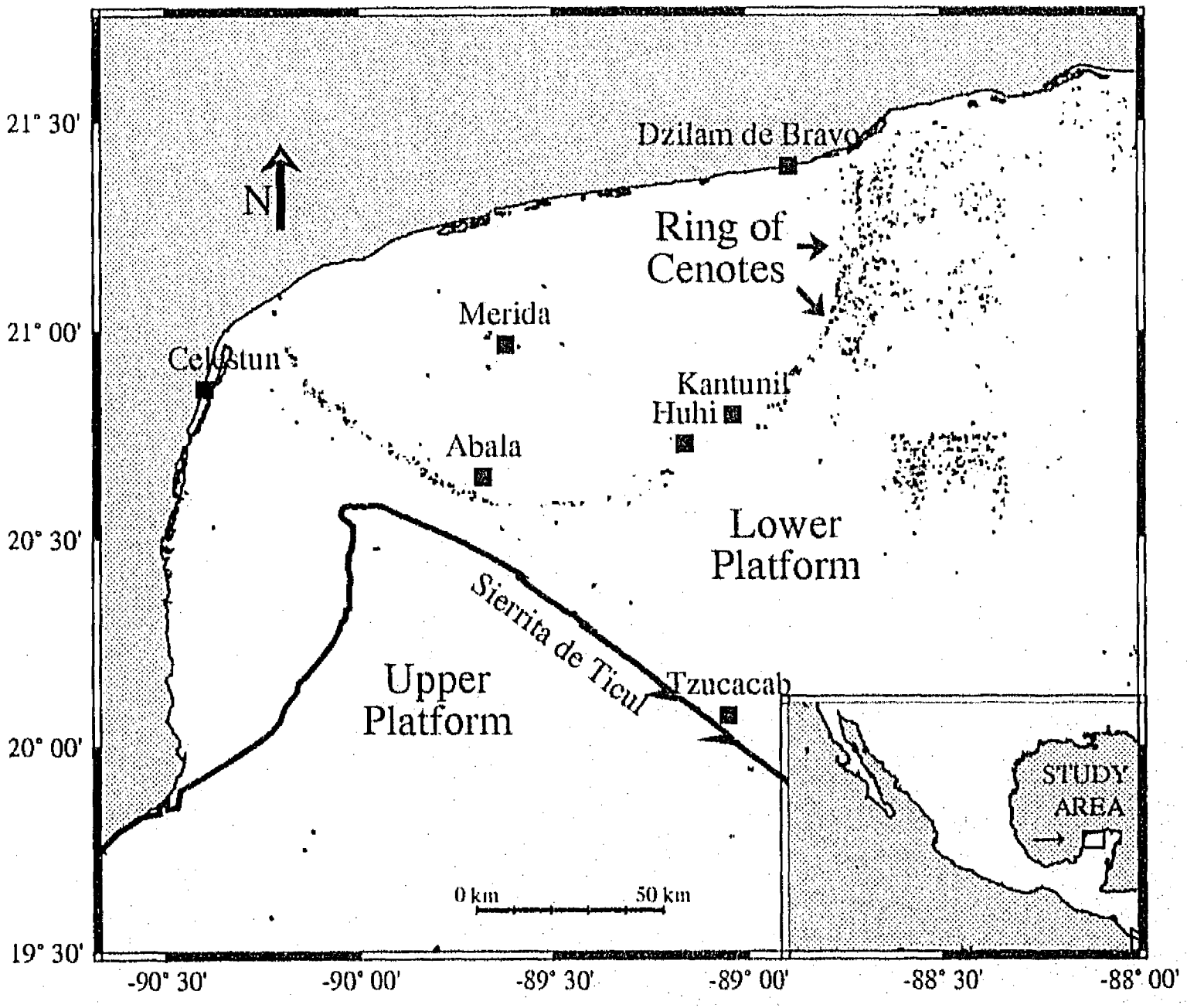

Fig. 1 Study Area in the northwestern part of the Peninsula of Yucatan, Mexico. Small black dots are submerged sinkholes (cenotes). Dry sinkholes are not represented in this Figure.

Currently, there are two schools of thought regarding the size of the crater. Sharpton et al. [1993] have proposed that it is on the order of 300 *km* in diameter, whereas Hildebrand et al. [1995] have suggested that it is on the order of 180 *km*. Only about half of the structure is located on-shore, the remaining part is off-shore in the Gulf of Mexico [Sharpton et al., 1992]. The virtual projection of the crater rim onto the surface intersects therefore once the western segment and once the northern segment of the coast line. As a consequence of millions of years of sedimentation, the structure is now buried beneath a thick layer of Tertiary carbonate sediments ranging from 220 *m* at the crater rim to 1000 *m* near the center [Perry et al., 1995; Marín, 1994]. The meteorite that created the Chicxulub Crater fell upon another tectonic structure related to the opening of the Gulf of Mexico. This tectonic process corresponds to a rotation of the Yucatan block with respect to the North American Continent which began in the Late Jurassic [e.g. Hall et al., 1982; Burke, 1988; Dunbar & Sawyer, 1987]. An observed gravity low on the Yucatan block was interpreted as crustal thinning or incipient rifting associated with the opening Gulf [e.g. Sharpton et al., 1993].

2. Objectives

The objectives of this study are: 1) to describe the spatial distribution of the sinkholes of the northwestern Peninsula of Yucatan; 2) to identify the relationship between the surface karst features, the Chicxulub Crater, and the transform fault; and 3) to determine the role of the Chicxulub Crater and the transform fault in the hydrogeology of the Peninsula of Yucatan.

3. Methodology

The sinkhole locations were obtained by digitizing topographic maps with a scale $1:50,000$ provided by the Instituto Nacional de Estadística, Geografía e Informática

(INEGI) of Mexico [Anonymous, 1984]. Gravity data was provided by the Lunar and Planetary Institute in Houston, U.S.A. as a $0.01^o x 0.01^o$ gravity matrix. Interpolation and graphical representation of the gravity data was conducted with the Generic Mapping Tool (GMT) software package [Wessel and Smith, 1992] on a SUN workstation. Computer programs for the interpretation of the digitized data were written by the senior author. All figures were generated with the GMT package.

4. Local tectonics

4.1 The transform fault

The tectonic history of the Peninsula of Yucatan is related to that of the opening of the Gulf of Mexico. Different authors agree that the Yucatan block obtained its actual position as a result of a rotational movement away from the North American Continent, nevertheless, differing models of the type of movement have been proposed. Hall et al. [1982] suggested a 24^o counterclockwise rotation with a rotation center approximately 90 *km* northeast of Acapulco in Mexico, while Dunbar and Sawyer [1987] proposed a 45^o clockwise rotation with a rotation center south of the Florida Peninsula.

A linear, slightly curved gravity low starting near $89^o30'$ west and $19^o30'$ and crossing the study area from south to north was observed [e.g. Hildebrand et al., 1991; Sharpton et al., 1993] and interpreted by Sharpton et al. [1993] as crustal thinning or incipient rifting related to the opening of the Gulf of Mexico. Thick evaporite units were found [e.g. Sharpton et al., 1993] in cores from several wells drilled by PEMEX in this area, suggesting that the possible end of the transform fault represented a stationary sea basin, necessary for the accumulation of such thick evaporite layers [Tucker, 1985]. The gravity map shows two additional gravity lows west and east of the main structure, which may be related to the same tectonic process.

4.2 The Chicxulub Crater

A nearly circular anomaly observed in gravity and magnetic data on the Peninsula of Yucatan was first interpreted to be a meteoritic impact by Penfield and Camargo [1981]. This impact event took place 65 Million years ago and is believed to be responsible for the mass extinction at the Cretaceous-Tertiary boundary [Hildebrand et al., 1991]. Sharpton et al. [1993] proposed that the crater resulted from an impact event that excavated initially to a depth of 17 to 20 *km* with a transient crater of up to 60 *km* deep. Part of the material ejected during the impact collapsed back into the excavation and partly filled it up again. These breccia deposits where found in several cores from deep wells drilled by the Mexican Petroleum Company (PEMEX) [Sharpton et al., 1992] as well as in cores of two wells drilled recently in the area [Marín, 1994]. Camargo & Suárez [1994] interpreted a thick, acoustically transparent sequence as the layer of these breccias deposited shortly after the impact.
The area inside the crater became a depositional basin during the Tertiary. Perry et al. [1995] reported the presence of Oligocene strata inside the line of the Ring of Cenotes but absent outside of it. The seismic sections presented by Camargo & Suárez [1994] show the complete sequence of Tertiary carbonate rocks whith increasing thickness towards the center of the basin. Presently, there is no major topographic evidence left of this sedimentary basin [Anonymous, 1984]. Progressive flattening of the seismic reflectors can be observed in the seismic sections of Camargo & Suárez [1994] during the Tertiary.

Results and discussion

5. Spatial distribution of the sinkholes on the northwestern Peninsula of Yucatan

The topography of the study area consists of two major, nearly horizontal platforms which are separated by a small land step, the Sierrita de Ticul (Fig. 1). The surface

of the lower platform, between the land step and the coast, cuts carbonate layers from the Eocene to the Pliocene [Gerstenhauer, 1987]. The area inside the Ring of Cenotes (Fig. 1) was proposed to be a sedimentary basin during the Oligocene [Perry et al., 1995] which was concluded from the absence of the Oligocene outside the Ring of Cenotes.

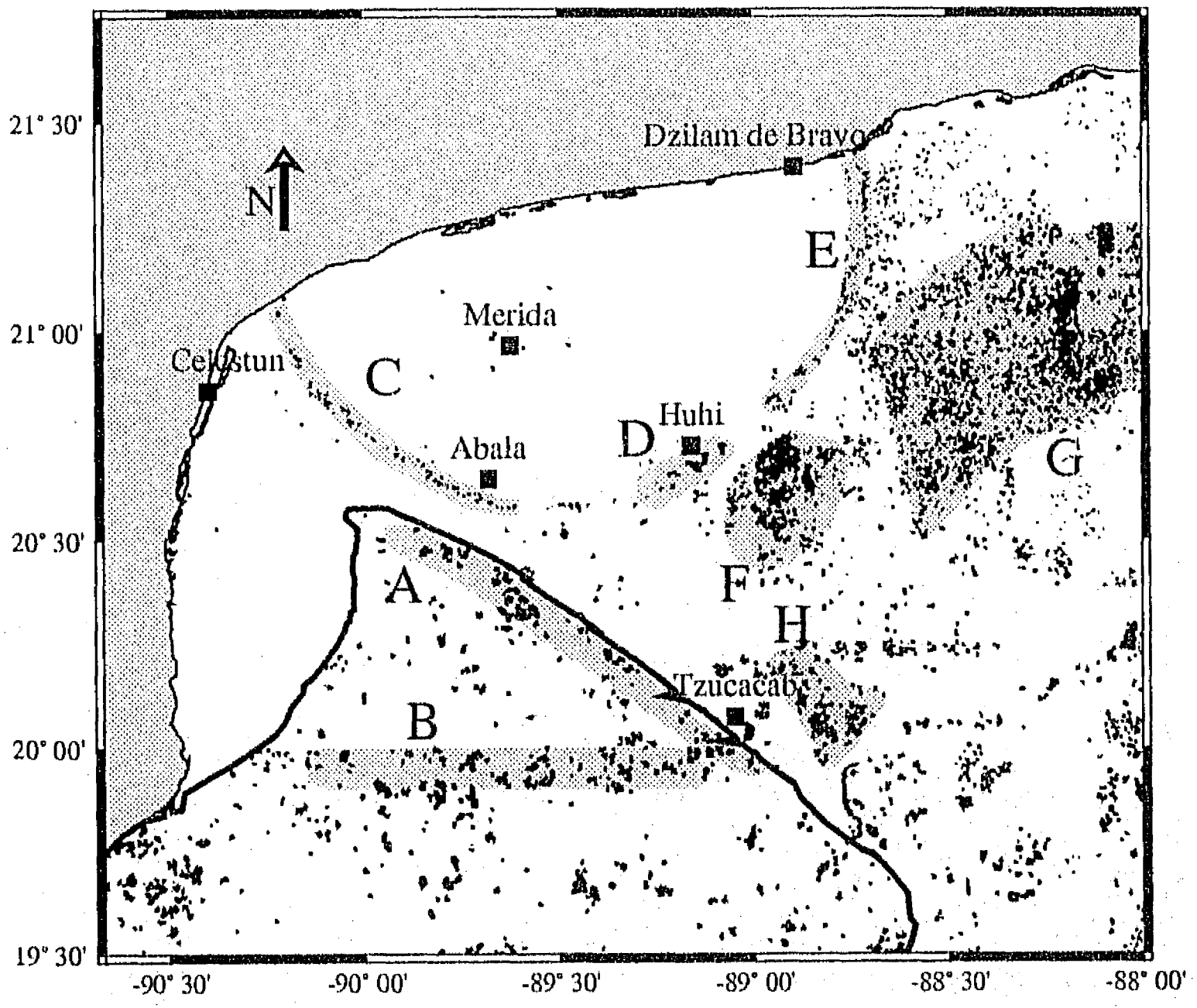

Fig. 2 Representation of submerged (cenotes) and dry sinkholes in the study area. Gray shaded areas, labeled (A) to (G), are clusters and alignments of sinkholes discussed in the text.

The formation of the upper platform was dated as Eocene [Gerstenhauer, 1987]. Both platforms show intensive karstification. Nearly 7000 sinkholes have been mapped in the study area [Anonymous, 1984] and are shown in Figure 2. In the case of the upper platform south of the land step, the karstification was active prior to the emergence of the lower platform, e.g. during the upper Eocene, the Miocene and the Pliocene [Gerstenhauer, 1987]. On the lower platform, the same author proposed the period from the Miocene to the Pleistocene for the karstification process.

5.1 Sinkholes on the upper platform

The sinkhole distribution of the upper platform has two characteristics. 1) An important number of the sinkholes are large in size (Fig. 3); 2) two alignments can be observed, one in a southeast to northwest direction (A in Fig. 2), and another in an east to west direction (B in Fig. 2). The alignment (A) is parallel to the Sierrita de Ticul; sinkhole locations start immediately south of the crest of the land step. The second alignment (B), however, shows no obvious relationship to any topography limit. Several sinkholes can be observed between these two alignments, the sinkhole density, however, is clearly lower. Almost all sinkholes located on the upper platform are dry, because the depth to the water table is in the range of 30 m to 140 m [Anonymous, 1988], (Fig. 4).

5.2 Sinkholes on the lower platform

As on the upper platform, the spatial distribution of the sinkholes on the lower platform is not uniform. The most striking feature is a circular alignment, described by various authors as the Ring of Cenotes [e.g. Pope, 1991; Marín, 1990; Perry et al., 1995]. The Ring is not continuous, but consists of several clusters of sinkholes, labeled in Figure 2 as (C) to (E).

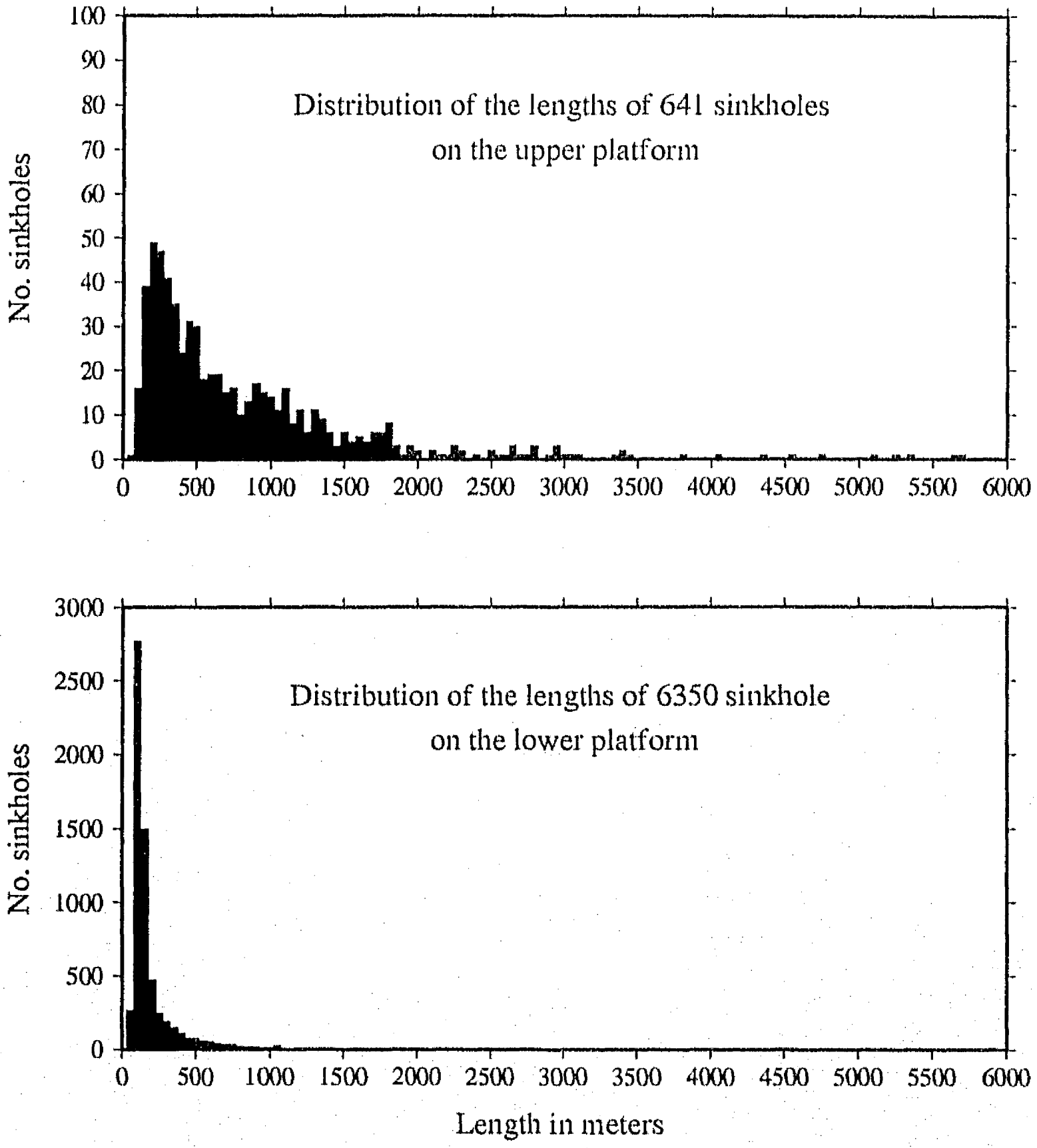

Fig. 3 Distribution of the lengths of sinkholes on the upper and the lower platform. Sinkhole lengths are based on digitized data.

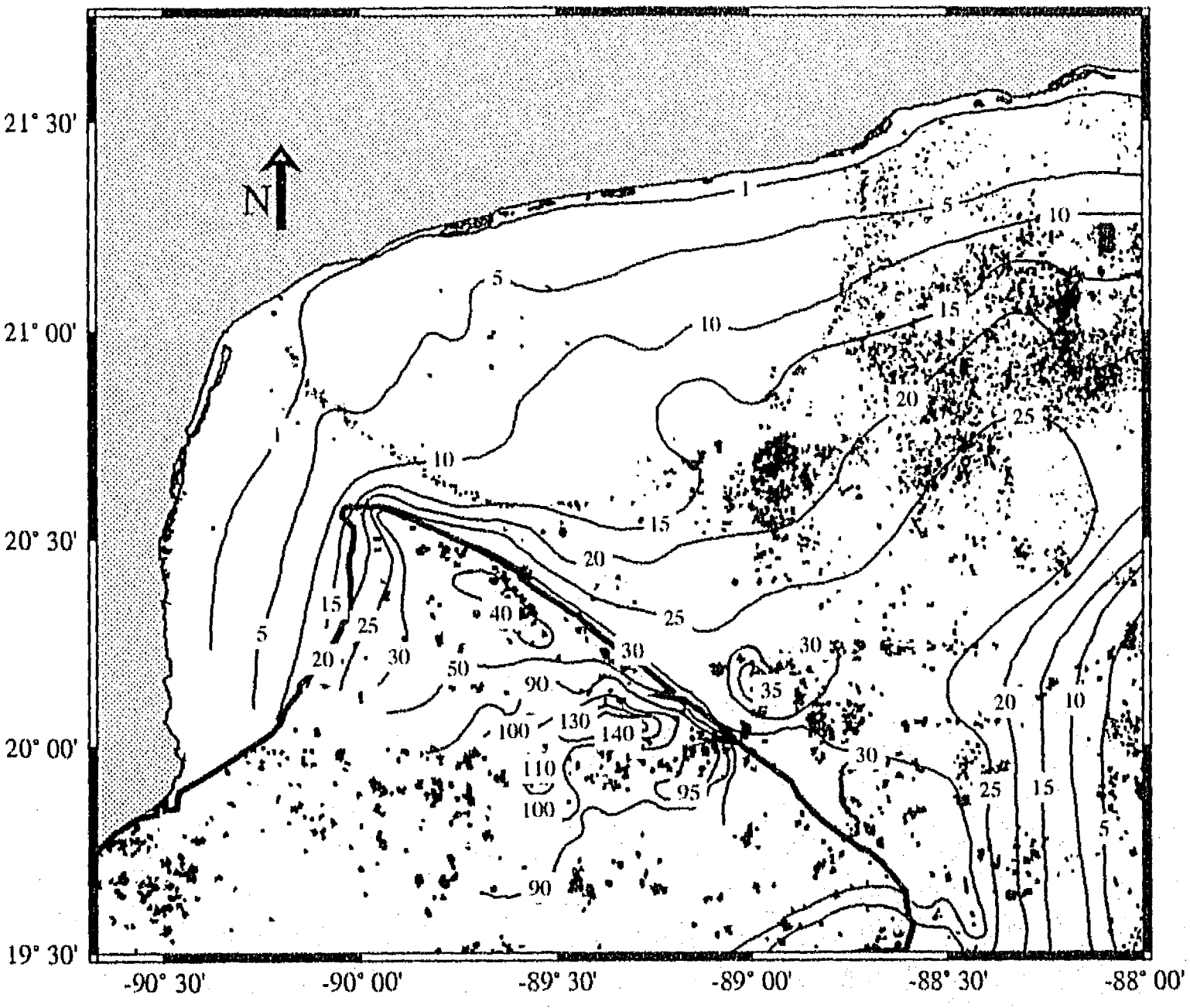

Fig. 4 Lines of equal depth to the water table, modified after Anonymous [1988]. Labels are depths in meters.

The western part of the Ring of Cenotes is the segment where the alignment is best developed. The segment closest to the west coast is accompanied by a minor, second ring, described by Perry et al. [1995] and Steinich and Marín [1996]. The Ring of Cenotes is interrupted on its southern part southeast of the village of Abala (Fig. 2).

The following, westward part of the Ring of Cenote is characterized by a decrease in sinkhole density and further eastward by an increase in dispersion of the sinkhole locations (zone D in Fig. 2 near Huhi). The westernmost part of the Ring of Cenotes (E in Fig. 2) can be described as a limit between an extensive sinkhole field east of the ring and an area with low sinkhole density which corresponds to the area inside the Ring of Cenotes. In this area which is characterized by an extremely low sinkhole density, only a few sinkholes are mapped near the City of Merida. The depth to the water table on the lower platform varies between 0 m and 35 m [Anonymous, 1988; Marín, 1990] (Fig. 4). In an extensive area between the Sierrita de Ticul and the coast line, sinkholes are submerged and are mapped as small, circular lakes (cenotes in the local language, Fig. 1). Especially, the sinkholes of the Ring of Cenotes are nearly all submerged except the short segment labeled (D) in Figure 2. A local high is mapped for the depth to the ground water table [Anonymous, 1988] which coincides with the area (D). Sinkholes in this segment are typically bigger than the others along the ring.

6. Distribution of the size of the sinkholes

The formation of the sinkholes of the Yucatan Peninsula is described by Gerstenhauer [1987]. He proposed a corrosion process by percolation from rainfall during humid periods, the subsequent formation of a resistant crust by reprecipitation of calcite near the surface during dry periods and the washing out of the corroded material beneath the crust. The more resistant crust forms the roofs of the cavities and is partly collapsed in an unknown percentage of the latter. The initiation of the corrosion process is facilitated by the presence of initial vertical fractures and bedding plane partings allowing the necessary circulation of the infiltrated water [Gerstenhauer, 1987; Sasowsky and White, 1994]. The heterogeneous distribution of the sinkholes in the study area implies that there are well defined locations where the conditions for corrosion were especially favorable in the past. This point is further discussed

in Section six. Figure 4 shows the depth to the water table. Comparison with the distribution of the size of the sinkholes shows that big sinkholes are related to large values of the depth to the water table. This relationship is obvious for the upper platform south of the Sierrita de Ticul (Fig. 1). The local high of the depth to the water table in the center of the study area at $89^o15'$ west and $20^o45'$ north coincides with the sinkhole area (D) in Figure 2. This area is characterized by large sinkholes which are only temporarily flooded [Anonymous, 1984]. The lowering of the water level within a cavity results in a removal of buoyant support and in an increase of the effective weight on the span. When the strength is exceeded, the roof of the cavity collapses [Ford and Williams, 1989]. These observations imply that buoyant support is a decisive factor for the actual size of the collapsed part of the roofs. The emergence of the upper platform during the Mio-Pliocene [Gerstenhauer, 1987] may have initiated the collapse of the major part of the roof of the cavities. The older karst features on the upper platform can therefore be assumed to have a higher collapse percentage which is reflected by the large sizes of its sinkholes with respect to the smaller ones on the lower platform. The lack of sinkholes on the lower platform in areas where favorable corrosion conditions can be assumed (as discussed in Section six) may be due to the low depth to the water table which maintains the necessary buoyant support and impedes in this way the massive collapse of the roofs. This may explain the lack of sinkholes in the central part of the high gravity gradient area near the City of Merida (Fig. 5).

7. Relationship between the surface karst features, the Chicxulub Crater and the transform fault

The early initiation of the corrosion process in a carbonate platform is favored by the existence of vertical fractures and bedding planes [Groves and Howard, 1994]. In the case of competent brittle rock, fracturing occurs when stress exceeds the rock's strength [Ford and Williams, 1989]. Two tectonic phenomena contribute to the

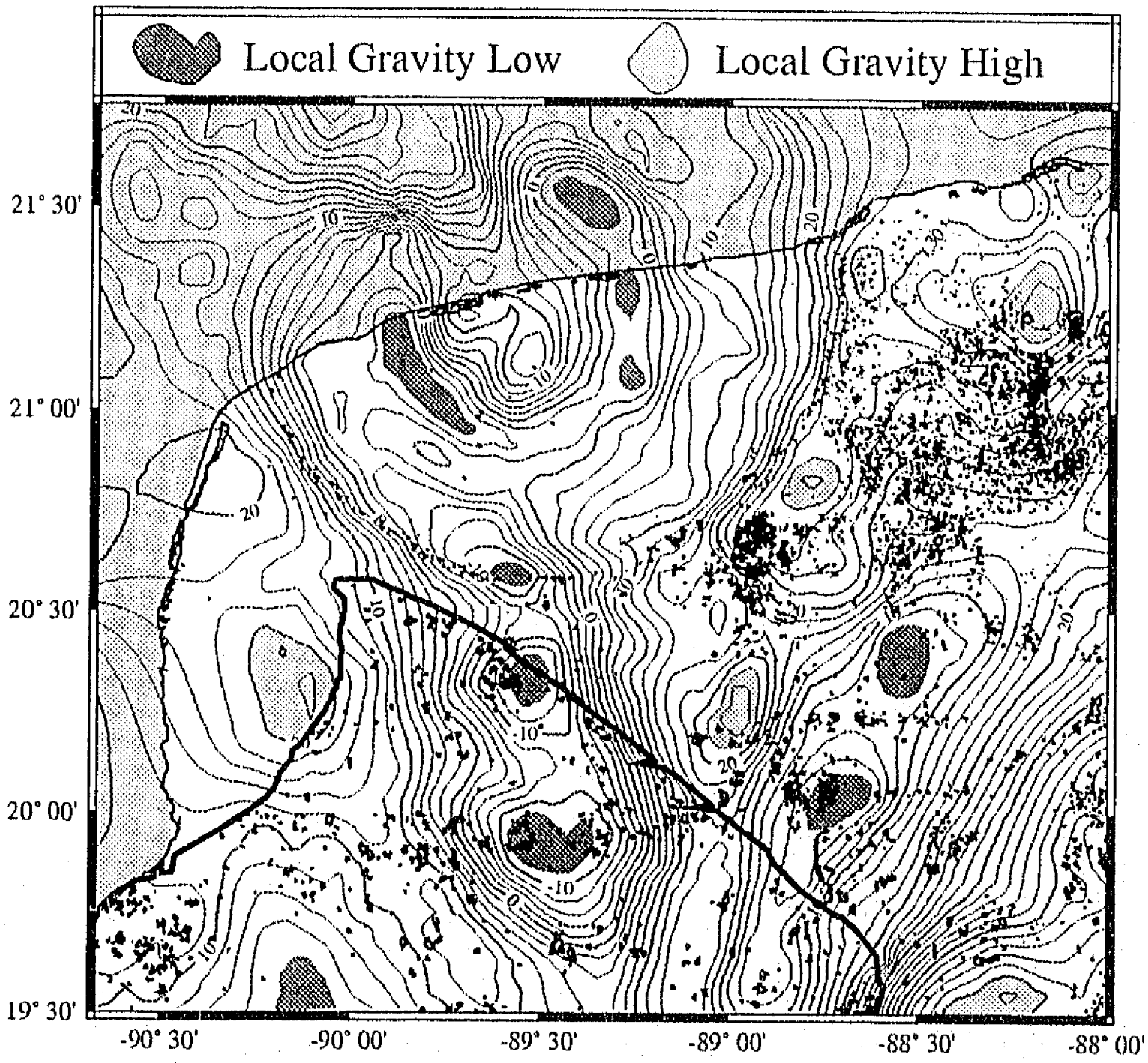

Fig. 5 Figure allowing a comparison of gravity data and sinkhole location in the study area. Contoured gravity anomaly data modified after Sharpton et al. [1993], the contour interval is 2 *mGal*. Local gravity lows are represented as dark gray shaded areas, local gravity highs as bright gray shaded areas.

distribution of the stress patterns in the study area, the transform fault and the Chicxulub Crater, described in Sections three and four, respectively. Both features provided special sedimentation environments during a certain time period in the form of sedimentation basins [Sharpton et al, 1993; Perry et al., 1995]. Two recent models of the Chicxulub impact basin [Camargo and Suárez, 1994; Sharpton et al., in press] show that the thickness of the impact breccia and the overlaying Tertiary carbonate sediments vary significantly along a profile perpendicular to the crater rim. These models are based on geophysical data (gravity and seismic data) and the interpretation of cores from several boreholes. The differences in the thickness of this loose material may have caused a different compaction behavior and rate. The deposition of the sediments on slopes may have provoked a shear deformation rather than compaction [Jones, 1994]. Stress release fracturing in relation with different compaction rates and shear deformation along steep slopes may be the most important factor for fracture creation. Sasowsky and White [1994] stressed the importance of stress release fracturing for the distribution of karst features along valley walls. Figure 5 shows gravity data [Sharpton et al., 1993] together with the sinkholes in the study area. The wall of the former sedimentation basin related to the transform fault is reflected in the gravity data by the steep gradients around the north-south axis at approximately $89^o30'$ west. In the case of the Chicxulub Crater, two walls are proposed by a recent model [Sharpton et al., in press]. They coincide with the two steep gravity gradient rings in Figure 5. Sinkhole accumulations can be observed along the outer ring, but not along the inner ring of the Crater. Sinkhole zones (F), (G) and (H) are also located upon steep gravity gradients (Fig. 5). Peak zones in the gravity data, however, coincide with zones of low sinkhole density. Examples of this are the axis of the transform fault, the area between the two steep gradient circles of the Chicxulub Crater and various other gravity minima and maxima in the eastern part of the study area. In the case of the Yucatan karst, we propose that walls of the former sedimentation basins related to the transform fault and the Chicxulub Crater offered the most favorable locations for initial fracturing and the subsequent

corrosion processes as a consequence of stress release fracturing related to differential sedimentation rates.

8. The influence of the Chicxulub Crater and the transform fault on the hydrogeology

The various tectonic features described so far played a determinant role for the initial conditions of the karstification process. We propose that variations of the compaction rates and shear deformation along the basin walls gave the fracture design to the Yucatan limestone. This implies a close relationship between the local tectonics and the hydrogeology in the study area, as a result, different 'hydrotectonic domains' [Brown, 1994] can be defined. The Ring of Cenotes is the most obvious hydrotectonic domain (HD) and is related to the steep slope of the transient cavity or the crater rim (depending on the actual size of the structure). Sinkhole-zones (C), (D) and (E) are part of this hydrotectonic domain. The Ring of Cenotes was proposed to be a high permeability zone, acting as an underground river system [Marín, 1990]. Steinich and Marín [1996] showed that a low permeability zone interrupts this underground river on its segment southeast of Abala. We propose that this decrease in permeability can be explained by the decrease of initial fracture density along the axis of the transform fault. Figure 5 shows that the axis and the crater rim are superimposed at this location. Velázquez [1995] and Steinich et al. [in review] proposed that within this zone there is a ground water divide in the aquifer system. Steinich and Marín [in review] described a highly variable zone of hydraulic gradient and proposed the existence of at least two fracture systems perpendicular and parallel to the Ring of Cenotes. Assuming that the eastern wall of the transform fault basin as well as the crater rim contributed to the initial fracturing, a multidirectional fracture pattern may be expected at the overlap of the two tectonic features and may explain the special hydraulic conditions of this highly variable zone. The second, inner steep gravity gradient circle (Fig. 5) might have generated favorable conditions for stress

release fracturing equal to the crater rim. A similar karst feature like the Ring of Cenotes may exist and may show up on the surface as the water level lowers and roof collapse reveals the existing cavities. Figure 5 shows that the few existing sinkholes near the City of Merida are located on the steep gravity gradient of the inner rings of the Chicxulub Crater. Several cavities with uncollapsed roofs have been observed by Marín [unpublished observation] in this area.

The extensive sinkhole field (G) (Fig. 2) coincides with the transition zone between a gravity high in the northeastern edge of the study area and a deep gravity low southwest of it. This zone can be defined as another hydrotectonic domain, characterized by especially good recharge conditions for the aquifer. Areas like the alignments (A) and (B) on the upper platform are other good candidates for hydrotectonic domains, however, further investigation is required to define their role in the hydrogeology of the study area.

9. Evidence of other phenomena influencing the distribution of sinkholes

In the former section, we stressed mainly two phenomena that influence the spatial distribution of sinkholes. 1) The initial fracture design which is determined by the local tectonic and give the initial conditions for the corrosion process. 2) The influence of the water level variations that either maintain or remove buoyant support of the cavity roofs and control the collapse rate of the latter. This phenomena is determinant at the end stage of the sinkhole history, e.g. whether the existing cavity makes its manifestation at the surface. However, several other phenomena influenced the karstification process. The 'Sierrita de Ticul' divides the lower and the upper platform. Emptying of the cavities on the upper platform occured in a phreatic environment prior to the emergence of the upper platform [Gerstenhauer, 1987]. The difference of elevation between the upper and the lower platforms is at least 25 m and a higher water level by this amount would place the coast line to what is now the Sierrita de Ticul [E. Perry, pers.commun.]. A narrow band behind the coast line

hosted then the mixing zone of salt and fresh water. The alignment (A) (Fig. 2) may therefore be explained by mixed water corrosion. A similar accumulation can be found parallel to the present coast line [Marín et al., 1988] and may be the actual equivalent to the alignment (A).

In the eastern part of the Peninsula, the climatic conditions provide actually favorable conditions for the destruction of the more resistant crust [Gerstenhauer, 1987]. Part of the numerous small dolines in the sinkhole zone (G) may be the result of surface solution rather than cave roof collapse [McConnell and Horn, 1972]. The described phenomena are important factors in the initiation of the karstification process, however, they have to be classified as secondary with respect to the tectonic features. A simulation study by Groves and Howard [1994] showed that only a few of the numerous initial fractures and bedding planes are enlarged into cave passages. Following this model, we propose that in the study area, the tectonic features gave the initial fracture design to the limestone rocks, while the phenomena discussed in this section contributed as the selection factor, which resulted in the opening of existing fractures to form the large karst pathways.

In this model the unexplained second alignment on the upper platform (B in Figure 2) should correspond to another tectonic feature which provided the initial fractures to this alignment. However, further study is necessary to identify the karst history of the latter.

10. Conclusions

Size and the location of nearly 7000 sinkholes of the Yucatan Karst were analyzed and were divided into various zones according to these parameters. The spatial distribution of the sinkholes in the study area was compared with the features of the local tectonics, a transform fault related to the opening of the Golf of Mexico and an impact structure, the Chicxulub Crater. This comparison showed that the locations of the sinkholes are related to these tectonic features. We propose that the stress re-

lease model proposed by Sasowsky and White [1994] apply as well to buried valleys. We proposed a model for the influence of the various factors on the formation of the Yucatan Karst in which the local tectonic features give the initial fracture design to the Yucatan limestone, while other phenomena like mixed-water corrosion or climatic conditions, act as selection factor for the opening of part of the existing initial fractures. Finally, the variations of the water level in time represents the decisive factor for the collapse of the cavity roofs and determines in this way if the karst features have a surface expression. In this way, different factors were identified as decisive for the karstification process and their influence on different stages of the latter was stressed.

Different 'hydrotectonic domains' can be identified. The two independent tectonic features, the transform fault and the Chicxulub Crater, are in narrow relationship with the actual hydrogeology of the Yucatan aquifer. This study shows that the exclusive and isolated discussion of the role of the Ring of Cenotes is not appropriate for the understanding of the hydrogeology of the Yucatan Peninsula. The existence of another circular high permeability zone similar to the Ring of Cenotes was proposed based on the conclusions of this study.

Acknowledgments

Birgit Steinich thanks the Dirección General de Asuntos del Personal Académico (grant IN107595) for a graduate fellowship and PADEP for financial support. We thank V. Sharpton for making available the gravity data.

References

Anonymous, Cartas Topográficas de Yucatán 1:50000, *Instituto Nacional de Estadística, Geografía e Informática,* Mérida, Yucatán, 1984.

Anonymous, Sinopsis Geohidrológica del Estado de Yucatán, 51 pp., 7 maps, Secretaría

de Agricultura y Recursos Hidráulicos, 1988.

Brown, K., Fluids in deforming sediments, in *The Geological Deformation of Sediments*, edited by A. Maltman, pp. 205 - 237, Chapman & Hall, London, 1994.

Burke, K, Tectonic Evolution of the Caribbean, *Ann. Rev. Earth Planet Sci.,* vol. 16, pp. 201-230, 1988.

Camargo, A. and G. Suárez, Evidencia Sísmica del Cráter de Chicxulub, *Boletín de la Asociación Mexicana de Geofísicos de Exploración,* vol. 34(1), pp. 1-28, 1994.

Dumbar, J.A. and D.S. Sawyer, Implications of Continental Crust Extension for Plate Reconstruction: An Example from the Gulf of Mexico, *Tectonics,* vol. 6(6), pp. 739-755, 1987.

Ford, D. and P.W. Williams, Karst Geomorphology and Hydrology, Unwin Hyman, London, 601 pp., 1989.

Gerstenhauer, A., Kalkkrusten und Karstformenschatz auf Yucatán, México, *Erdkunde,* vol. 41, pp. 30-37, 1987.

Groves, C.G. and A.D. Howard, Early development of karst systems: 1. Preferential flow path enlargement under laminar flow, *Water Resour. Res.,* vol. 30(10), pp. 2837-2846, 1994.

Hall, D.J., T.D. Cavanaugh, J.S. Watkins, K.J. McMillen, The Rotational Origin of the Gulf of Mexico Based on Regional Gravity Data, *AAPG Studies in Continental Margin Geology,* Memoria 34, 1982.

Hildebrand, A.R., G.T. Penfield, D.A. Kring, M. Pilkington, A. Camargo Z., and S.B. Jacobsen, Chicxulub Crater: A possible Cretaceous/Tertiary boundary impact crater on the Yucatán Peninsula, Mexico, *Geology,* vol. 19, pp. 867-871, 1991.

Hildebrand, A.R., M. Pilkington, M. Connors, C. Ortíz-Alemán, and R.E. Chávez, Size and structure of the Chicxulub crater revealed by horizontal gravity gradients and cenotes, *Nature,* vol. 376, pp. 415-417, 1995.

Jones, M., Mechanical principles of sediment deformation, in *The Geological Deformation of Sediments,* edited by A. Maltman, pp. 37-71, Chapman & Hall, London, 1994.

Marín, L.E., Field Investigations and Numerical Simulation of Groundwater Flow in the Karstic Aquifer of Northwestern Yucatan, México, Ph. D. Thesis. 183 pp., Northern Illinois University, 1990.

Marín, L.E., Informe final sobre las perforaciones en Yucatán, Reporte Técnico, Instituto de Geofísica - UNAM, 1994.

Marín, L.E., R. Sanborn, A. Reeve, T. Felger, J. Gamboa, E.C. Perry, and M. Villasuso, Petenes: A key to understanding the hydrogeology of Yucatan, Mexico (abstract), *Int. Symposium on Hydrogoly of Wetlands in Semiarid and Arid Regions,* pp. 119-122, Seville, Spain, 1988.

McConnell, H, and J.M. Horn, Probabilities of surface karst, in *Spatial Analysis in Geomorphology,* edited by R. Chorley, pp. 111-133, Methuen, Loudon, 1972.

Penfield, G., and A. Camargo, Definition of a mafic igneous zone in the central Yucatan platform with aeromagnetic and gravity (abstract), *Abstracts and Biographicies,* Society of Economic Geologists 51st Annual Meeting, p. 11, 1981.

Perry, E., L. Marín, J. McClain, and G. Velázquez, Ring of Cenotes (sinkholes), northwest Yucatan, Mexico: its hydrogeologic characteristics and possible association with the Chicxulub impact crater, *Geology,* vol. 23(1), pp. 17-20, 1995.

Pope, K.O., Mexican site for K/T impact crater?, *Nature,* vol. 351, p. 105, 1991.

Pope, K.O., A.C. Ocampo, and C.E. Duller, Surficial Geology of the Chicxulub Impact Crater, Yucatan, Mexico, *Earth, Moon, and Planets,* vol. 63, pp. 93-104, 1993.

Sasowsky, I.D. and W.B. White, The role of stress release fracturing in the development of cavernous porosity in carbonate aquifers, *Water Resources Research,* vol. 30(12), pp. 3523-3530, 1994.

Sharpton, V.L., G.B. Dalrymple, L.E. Marín, G. Ryder, B.C. Schuraytz, and J. Urrutia-Fucugauchi, New Links Between the Chicxulub Impact Structure and the Cretaceous-Tertiary Boundary, *Nature,* vol. 359, pp. 819-821, 1992.

Sharpton, V.L, K. Burke, A. Camargo-Zanoguera, S.A. Hall, D.S. Lee, L.E. Marín, G. Suárez-Reynoso, J.M. Quezada-Muñeton, P.D. Spudis, and J. Urrutia-Fucugauchi, Chicxulub Multiring Impact Basin: Size and Other Characteristics Derived from

Gravity Analysis, *Science,* vol. 261, pp. 1564-1567, 1993.

Sharpton, V.L., L.E. Marín, C. Carney, S. Lee, G. Ryder, B.C. Shuraytz, P. Sikora, and P.D. Spudis, A Model of the Chicxulub Impact Basin Based on Evaluation of Geophysical Data, Well Logs and Drill Core Samples, *Geological Society of America Special Paper 307,* in press.

Steinich, B., and L.E. Marín, Hydrogeological investigations in northwestern Yucatan, Mexico, using resistivity surveys, *Ground Water,* in press, 1996.

Steinich, B., and L.E. Marín, Determination of flow characteristics in the Aquifer of the Northwestern Peninsula of Yucatan, Mexico, *Journal of Hydrology,* in review.

Tucker, M.E., Einführung in die Sedimentpetrologie, Ferdinand Enke Verlag, Stuttgart, 265 pp., 1985.

Velázquez Olimán, G., Estudio Geoquímico del Anillo de Cenotes, Yucatán, (Geochemical study of the Ring of Cenotes, Yucatan (spanish), *M.S. Thesis,* Instituto de Geofísica, Universidad Nacional Autónoma de México, 77 pp., 1995.

Wessel, P. and W.H.F. Smith, The GMT-SYSTEM v. 2.1., Technical Reference & Cookbook *SOEST/SIO,* 1992.

VI. Conclusiones

En el presente trabajo se estudiaron aspectos hidrogeológicos y geofísicos del noroeste de la Península de Yucatán, México.

El acuífero cárstico de la Península de Yucatán consiste en un lente de agua dulce el cual flota sobre agua salada. Está caracterizado por su alta permeabilidad. El Anillo de Cenotes es un alineamiento circular de cenotes que posiblemente funge como un sistema de río subterráneo en el acuífero. Se ha propuesto su relación con el Cráter de Chicxulub, una estructura de impacto creada por un meteorito en el límite del Cretácico-Terciario. El presente estudio del acuífero de Yucatán permite obtener las siguientes conclusiones.

1) El espesor del lente de agua dulce varía entre 18 metros cerca de la costa a 110 metros en la parte sureste de la zona estudiada. Estos resultados se obtuvieron de la interpretación de datos eléctricos.

2) La parte superior del acuífero es electricamente anisotrópica. Se propone que esta anisotropía se debe a la existencia de direcciones preferenciales de la permeabilidad.

3) El Anillo de Cenotes es una zona de alta permeabilidad en relación a sus alrededores. Sin embargo, la interpretación de datos eléctricos ha demostrado que la permeabilidad varía a lo largo del anillo. Existe una zona de baja permeabilidad en la parte sur del anillo al sureste de la población de Abalá que interrumpe el flujo del agua subterránea a lo largo del anillo. Segmentos de alta permeabilidad del anillo se manifiestan en la superficie por una alta densidad de cenotes.

4) El área al oriente de la zona de Abalá, la cual representa la parte central del Anillo de Cenotes, se caracteriza por su alta variabilidad de los niveles de agua

y del régimen de las líneas equipotenciales. En esta área se identifican varios sistemas de fracturas bien conectadas y con diferentes direcciones. La zona de baja permeabilidad de Abalá representa el límite occidental de la zona de alta variabilidad. Sus características permiten una rápida respuesta a las condiciones de recarga superficial, cambios importantes de las direcciones de flujo así como un drenaje más rápido respecto a otras áreas del acuífero.

5) La comparación de datos eléctricos e hidráulicos en la zona de alta variabilidad muestra que las direcciones de las fracturas interconectadas corresponden en la mayor parte del área a las direcciones del gradiente hidráulico. Ello implica que este último tuvo un papel determinante en la formación de las vías de flujo del agua subterránea. Registros eléctricos muestran que los diferentes sistemas de fracturas son desarrollados de una manera similar por lo que se propone que los cambios de los gradientes hidráulicos en la zona de alta variabilidad son muy frecuentes.

6) Basado en datos geofísicos e hidráulicos se propone que la zona de Abalá desconecta hidraulicamente la zona de alta variabilidad de la parte occidental del Anillo de Cenotes formando de esta manera dos subsistemas en el acuífero de Yucatán. Se propone que la zona de Abalá funge como parteaguas en el acuífero. Este resultado está apoyado por la interpretación de datos geoquímicos en la zona.

7) Como consecuencia de los cambios en los gradientes hidráulicos y en las direcciones de flujo se propone que la zona de alta variabilidad tiene una elevada vulnerabilidad frente a la contaminación proveniente de la zona urbana e industrial de la Ciudad de Mérida.

8) Se realizó un estudio de la distribución y los aspectos de la formación de las

depresiones en el carst de Yucatán con el fin de identificar otras posibles zonas de importancia para la hidrogeología de la Península. Se propone que la formación y las características de las depresiones están estrechamente relacionadas con la tectónica local. Se estudiaron dos elementos tectónicos: una falla relacionada con la apertura del Golfo de México y el Cráter de Chicxulub. Ambas estructuras representaron en su epoca cuencas de sedimentación marina.

9) Se propone que las paredes de las cuencas de sedimentación ofrecieron condiciones favorables para la formación de fracturas de la roca del acuífero, debido a la liberación de fuerzas de tensión que se acumulan por el cambio de los índices de compactación de los sedimentos en la cercanía de las paredes de las cuencas.

10) Como modelo para la formación del carst de Yucatán, se propone que la tectónica local determinó el diseño de fracturas iniciales en la zona estudiada, dando de esta manera las condiciones iniciales para el subsiguiente proceso de carstificación. Fenómenos como el gradiente hidráulico, las condiciones climatológicas o la disolución por la mezcla de agua dulce y agua salada representaron los factores determinantes para la selección de las fracturas que se abrieron por disolución. La profundidad al nivel freático ha sido el fenómeno importante para la manifestación de las cavidades cársticas en la superficie, manteniendo o quitando el apoyo de los techos de las cavernas.

11) Basado en este modelo, se realizó una división de las depresiones cársticas en varios grupos según su formación y sus dimensiones. Se propuso una identificación de diferentes 'dominios hidrotectónicos' que determinan el régimen del flujo de agua en el acuífero de Yucatán.

A base de los resultados obtenidos en este estudio se podrá elaborar un nuevo modelo conceptual del funcionamiento hidrogeológico del acuífero de Yucatán. El

conocimiento de las profundidades a la interfase permitirá estimar los espesores del lente de agua dulce. La investigación de las características del carst yucateco respecto a la distribución y tamaño de las dolinas así como la identificación de zonas con sistemas de fracturas alineadas permitirá definir la permeabilidad en la zona de estudio con más detalle espacial y tomando en cuenta aspectos de heterogeneidad y de anisotropía. La división del acuífero en dominios hidrotectónicos representará una base para dicha tarea. La observación de las oscilaciones de los niveles de agua en algunas partes del acuíferos da nuevos elementos para el estudio de la vulnerabilidad del acuífero frente a la contaminación.

Agradecimientos

Agradezco al Dr. Luis E. Marín por la dirección de esta tesis, por el apoyo durante todo el tiempo de mi estancia en el Posgrado del Instituto de Geofísica y por el trabajo compartido. A los Doctores E. Perry y P. Carpenter, ambos de la Northern Illinois University, por sus consejos y por prestar equipo de campo. Al Dr. B. Sharpton por poner a mi disposición los datos gravimétricos. Al personal del Instituto Nacional de Estadística, Geografía e Informática (INEGI) y de la Comisión Nacional de Agua (CNA) en Mérida, por su apoyo en diferentes etapas de los trabajos de campo en Yucatán. Agradezco a los Doctores J. Urrutia-Fucugauchi, D. Morán Zenteno, A. Ortega Guerrero, O. Campos Enríquez, J. Arzate Flores y E. Perry, que en su función de sinodales, me ayudaron con sus valiosos comentarios en la fase final de esta tesis. Agradezco al Deutscher Akademischer Austausch Dienst (DAAD) de Alemania, a la Secretaría de Relaciones Exteriores de México , a la Dirección General de Asuntos del Personal Académico (DGAPA), al Consejo Nacional de Ciencia y Tecnología (CONACyT); todas esas instituciones me proporcionaron ayuda económica en forma de becas y/o financiamiento de trabajo de campo que hizo posible la realización de este trabajo.

Agradezco a Norma Bravo por acompañarme en los numerosos tramites que implica la estancia en el Posgrado y por su eterna paciencia con mi impaciencia con ellos. Agradezco a todos los compañeros del Posgrado en Geofísica por el tiempo compartido.

De manera muy especial agradezco a Carlos Fuentes por su apoyo incondicional en todos los sentidos. Sin el no se hubiera llevado a cabo este trabajo. Agradezco a mi familia que, remotamente, nos esta brindando su apoyo.